

Study of a New Healing Precursor Derived From Waste Streams For Bacterial Self-Healing Concrete

(Master Thesis)

A. Hazarika

Technische Universiteit Delft

STUDY OF A NEW HEALING PRECURSOR DERIVED FROM WASTE STREAMS FOR BACTERIAL SELF-HEALING CONCRETE

A thesis submitted to the Delft University of Technology in partial fulfillment
of the requirements for the degree of

Master of Science in Civil Engineering

by

Amrita Hazarika

June 2021

Thesis Committee: Prof.dr. Henk Jonkers (Chair, Supervisor)
Ir. Emanuele Rossi (Supervisor)
Prof. dr. Roel Schipper (External Member)

*To Maa and Deta, whose both
love for me, and belief in my potential
far exceed my own.*

ACKNOWLEDGEMENTS

“And when all the wars are over, a butterfly will still be beautiful.”

— *Ruskin Bond.*

For me, the *butterfly* is my masters journey - my odyssey of sorts, in the Netherlands. Despite the mayhem of the current pandemic, and the perennial chaos and confusion with regard to my health, personal life and academics throughout the masters period, I still find this journey to be an extraordinarily beautiful one. It will always be so. I owe this to the handful of gracious people without whose unceasing support, guidance, time, company, love, and upliftment, I and this thesis could have been a lost cause a good while back. I therefore take generous space in this section for honouring the key people who all made this journey a success.

First and foremost, I am indebted to the chair of my thesis committee, Prof. Dr. Henk Jonkers, for being immensely kind in the process and enabling me to complete the thesis despite all the odds in the way. His ready help whenever I needed it, flexibility in adapting to my plans, time and guidance, were all majorly instrumental for the completion of my thesis. Dr. Jonkers is one character in the world of academia whose humility and ever-approachable disposition make the whole profession a better, kinder place for struggling enthusiasts in the field like myself.

I thank my external committee member, Prof. Dr. Roel Schipper, for being very empathic and patient with me. His eagerness to help me in whatever way possible, earnest interest in my progress, and the reminders regarding all the academic formalities, made me feel very supported and guided. Major thanks and appreciation goes to my daily supervisor Emanuel Rossi for being outstandingly understanding and patient with me all throughout the course of this thesis work. Through his unceasing effort to push my boundaries at work and quality of my research, he indeed sets an exemplary precedent for all daily supervisors to emulate. Thanks to his vast reserves of energy, that I felt quite enthusiastic when we worked at the lab.

I take this opportunity to thank our lab assistants at Microlab and Stevinlabs, John van den Berg, Maiko van Leeuwen, Arjan Thijssen, and Ton Blom for the assistance and support in conducting my experiments. Also big thanks to the colleagues at microlab, Boyu, Claudia, Marija, Yu Zhang, Anna Linda and Renee, who were all ever so kind to help me out with different experiments. I also thank the secretary of our section (Materials and Environment), Jacqueline van Unen Bergenhenegouwen for all the administrative assistance with regard to office space, computer, and formalities thereof, during my term as a student assistant and during the master thesis time as well.

A big shoutout to my friends and family both at the Netherlands and back home in Assam, India for keeping my sanity intact. In no particular order, I thank Ritu for being a pillar of support and the proverbial friend in need and deed, Mayuri for keeping me afloat through the roughest of storms and for all the humor when I needed, Dikshita for

supporting me when the academics became a little too overwhelming, and Bhaswati ba for just existing and providing a safe haven for me at her place whenever I contemplated fleeing the pressures of this journey! Thanks to all the people that I met and became friends with at the Netherlands who through their own ways, helped make this journey a bit more amusing and colorful for me.

Finally, I thank the relentless pursuit of my parents to provide their daughters with the kind of opportunities and experiences that they believe to be exponentially better than their share. Thank you for being my heroes. Thanks to Pba for having my back through thick and thin, and to Anav for bringing rays of sunshine to all our lives.

ABSTRACT

The introduction of autonomous and stimulated autogenous self - healing of concrete cracks has been a wonderful technological breakthrough for our built infrastructure. By reducing manual dependence on repair and maintenance activities on concrete public structures, the application of self-healing can potentially save millions in public economy. However, despite the existence of a large body of research on the domain, the judgement to choose one out of several potential strategies to effectively heal a crack is still met with heavy contestation. Currently, the approach to biologically heal a crack by promoting bacterial precipitation of Calcium Carbonate crystals, is deemed the most environment friendly of all. Research on this has proved that this approach is indeed successful in closing cracks up to at least 0.4mm. However, the bacteria responsible for the precipitation is dependent on the constituent precursor and the nutrients of the healing agent. The bacterial precursor that has been successfully applied so far in OPC cementitious composites is often based on lactic acid derivatives, that involve substantial costs in its production process. Recent studies have also demonstrated some incompatibility of the same precursor on low pH environments, such as that characterised by the addition of supplementary cementitious materials like blast furnace slag. For instance, a higher dosage of the lactic acid based precursors lead to negative effects in strength in blast furnace slag cements. In the Netherlands, CEMIII/B (slag cements) finds reasonably larger market share than OPC cements. As such, the incompatibility of lactic acid based bacterial self-healing agents presents a discouraging scenario.

Polyhydroxyalkanoates or PHA extracted from waste streams, have been suggested to be a low cost biodegradable polymer that can effectively replace high cost polymers such as PLA (poly lactic acid). It is also established in recent literature, that PHAs can be metabolically converted by bacterial species to form Calcium Carbonate. Besides, unlike the PLAs, these are hypothesized to be applicable in higher dosages in even low pH environments. Taking these into consideration, the current study delves into the potentials of this possible new alternative for bacterial precursor. Scientific questions and objectives based on the probable effects of the PHA on functional properties, healing efficiency, durability, sustainability and economy, were explored. It was found through a number of experimental and analytical data, that the new healing agent demonstrates ample promise to be used as an effective healing precursor for the bacterial self-healing of cement based applications. This holds true in both OPC and Slag rich cement types. With this, numerous novel possibilities are now open for further research into the large-scale application of PHA based self-healing.

*Amrita Hazarika
Delft, June 2021*

CONTENTS

Acknowledgements	v
Abstract	vii
List of Figures	xi
List of Tables	xv
Abbreviations	xvii
1 Introduction	1
1.1 Background	1
1.2 Problem definition and significance of study	2
1.3 Research questions and scope	3
1.4 Hypotheses	5
1.5 Outline of thesis.	6
2 Literature Study	9
2.1 Concept of self healing	9
2.2 Autogenous self healing.	11
2.3 Autonomous self healing	14
2.4 Bacterial self healing	16
2.5 Future of self-healing in concrete	22
3 Methodology	23
3.1 Experimental Program	23
3.1.1 Materials.	23
3.1.2 Sample preparation	24
3.1.3 Methodology.	26
3.2 Environmental and Economical assessment	33
3.2.1 Materials.	34
3.2.2 Methodology for environment assessment.	35
3.2.3 Methodology for Economic assessment	38
3.2.4 Assumptions and considerations	38
4 Results	41
4.1 Experimental Analysis	41
4.1.1 Compatibility analysis with hydration	41
4.1.2 Influence on functional properties.	42
4.1.3 Influence on healing efficiency.	43
4.1.4 Influence on degradation	48

4.2	Environmental and economical Assessment	51
4.2.1	Environmental Assessment	51
4.2.2	Economic Assessment	52
5	Discussion	55
5.1	Experimental analyses for research questions 1,2,3	55
5.1.1	Compatibility Analysis with Hydration	55
5.1.2	Influence on functional properties	56
5.1.3	Healing efficiency	57
5.1.4	Influence on degradation	58
5.2	Environmental and Economic Assessment	58
6	Conclusion	61
6.0.1	Compatibility w.r.t hydration.	62
6.0.2	compatibility w.r.t functional properties	62
6.0.3	Healing Efficiency	62
6.0.4	Influence on degradation mechanisms	63
6.0.5	Environmental and Economical Assessment	63
7	Future scope and recommendation	65
A	Appendix	77
A.1	Workability :Flow table photographs	77
A.2	Healing Efficiency.	78
A.2.1	Stereomicroscopy and Water Permeability	78
A.3	Influence on Dual Degradation Mechanisms	86

LIST OF FIGURES

1.1	Outline of the thesis	7
2.1	Publications on the topic of self-healing concrete	10
2.2	Citations garnered over the years on the topic.	10
2.3	Performance (a) and costs (b) with elapse of time for normal (A) and high quality (B) structures. Direct costs of repair included. Performance (c) and cost (d) of a structure made with self-healing material (concrete) with elapse of time. Interest and inflation ignored. (Reproduced from [25]) . . .	10
2.4	Classification of processes behind autogenous self healing, [25]	12
2.5	Permeability in never-dried concrete (a),and the same after drying-resaturating (b) [37]	13
2.6	Surface and diffusion controlled process of calcite growth [35]	13
2.7	Influence of healing strength versus water cement ratio. [28]	14
2.8	Schematic of mechanically triggered capsule-based self-healing in cementitious matrix. (Reproduced from [45])	15
2.9	Formation of calcium carbonate on bacterial cell wall. Schematic by [58] .	16
2.10	ESEM image of bacterial imprint that are found on the surface of cracks. [10]	17
2.11	Schematic of a crack-healing by concrete-immobilized bacteria. [26] . . .	18
2.12	Compounds used for studying the feasibility in 2 component bacterial self-healing in concrete. [76]	19
2.13	Effect on compressive strength development of mortar cubes containing different organic compounds [76].	19
2.14	a) Stereomicroscopic observations of cracks observed at 28 days of healing. b) Observations at 56 days of healing. These demonstrate LWA encapsulated healing in both wet-dry and underwater regimes. [77]	20
2.15	ESEM images of precipitates that were found on the surface of the crack after healing treatments a. REF specimen, b. CTRL specimen, c. B specimen submerged in water for 28 days; d. REF specimen, e. CTRL specimen, f. B specimen subjected to wet-dry cycles for 56 days; g. REF specimen, h. CTRL specimen, i. B specimen submerged in water for 28 days; j. REF specimen, k. CTRL specimen, l. B specimen subjected to wet-dry cycles for 56 day. [77]	21
3.1	Schematic of the preparation steps involved in forming the healing agent. .	24
3.2	A twin type eight channel TAM Air calorimeter with 20ml glass ampoules [4]	27
3.3	Typical isothermal conduction calorimetry curve for the hydration of ordinary Portland cement and blastfurnace slag blended cement. [5]	27

3.4	Schematic of the compatibility tests: a) Hydration curves obtained from isothermal calorimetry on paste; b) Slump formed in a flow table test for workability on fresh mortar; c) Vicat test for setting time on fresh mortar; d)Compressive strength test on hardened and cured mortar.	28
3.5	Crack induction via Instron hydraulic testing machine.[11]	30
3.6	Water permeability set-up.[11]	31
3.7	Schematic of the steps and the time-line of healing efficiency tests.	32
3.8	Schematic of the steps involved in the degradation studies. This is representative of each of the 8 prisms cast per cement type. Parts 'A' of the prism were used for carbonation studies, and parts 'B' were used for salt-frost attack studies.	34
3.9	Schematic drawing of the 4 required phases of an LCA procedure[27]	36
3.10	System Boundary for the study depicted by the red border.	37
4.1	Energy evolution in CEM I	42
4.2	Energy evolution in CEMIII/B	42
4.3	Setting times in CEM I composites	43
4.4	Setting times in CEMIII/B composites	43
4.5	Compressive strength of CEM I composites	43
4.6	Compressive strength of CEMIII/B composites	43
4.7	Workability results	43
4.8	Crack width of CEMI based control sample.	44
4.9	Crack width of CEMI based PLA-1 sample.	44
4.10	Crack width of CEMI based PLA-2 sample.	44
4.11	Crack width of CEMI based PHA-1 sample.	44
4.12	Crack width of CEMI based PHA-2 sample.	44
4.13	Crack width of CEMIII/B based control sample.	45
4.14	Crack width of CEMIII/B based PLA-1 sample.	45
4.15	Crack width of CEMIII/B based PLA-2 sample.	45
4.16	Crack width of CEMIII/B based PHA-1 sample.	45
4.17	Crack width of CEMIII/B based PHA-2 sample.	45
4.18	Reduction of the effective widths after 70 days of healing, as calibrated by optical microscopy.	45
4.19	Effective widths at days 0 and 70 of healing in control specimens.	46
4.20	Effective widths at days 0 and 70 of healing in PLA-1 specimens.	46
4.21	Effective widths at days 0 and 70 of healing in PLA-2 specimens.	46
4.22	Effective widths at days 0 and 70 of healing in PHA-1 specimens.	46
4.23	Effective widths at days 0 and 70 of healing in PHA-2 specimens.	46
4.24	Self-healing capacity of CEMI composites.	47
4.25	Self-healing capacity of CEMIII/B composites.	47
4.26	Deposition of precipitation along crack periphery	48
4.27	Deposition of precipitation across crack width	48
4.28	Clusters of precipitated crystals	48
4.29	XRD data of CEM I composites	49
4.30	XRD data of CEMIII/B composites	49

4.31 TGA data of CEM I composites	49
4.32 TGA data of CEM III/B composites	49
4.33 Observed carbonated front after pH test	50
4.34 Average depth data	50
4.35 Total mass loss across both cement types after 10 cycles	50
4.36 Progressive mass loss of the control mortars	51
4.37 Progressive mass loss of the PHBV mortars	51
4.38 Progressive mass loss of the PDLA mortars	51
4.39 Progressive mass loss of the B mortars	51
4.40 Environmental impact assessment per category. It is clear from the assess- ment that the the GWP impact of using CEMI without the healing agents, is most damaging. The same while using the healing agent, drops signifi- cantly, implying the positive effects of using the biogenic healing agent. . .	52
4.41 Total ECI of the 4 RC mix designs.	53
4.42 Economic costs of the mixes.	53
A.1 CEMI PLA-1	77
A.2 CEMI PLA-2	77
A.3 CEMI PHA-1	77
A.4 CEMI PHA-2	77
A.5 CEMIII/B PLA-1	78
A.6 CEMIII/B PLA-2	78
A.7 CEMIII/B PHA-1	78
A.8 CEMIII/B PHA-2	78
A.9 Control	78
A.10 PLA1	79
A.11 PLA2	79
A.12 PHA1	79
A.13 PHA2	79
A.14 CEMI Control 0 day	79
A.15 CEMI Control 70 days	80
A.16 CEMI PLA1 0 day	80
A.17 CEMI PLA1 70 days	80
A.18 CEMI PLA2 0 day	81
A.19 CEMI PLA2 70 days	81
A.20 CEMI PHA1 0 day	81
A.21 CEMI PHA1 70 days	82
A.22 CEMI PHA2 0 day	82
A.23 CEMI PHA2 70 days	82
A.24 CEMIII/B Control 0 day	83
A.25 CEMIII/B Control 70 days	83
A.26 CEMIII/B PLA1 0 day	83
A.27 CEMIII/B PLA1 70 days	84
A.28 CEMIII/B PLA2 0 day	84
A.29 CEMIII/B PLA2 70 days	84

A.30 CEMIII/B PHA1 0 day	85
A.31 CEMIII/B PHA1 70 days	85
A.32 CEMIII/B PHA2 0 day	85
A.33 CEMIII/B PHA2 70 days	86
A.34 CEMI Control	86
A.35 CEMI PHA	86
A.36 CEMI PLA1	86
A.37 CEMI PLA2	86
A.38 CEMIII/B Control	86
A.39 CEMIII/B PHA	87
A.40 CEMIII/B PLA1	87
A.41 CEMIII/B PLA2	87
A.42 CEMI Control	87
A.43 CEMI PHA	87
A.44 CEMI PLA1	88
A.45 CEMI PLA2	88
A.46 CEMIII/B Control	88
A.47 CEMIII/B PHA	88
A.48 CEMIII/B PLA1	88
A.49 CEMIII/B PLA2	88
A.50 Mass loss, day 1	89
A.51 Mass loss, day 3	89
A.52 Mass loss, day 7	89

LIST OF TABLES

3.1	Healing agents used in the study	24
3.2	Mix design variations and abbreviations used for the compatibility studies. The w/c ratio was kept constant at 0.5 for all tests. For mortars, the cement:sand:water ratio was 1:3:0.5 by mass.	28
3.3	The mix designs considered for the environmental and economic analyses	35
3.4	11 impact categories, their definitions and their shadow prices[28]	37
4.1	Calculation of the ECI against 11 impact categories	52
4.2	Material costs without Healing Agent.	53
4.3	Cost of healing agent excluding labour, transportation and energy costs.	53
5.1	Reductions observed in 11 impact categories due to addition of PHA based healing agent.	59

ABBREVIATIONS

SHA	Self-Healing Agent
HA	Healing Agent
PLA	Poly-Lactic-acid
PHA	Polyhydroxyalkanoates
CH	Calcium Hydroxide
CSH	Calcium-Silicate-Hydrate
OPC	Ordinary Portland Cement
BFSC	Blast Furnace Slag Cement
TGA	Thermogravimetric Analysis
XRD	X-Ray Diffraction
ESEM	Environmental Scanning Electron Microscopy
OM	Optical Microscopy
RCC	Reinforced cement concrete
RC	Reinforced concrete
SHC	Self-Healing Capacity
LCA	Life Cycle Assessment
ECI	Environmental Cost Indicator

1

INTRODUCTION

1.1. BACKGROUND

When we address the growing consciousness behind enhancing the service life of our concrete infrastructure, we invariably imply upgrading its durability. Concrete, by far, has been a reliable construction material, but because of its characteristic and quite unavoidable cracking phenomenon, it ages and degrades. Over the current century, this has led to heightened concerns related to structural health and safety, along with an unprecedented surge in service and maintenance costs of infrastructure world over. In Europe, in the past decade, a conservative cost estimate of replacing just highway structures alone, amounted to €600 Billion whereas an additional €2 to 3 billion was spent annually on their upkeep [1]. At the same time in the US, annually about €18 billion was needed for repair and retrofitting of civic infrastructure, and €1.6 trillion was projected for repairing or replacing infrastructure in Asia [2, 3].

Besides the immense economic impact associated with repair and maintenance of constructions, the production of cement is also single handedly responsible for up to 8% of global anthropogenic CO₂ emissions. With escalating demand on new public constructions in fast growing economies like India and China, and the burgeoning repair activities in developed nations, the concerns related to socio-environmental costs have become equally alarming as of 21st century. All in all, this calls for an urgent intervention not only in the technology behind producing our built infrastructure, but also one that ensures their longevity.

Notwithstanding the massive research and developmental advances in the field of concrete durability, the problem of ageing and degradation due to cracks in concrete still remain unresolved. In the past decade, numerous studies have therefore been devoted to the concept of self-healing of concrete infrastructure. These studies demonstrate the possibility of future civil infrastructure that, via a multitude of likely approaches, is smart enough to detect its own damage and undergo repair by itself. This then would drastically reduce dependence on human intervention and the associated economic, social and environmental costs after damage initiation. Thus, self-healing of concrete holds

significant promise towards sustainably addressing the issues of damage associated with cracking

The self-healing approaches studied and implemented so far, are varied. They range from traditional autogenous self-healing of concrete, wherein the concrete demonstrates an intrinsic healing ability, to introduction of stimulated autogenous healing via mineral additives, super absorbent polymers, and to autonomous healing via minerals and bacteria. Of these, autonomous healing via bacterial metabolic precipitation of CaCO_3 crystals represents a biogenic self-healing technology and is deemed to be a potentially environment-friendly approach. This forms the broader subject of my current study.

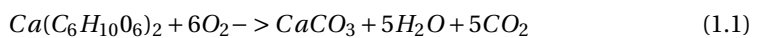
1.2. PROBLEM DEFINITION AND SIGNIFICANCE OF STUDY

In 2007, Dr. Jonkers introduced a two component biogenic healing agent at TU Delft [4]. These are:

- Alkali resistant, spore-forming bacterial strain that has a high carbonate production capacity
- A mineral precursor compound or food.

In practice, these are usually packed with growth vitamins or nutrients for the spores, like yeast extract. In addition to being a source of nutrient for bacteria germination and growth, it has also been suggested that the addition of YE improves calcium carbonate precipitation [5]. All these are incorporated as a package, into the concrete during the mixing stage. Upon hardening and cracking of concrete due to shrinkage or other crack initiating mechanisms, ingress of water via the cracks help activate the otherwise dormant bacterial spores. Upon activation, the spores metabolically convert the mineral compounds into calcite like crystals that deposits along the cracks. Accordingly, the cementitious matrix becomes denser and resistant against the transport of undesirable compounds (like chlorides, sulfates, etc) that cause degradation [6], [7]. This is the general concept of the biogenic healing mechanism.

In the past decade, several studies have successfully demonstrated the feasibility of using lactic acid derivatives, such as calcium lactates, as a mineral precursor [7], [8], [9], [10]. Lactic acid is a good source of carbon required for microbial metabolism of bacteria. Under alkaline pH, poly lactic acid are hydrolyzed to form lactic acid units that can be converted to CaCO_3 and CO_2 via bacterial metabolic activity [as shown in equation 1.1]. The produced CaCO_3 crystals fill the crack and provide water tightness to the matrix. CO_2 further reacts with portlandite (CH) available in the cementitious matrix, to produce additional limestone. This second reaction mirrors the carbonation reaction typically observed in OPC systems. Thus, it appears to be an effective strategy to further densify the microstructure. In addition to reducing water permeability, the presence of calcium lactate has also been demonstrated to increase the compressive strength of mortars by up to 10% [11], [12].



However, the above holds true only in OPC, or CEMI as it is called in the Netherlands. In slag-rich cements, or CEMIII/B, as is typically used in the Netherlands, the

amount of CH in the system is limited which leads to a lower pH environment than in OPC. Since calcium lactate derivatives need high pH alkalinity to be hydrolyzed and then become available for bacterial metabolic conversion, their reaction in CEMIII/B yields much lower CaCO_3 production. Further, the CO_2 that is produced as a byproduct reacts with CSH in the absence of CH, thereby resulting in an open microstructure and substantially high surface water absorption. Studies have also shown a unacceptably reduced compressive strength (50% lower) in blast furnace slag cements that contained calcium lactate based healing agents [9]. Furthermore, calcium lactate is produced via homoplastic fermentation of sugars. It undergoes a complex purification process that is associated with exceptionally high costs, apart from also producing large amount of chemical effluents, like calcium sulfates [13]. The production process of calcium lactate is therefore economically and environmentally rather unviable.

The aim of the current study is to find a viable alternative that is able to overcome these limitations of calcium lactate based precursors. The focus is on checking Polyhydroxyalkanoate (PHA), an alkanooate based derivative, that is extracted from waste streams, for its potential as a healing precursor in cementitious composites.

PHA is a known biodegradable polymer that is increasingly being researched as a desirable substitute for synthetic plastics. It is produced by microorganisms under imbalanced growth condition due to carbon source surplus and/or limitation of essential nutrient such as phosphorus and nitrogen [14], [15]. Several studies demonstrate the feasible utilization of industrial and bio mass waste streams as carbon source/feedstock for microbial growth, in order to produce PHA [15], [16], [17], [18]. These advances can substantially offset the otherwise high cost associated to carbon sourcing in the production of PHA. Additionally, this also leads to recycling of agro-industrial wastes which implies that the production process and application of the potential healing precursor in cementitious composites, is already more circular compared to its calcium based predecessors.

Functionally, unlike the PLA, PHA does not require to undergo chemical hydrolysis in high pH to be available for bacterial metabolic activity. They can be enzymatically hydrolyzed by bacteria. As such it is hypothesized to perform better in low pH environments as in CEMIII/B in comparison to calcium lactate derivatives. Upon crack initiation and activation of bacterial spores by ingress of water, PHA can be readily available for metabolic conversion into CaCO_3 . Preliminary studies on this have demonstrated promising compatibility of PHA with blast furnace slag cements. This study is an attempt to investigate further, the compatibility of PHA with cementitious composites made of both OPC and BFSC cement types and the influences on functional, healing, and durability properties of varying mix designs. To that end, the following research questions have been sought to be answered through the investigation.

1.3. RESEARCH QUESTIONS AND SCOPE

The following six research questions are examined through the current study:

1. **Research question 1:** *What is the compatibility and influence of the new healing precursor with CEM I and CEM III/B, with respect to rate of cement hydration, workability, setting time and compressive strength?*

- **Objective:** To study the heat of hydration curves, via isothermal calorimetry, of the healing agent based composites and compare the same with that of a reference composite. From these curves, the rate of hydration can be studied. Further, two fresh state and one hardened state properties, viz., workability, setting time, and compressive strength respectively, are investigated with experiments adopted from standards.
2. **Research question 2:** *What is the healing efficiency of the new precursor in comparison to PLA based precursors?*
 - **Objective:** Quantification of the crack-sealing potential with respect to watertightness after healing. This will be conducted with a water permeability test. Healing characteristics of an artificially induced crack are to be analysed both quantitatively and qualitatively with the aid of Electron Scanning Microscopy (ESEM) and Optical Microscopy (OM).
 3. **Research question 3:** *What is the effect of healing agent addition on the two concrete degradation mechanisms of carbonation and salt-frost attack?*
 - **Objective:** The aim is to investigate the dual-degradation mechanisms of carbonation and salt-frost attack on composites containing healing agents and those without. Physical (natural carbonation, pH test, freeze thaw cycles) and characterization tests (TGA, XRD) are undertaken to arrive at an answer to the research question.
 4. **Research question 4:** *What is the environmental and economical impact potential of adding the new healing agent in reinforced concrete structures?*
 - **Objective:** To test possible reduction in environmental impact costs and economic impact upon using the proposed healing agent in real-life applications.
 5. **Research question 5:** *Is the quality of produced healing agent batches stable with respect to functional performance properties?*
 - **Objective:** To check if varying batches produce near-consistent results for the first two research objectives. Since, the raw materials of the proposed healing agent are derived from bio-mass from waste streams, their properties are dependent on the contents present in the latter. This is often not consistent.
 6. **Research question 6:** *What is the functional property, healing and durability performance of the proposed healing agent with respect to the currently commercially available lactate derived healing agents?*
 - **Objective:** To check for potential discrepancies in test data for the first 3 research questions..

1.4. HYPOTHESES

To investigate for the above research questions, the following hypotheses have been made.

1. **Compatibility with respect to hydration:** As explained in section 1.2, because the new HA does not necessarily require alkaline activation for metabolic conversion by bacteria, it is potentially more compatible than lactate based derivatives, in low pH environments in low clinker cements. The heat evolution of hydration is not expected to deviate substantially upon addition of new healing agent in both the cement types.
2. **Compatibility with respect to functional properties:** Since PHA is not necessarily dependent on alkalinity for metabolic conversion in contrast to PLA, their performance, or rather their influences, in low pH matrices are expected to be disparate. It is expected that the microstructure will be denser and strength behavior will be better for PHA based slag systems than what was observed by [9] for PLA. However, possible presence of air-entrainment upon addition of PHA and PLA is suspected, as both biopolymers are known to be employed as "pore-forming agents" in cementitious mixtures [19]. If these healing agents do administer additional air voids, they will affect the compressive strength negatively. This might offset the positive effect of the healing agents densifying the microstructure.
3. **Healing efficiency:** Studies on the subject of PHA decomposition show that PHA can be decomposed or consumed by microbial activity given that a specific extracellular PHA depolymerases is secreted [20], [21]. In another study [22], the *B. Cohnii* related bacterial strains, the ones used also for bacterial SHC, were stated to secrete the extracellular PHA depolymerases to metabolically convert PHA. A recently concluded study by [23] further confirmed this to be true. As such, the metabolic conversion and consequently the crack healing capacity of the new HA can be hypothesized to be comparable to other bacterial precursors in CEM I. In CEMIII/B, the healing efficiency of new proposed HA is expected to be better than PLA, because of the reasons stated previously.
4. **Influence on degradation mechanisms:** In OPC systems, because of a potential increase in water tightness and densification owing to crack healing by the new HA, porosity induced degradation mechanisms such as carbonation, salt scaling by freeze thaw, and corrosion -both chloride and carbonation induced, is expected to be much lower. In BFSC, it is expected that the new HA will perform better in terms of densification by metabolic reaction, compared to calcium lactate based HA.

Additionally, a preliminary characterization study of a cement microstructure containing the new precursor, demonstrated the presence of well distributed, round air voids in the matrix. Presence of upto $\pm 0.5\%$ air voids were detected in PHA based composites, compared to the control. This could lead to a reduction of compressive strength, but also could imply higher resistance capacity against salt frost damage according to the "glue-spall" mechanism of salt scaling [24]. It is therefore

hypothesized that the entrained air voids could possibly resist salt scaling better than reference samples and former HAs.

5. **Environmental and economical impact:** In RCC, steel reinforcements are added to resist tensile cracking of concrete. If the new HA has comparable healing capacity to PLA based HAs, then it might be able to heal cracks upto 0.4mm or beyond. Thus, if incorporated in real life applications, the HA would potentially be able to make a structure adaptive to heal cracks upto at least 0.4mm. This would then imply lesser dependence on crack-restraining steel reinforcement for cracks up till the aforementioned sizes. This would mean substantial monetary savings in constructions. Apart from that, since the production process of PHA is more circular, the possible use of HA instead of steel would imply much lower environmental footprint comparatively. The economic and environmental costs analyses of the new HA are therefore expected to yield favorable outcomes in comparison to traditionally used lactate derivatives.

1.5. OUTLINE OF THESIS

The study is presented in the following manner:

Chapter 1 introduces the research background, the topic definition, significance of the study, research questions and the related hypotheses.

Chapter 2 presents a thorough literature survey on the topic of SHC, the varied approaches, their drawbacks and future scope in the field of SHC.

Chapter 3 presents the methodology of the experimental program and the environmental and economic assessments followed to investigate and answer the research questions of this study.

Chapter 4 presents the results obtained and post processed from the experimental program, as well as the environmental and economic assessments.

Chapter 5 presents discussion of the results from the previous chapter.

Chapter 6 summarizes the conclusion of the study.

Chapter 7 presents future scope of this research.

The following flow-chart presents an outline of the study.

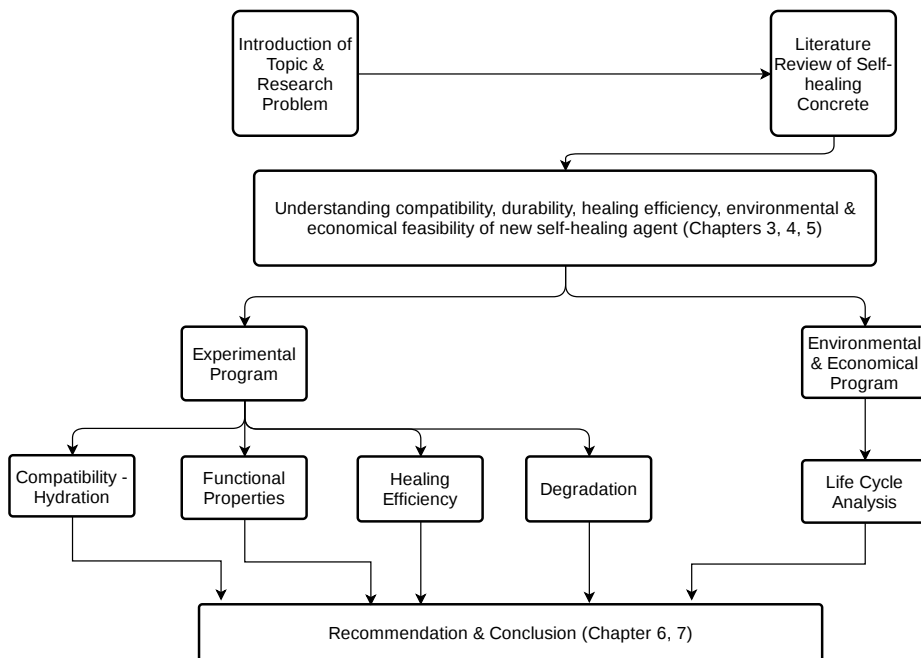


Figure 1.1: Outline of the thesis

2

LITERATURE STUDY

2.1. CONCEPT OF SELF HEALING

Rooij et al.[25] define self-healing materials as *man-made materials, which have the built-in capability to repair structural damage autogenously or with the minimal help of an external stimulus*. The numerous studies conducted on the topic of embedding this phenomena in cement based composites, demonstrate possibility of future civic infrastructure that, via a multitude of likely approaches, are smart enough to detect their own damage and undergo healing or repair by themselves. This then would drastically reduce dependence on human intervention and the associated economic, social and environmental costs after damage initiation. This therefore has piqued an escalating research and development interest on the topic of self-healing concrete within the last 50 years. The drive to make our structures smarter and more resilient towards damage has led to an evolution of varying engineered approaches in the said technology, especially in the last decade. Figures 2.1 and 2.2 show the growing scientific interest in the field. These data have been collected from *Scopus* under the phrase 'self-healing concrete' for the years 2010-2021.

The performance comparison of a structure equipped with self-healing technologies versus a structure without it, can be better gauged with the curves demonstrated in figure 2.3 [26]. Over time, as cracks appear on concrete structures and degradation initiates, the first repair becomes necessary (shown in a) to maintain the required level of strength. Thereafter, depending on the quality and the subsequent durability of the repair work, a second repair is usually required within a span of 10-15 years. The total costs (shown in b) at the end of service life of the structure, rise progressively, depending on the frequency of the repair and maintenance activities needed over the years. Comparatively, in a self-healing concrete structure (shown in c and d), the occurrence of crack is followed by self-healing, which is why the total costs of such a structure can be projected to remain constant over the years. However, the initial costs of such a structure would be higher because of additional functionalities provided to it, compared to normal structures. Nevertheless, the elimination of frequent repair and maintenance demands would

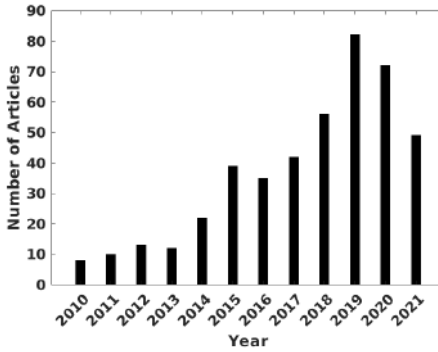


Figure 2.1: Publications on the topic of self-healing concrete

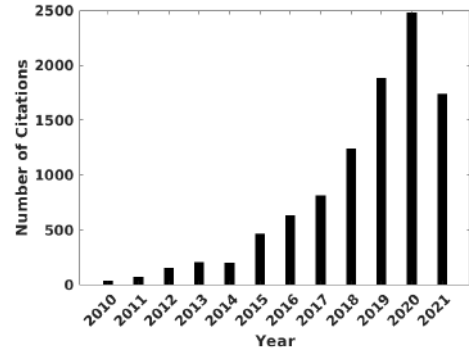


Figure 2.2: Citations garnered over the years on the topic.

prove to be financially beneficial for the owners. Thus, self-healing of concrete holds significant promise towards sustainably and economically addressing the issues of damage associated with cracking and ageing.

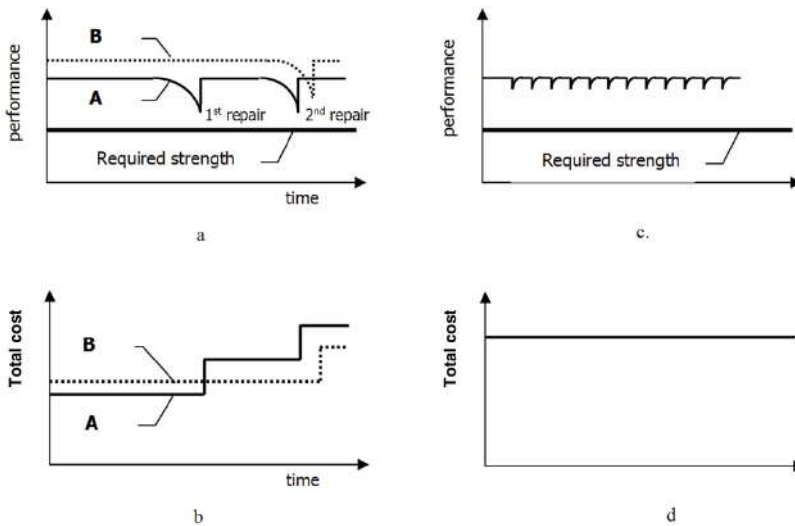


Figure 2.3: Performance (a) and costs (b) with elapse of time for normal (A) and high quality (B) structures. Direct costs of repair included. Performance (c) and cost (d) of a structure made with self-healing material (concrete) with elapse of time. Interest and inflation ignored. (Reproduced from [25])

The self-healing approaches studied and implemented so far, are varied. They range from traditional autogenous self-healing of concrete, wherein the concrete demonstrates an intrinsic healing ability, to introduction of stimulated autogenous healing via mineral additives, super absorbent polymers, and to autonomous healing via minerals and bacteria [5], [27]. The Rilem committee [25] proposes the following concise classifica-

tion, using which the entire field of self-healing can be described: autogenous and autonomous or engineered self healing. Bacterial self-healing, which is the topic of the current study, is categorised into autonomous classification. The following sections shed more light into the mechanisms and approaches of self-healing in concrete.

2.2. AUTOGENOUS SELF HEALING

Autogenous self healing is the process by which concrete intrinsically heals its own micro-cracks without external intervention. The observation and investigation into the mechanisms by which concrete can seemingly mimic natural healing as in tissues of living organisms, have been conducted since the early 19th century. In 1836 when it was first observed by the French Academy of Science, the white crystalline deposits in the cracks of concrete water retaining structures were reported to be calcium carbonate (CaCO_3) [28]. Early literature pertaining to the physicochemical analyses of the phenomenon indicate that CaCO_3 in the fractured concrete results either as a product of an ongoing hydration reaction between unhydrated cement grains and water [29], [30], [31], or the (carbonation) reaction between calcium hydroxide ($\text{Ca}(\text{OH})_2$) and atmospheric carbon dioxide (CO_2) [32]. Besides, Clear [33] from his investigation on effect of autogenous healing on permeability, found that the initial reduction of permeability is more likely to be a result of mechanical blockages of cracks by water-borne debris. Over time, the 5 mostly cited explanations offered by subsequent studies into the phenomenon were [34]:

1. Further hydration of the concrete.
2. Expansion of the concrete in the crack flanks.
3. Crystallization of calcium carbonate.
4. Closing of the cracks by solid matter in the water.
5. Closing of the cracks by spalling-off loose concrete particles resulting from the cracking.

Rooij et. al[25] [32] later condensed these into 3 main categories: physical (point 2), chemical (points 1 and 3), and mechanical (points 4 and 5), as depicted in figure 2.4. Among these processes, Edvardsen in 1999[35] and Neville in 2002 [36], postulated that crystallization of calcium carbonate within cracks is the primary mechanism for autogenous healing in mature concrete. Crystallization of calcium carbonate can result either from the chemical reactions between the calcium ions from concrete matrix and the carbonate ions in pore solution, or carbon dioxide available in the air entering the crack [5]. For this, the availability of water is a necessary criterion, including the presence of carbonates or bicarbonates [36].

The quantification and influence of autogenous healing on the durability and mechanical properties in fractured concrete was investigated under a variety of influences. The influence of age, mix properties, type of cement, curing conditions on autogenous healing were studied first by Lauer and Slate [28]. They reported that the presence of lime or fly-ash lowers the healing strength when samples were cured under water, but

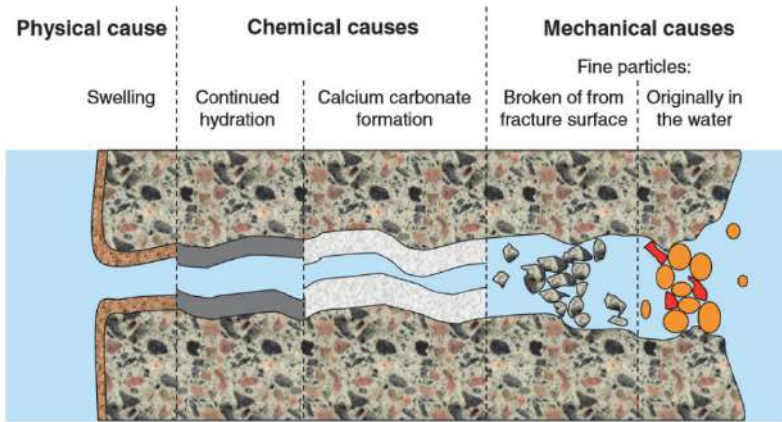


Figure 2.4: Classification of processes behind autogenous self healing, [25]

little impact was observed when curing was done in atmosphere with 95% RH. They also reported an increased healing with higher w/c ratio and that the presence of water is essential to obtain maximum healing strength (figure 2.7). On the other hand, [Dhir1973] showed that the ability of autogenous self-healing increased with a higher cement content and was more intensive at early age of hydration. Hearn and Morley [37] after conducting permeability tests on 26-year old concrete samples, reported that drying and re-saturation results in substantial enhancement of self-healing behavior in mature concrete (Figure 2.5). Shrinakge cracking was reported to make the self-sealing more pronounced as it enables previously unexposed hydrates to come into contact with pore water. In a subsequent study [32], Hearn states that the effect of continued hydration on reduction of permeability is insignificant in concrete, unless at an early age. Edvardsen [35] conducted permeability tests on plain concrete and found that presence of water in the initial 5 days was crucial for the occurrence of self healing. He further established that the growth rate of CaCO_3 crystals in the cracks was dependent on crack width and water pressure, while concrete composition and type of water had no major influence on the rate of healing. Additionally, he found that there were two different growth process of crystals - the early surface-controlled and the late diffusion-controlled as depicted in figure 2.6. Further, the location of the CaCO_3 crystals depends on the temperature, pH value, CO_2 , partial pressure, and saturation index of calcite and on the concentration of Ca^{2+} and CO_3^{2-} ions. Reinhardt and Jooss [38] also conducted permeability tests and reported that the decrease of the flow rate depends on crack width and temperature and that a higher temperature favors a faster self-healing process.

As far as composition of the healing products is concerned, Lauer and Slate [28] reported that bonding materials formed in the cracks were 100% CaCO_3 . This however was found to differ in the study conducted by [39]. In this study, the presence of ettringite and portlandite was detected in cracked high-strength concretes subjected to freeze/thaw condition. In later studies, C-S-H were detected cracks after cracked samples were cured in water [40]. Further supporting the findings of [35] regarding CaCO_3

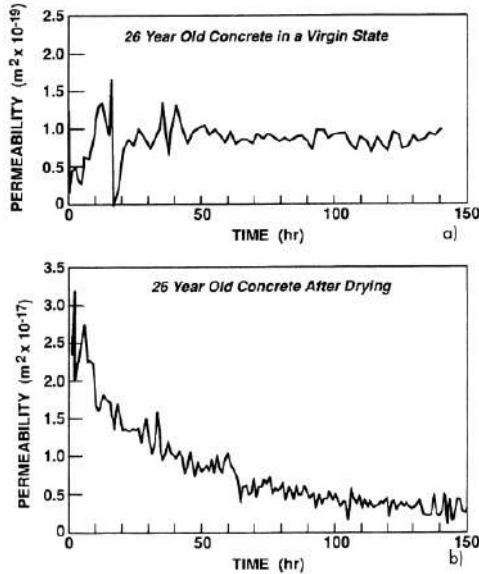


Figure 2.5: Permeability in never-dried concrete (a), and the same after drying-resaturating (b) [37]

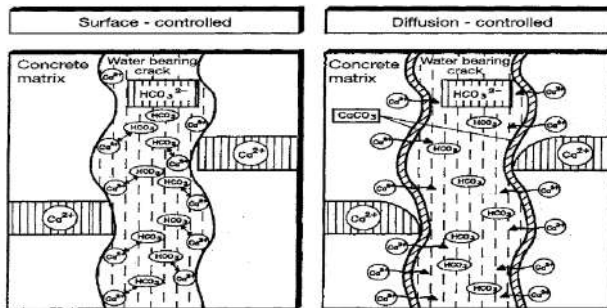


Figure 2.6: Surface and diffusion controlled process of calcite growth [35]

crystals in cracks,[41] stated that such formations could also be observed in slag cements. They also report that the width of crack is crucial for extent of healing as smaller cracks are easier to heal. The exact composition of healing appears to be inconsistent with findings which can be a challenge to fully understand the mineralogy of the healing agents.

Another challenge of autogenous self healing is with regard to slag cements. In these cements a high amount of slag particles that do not react early on, are later available for continuation of hydration and can aid in autogenous healing. However, the consumption of portlandite by slag reduces the chances of calcium carbonate precipitation which in turn could deter autogenous self-healing in such systems [42]. Finally, the cracks widths that can be effectively healed by autogenous healing is limited to 10–100 μm, and

sometime up to 200 μm but less than 300 μm , only in the presence of water [5]. Healing of larger cracks therefore needs external intervention. Nevertheless, autogenous self healing is the safest, most economical and environment friendly healing mechanism when compared to other mechanisms [43].

2

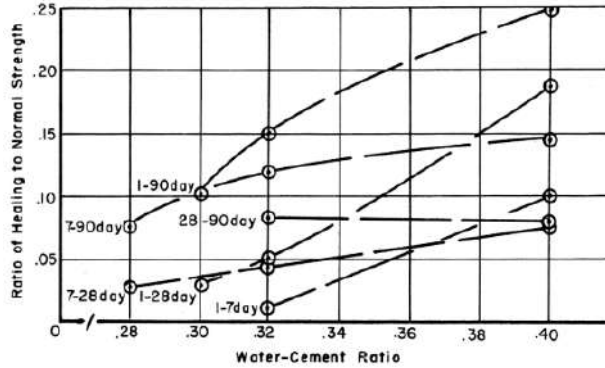


Figure 2.7: Influence of healing strength versus water cement ratio. [28]

Hence, to overcome its shortcomings and to enhance the efficiency of autogenous self healing of concrete, use of additives such as fibres, minerals such as fly-ash and silica fume, crystalline admixtures, superabsorbent polymers and other expansive minerals such as MgO, Bentonite clay have been explored [27]. These additives limit the crack width, provide water, or enhance hydration and/or crystallization. The autogenous healing process is then called *stimulated* or improved, as these additives help override its limitations. [5] [43], [44].

2.3. AUTONOMOUS SELF HEALING

In autonomous healing systems, active healing material are encapsulated into the cementitious matrix. These encapsulations upon being triggered mechanically, physically or chemically, release the cargo to the damaged area or the region that needs material recovery, as shown in figure 2.11 [45]. The maximum reported crack width that can be healed by autonomous healing is 0.5mm [46]. The successful working of this system however is governed by a variety of factors, such as compatibility of the encapsulation to both concrete and healing agent, trigger mechanism, cargo release rate, and repeatability of healing [5], [27]. DeBelie et al. [5], in their comprehensive review of autonomous healing classifies encapsulation into three distinctions, based on geometrical proportions: microencapsulations (<1mm), macroencapsulation, and vascular encapsulation. Depending on the material of shell, type of healing agent and technique of encapsulation, further classifications are offered by [47] and [48]. The type of trigger popularly adopted for these microcapsules is mechanical [45] although few studies have reported successful chemically stimulated encapsulated healing [49], [50]. The success of encapsulated autonomic healing can be gauged with respect to its ability to recover mechanical properties and durability of the cementitious matrix after damage

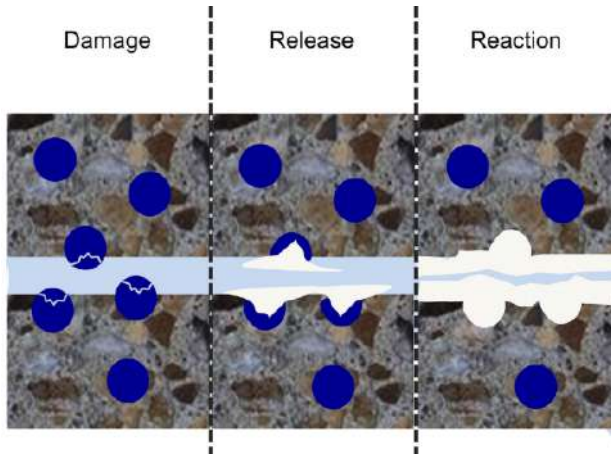


Figure 2.8: Schematic of mechanically triggered capsule-based self-healing in cementitious matrix. (Reproduced from [45])

initiation. The common properties affected by the use of encapsulated additives include compressive strength, flexural strength, water permeability, chloride diffusion and capillary absorption. There exists a significant body of research that attempts to investigate these properties. However, despite most of these studies reporting improved water-tightness upon addition of healing agents, find varying results for mechanical properties. For instance, [51] studied poly(phenol–formaldehyde) (PF) microcapsules and found that by incorporation of 4% microcapsules into cement paste, the strength decreased 32% from 7.4 kN to around 5 kN. [52] developed a system of concentric glass capsules and found that samples immersed in water had a strength recovery of upto 25% and a healing efficiency of upto 95%. [53] reported that 2% crystalline sodium silicate in polyurethane-encapsulated microcapsules with a diameter ranging from 40 to 800 m increased 24% mechanical load recovery compared to 12% in the control samples. [54] tested on gelatin–acacia gum as shell material and reported they decrease the strength by 25%. Nevertheless, they are able to survive mixing with cement and rupture successfully upon crack formation and release sodium silicate solution.

Polymeric capsules are potentially easier to produce due to lower processing temperatures, and the possibility for integrated extrusion, filling, and sealing steps [5]. On the other hand, the vascular method offer significant advantages over microcapsule as the healing agent can be continually supplied all across the matrix, using this approach. Microfluidics as an encapsulation technique is also now a popular investigated topic. This double emulsion template, a wide variety of shell materials can be explored, and the properties can be modulated to fine tune payload, permeability and shell properties of the microcapsules [45].

Regardless of the apparent benefits, these approaches for encapsulation need however answer the economic and sustainability in the construction sector. [55] used a polymer encapsulated polyurethane (PU) precursor to study the life cycle costs in SimaPro involving 10 environment impact categories. He reported that upto 72–78% reduction

in impact was enabled, mainly due to the service life extension possible with a properly working self-healing concrete. In another, cradle-gate study [56] involving (semi-)synthetic SAPs and 2 v% of polypropylene (PP) or polyvinyl alcohol (PVA) microfibre, they conclude that CML-IA impacts of 1m% SAP range between 4 and 52% of the cement impact. The highest impacts were recorded for semi-synthetic SAPs, due to high energy use during drying. They also suggest that PVA microfibre should be avoided since addition of 2 v% (= 26 kg/m³) can easily induce significantly higher CML-IA impacts than 572 kg cement. Studies involving thorough life-cycle cost assessment are scant in the field of self-healing concrete. This is majorly because autonomous healing is an evolving branch and the full extent information of upscaling or real-life applications are difficult to gather in order to calculate end of life impacts. The consensus so far is that, if 100% crack healing efficiency could be assumed, environmental impacts as well as service life costs remain lower than those of traditional concrete.

2.4. BACTERIAL SELF HEALING

The introduction of bacterial spores for the purpose of enabling self-healing of concrete, delivered the much needed breakthrough for the field. This mechanism involves the selective deposition of microbiologically induced Calcium Carbonate precipitates, for remediation of micro-cracks. Existing literature on the topic are suggestive of its potential as an environmentally safe method and one that can assure long-lasting crack repair in cementitious composites [57], [5], [58], [59], [25], [26]. Early researchers on the topic [60], [61] observed the ability of microbiological species that demonstrated improved selective plugging when sprayed or applied in porous cementitious composites. Building on top of these initial, promising researches, the feasibility of using bacterial species in terms of influence on functional properties and durability of concrete was checked by [62], [63] and [64] in the early 2000s. They observed deposition of dense layers of calcium carbonate in cracks and a consequent increase of water-tightness of the cementitious matrices. These studies studied with ureolytic strains of bacteria that necessitated substrates made of urea and calcium chloride that were applied externally to the damaged concrete.

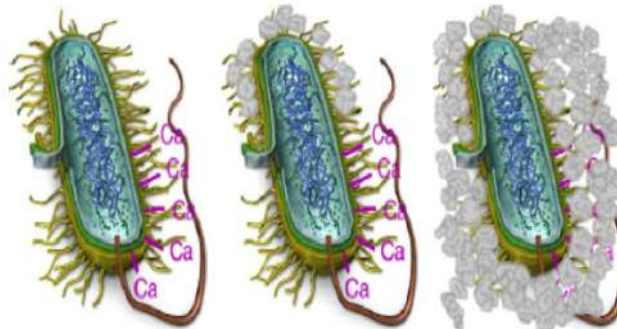
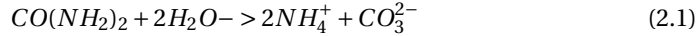


Figure 2.9: Formation of calcium carbonate on bacterial cell wall. Schematic by [58]

The bacterial species *Bacillus pasteurii*, *Bacillus sphaericus*, *Bacillus megaterium*

and *Sporosarcina ureae* belong to the group of ureolytic strains than decompose urea into ammonium and carbonate ions [5]. This approach to bacterial self-healing has been extensively studied by several researchers to be quite effective in improvement of watertightness and recovery of strength of damaged concrete [65], [66], [67], [68], [69], [70]. The reaction mechanism of ureolytic bacterial metabolism is shown in equations 2.1 and 2.2.



Another approach that was studied simultaneously in this period is denitrifying bacterial approach. For this, the bacterial species *Pseudomonas denitrificans* and *Castellaniella denitrificans* are used [5]. This could facilitate the functioning of microbial healing under low oxygen conditions. Although less precipitation yields were possible through this pathway compared to the ureolytic pathway, yet repetition of yields were achieved. [71] notes in their report that both ureolytic and denitrifying pathways produce massive amounts of ammonia and nitric oxide which are both harmful in different ways. Ammonia could drastically increase risk of reinforcement corrosion when it is oxidised to nitric acid by bacteria [72].

Jonkers and Schlangen [73] introduced the use of specialized alkaliphilic bacterial spores of species *Bacillus cohnii*, and *Bacillus pseudofirmus*, and an organic compound based healing to facilitate autogenous self-healing potential under aerobic conditions. This metabolic pathway based on organic calcium salts instead of urea hydrolysis, prevents the possible detrimental effect of the latter [72]. Since the scope of the current study is confined to aerobic bacterial pathway, the advances made on this, and very specifically those made in the TU Delft, have been emphasized. The two-component

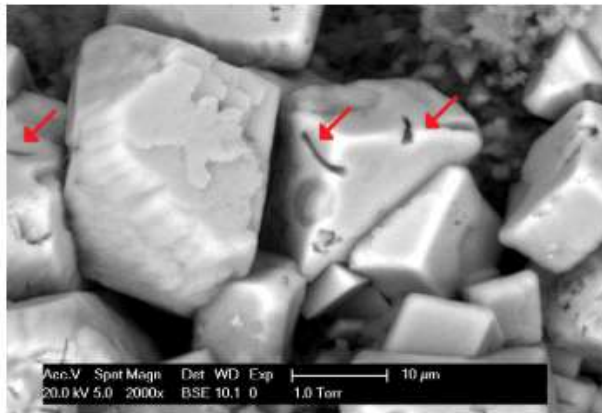
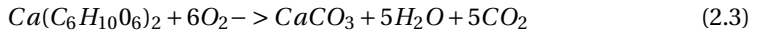


Figure 2.10: ESEM image of bacterial imprint that are found on the surface of cracks. [10]

healing agent were mixed with fresh cement paste, thereby becoming part of the subsequent concrete composite [74]. These bacterial spores when first administered into concrete mixes, remain as metabolically inactive and survives the surrounding of highly

alkaline concrete matrix. The organic compounds that they are used as substrates for these spores can be metabolically converted once the spores are activated by the water entering through the cracks.



Carbonate crystals that are produced through the above equation, are used to plug open cracks. The carbon dioxide produced along with it, further reacts with hydration product portlandite (CH), to produce even more calcium carbonate according to the following equation.

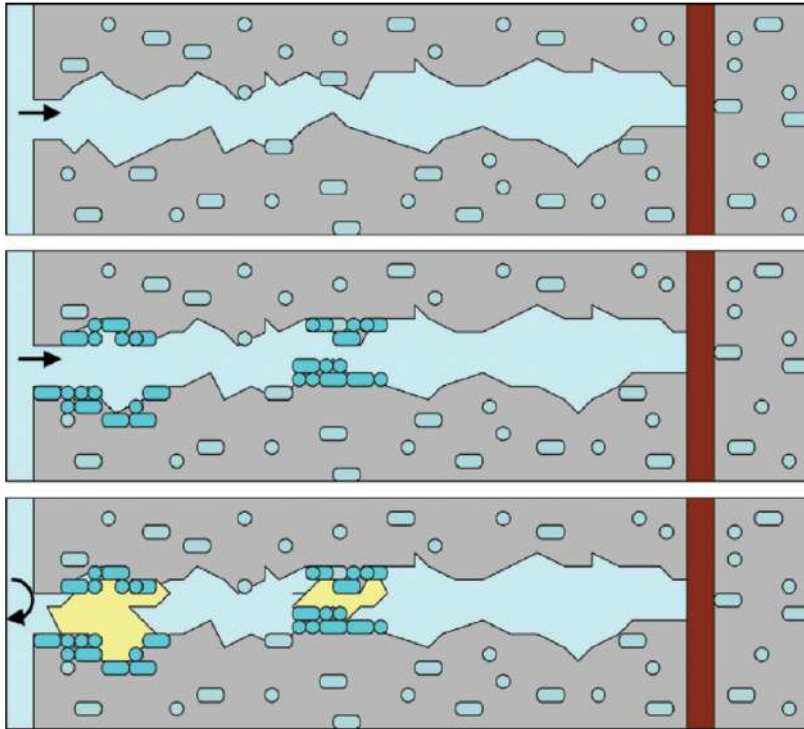
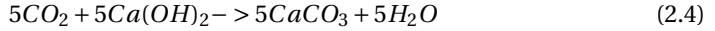


Figure 2.11: Schematic of a crack-healing by concrete-immobilized bacteria. [26]

In a following study [71], the compatibility of various organic compounds, such as yeast extract, peptone, calcium acetate and calcium lactate was tested for use as a precursor for the bacterial species. It was reported that only calcium lactate demonstrated in an positive effect (10% increase) on strength, whereas the rest proved unfavorable for the same. Palin et al. [75] found that for application of this two-component bacterial healing agent in marine environments, four organic precursors appear most feasible - magnesium acetate, magnesium lactate, saccharin sodium and gum Arabic. Other

organic compounds tested in following projects [76] are shown in figure 2.12 and 2.15. These studies report the the feasibility of magnesium acetate as a cost-effective concrete

Organic compound	Cost (€.kg ⁻¹)
(+)-Magnesium L-ascorbate	1
Carrageenan	2
Chitosan	2
D-(+)-Xylose	1
D-sorbitol	1
Glycerol	1
Gum arabic	1
L-Rhamnose	0.6
Magnesium D-gluconate	0.6
Magnesium L-lactate	1
Magnesium acetate	0.1
Maltodextrin	0.3
Pectin	1
Saccharin sodium	1

Figure 2.12: Compounds used for studying the feasibility in 2 component bacterial self-healing in concrete. [76]

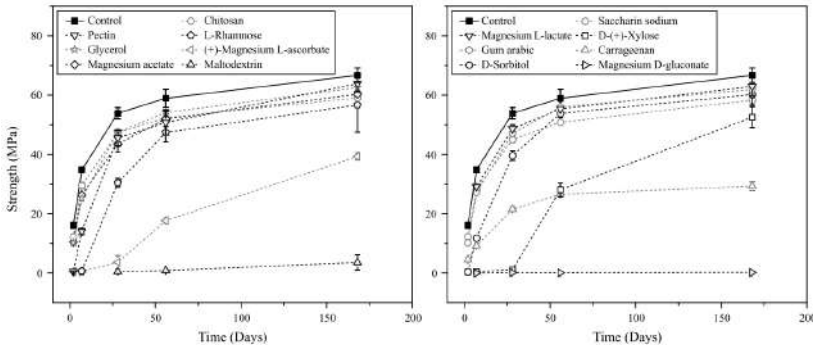


Figure 2.13: Effect on compressive strength development of mortar cubes containing different organic compounds [76].

compatible organic mineral precursor. On the other hand, from past researches and new investigations, [9] and [12] propose that lactate acid derivatives such as calcium or sodium lactate or polylactide, can be more effectively used as an organic precursor for bacterial self healing systems, in large scale or commercial OPC applications as it shows negligible influence on mortar strength development. Besides, it also demonstrated remarkable (almost 3 times) improvement of water-tightness compared to control samples. It also led an enhanced reduction of water absorption by concrete surface.

Additionally, [77] reported that the calcium lactate, which is usually quite soluble in water, can stay undissolved in cementitious matrices, until bacterial spores are activated and initiate their metabolic activity. [9] also checked the possible reduction of environ-

2

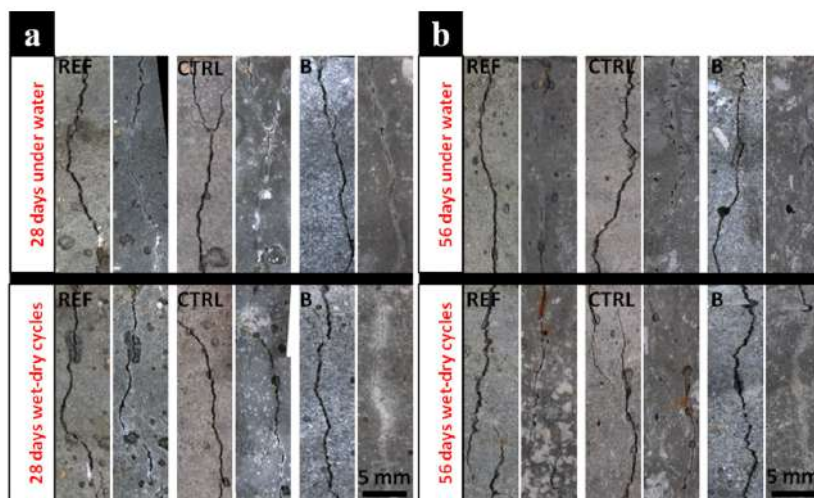


Figure 2.14: a) Stereomicroscopic observations of cracks observed at 28 days of healing. b) Observations at 56 days of healing. These demonstrate LWA encapsulated healing in both wet-dry and underwater regimes. [77]

mental and economical burden upon using calcium lactate based healing agent, which would make a structure water tight and lead to lesser dependence on reinforcing steel requirement. They propose that up to approximately 31.40kg less steel can be used if the healing agent is used. This however was shown to lead to same CED (environment burden) of 930.4MJ and an increased environmental prevention cost. They further propose that when the healing agent is applied only to the concrete cover, the environment impact is readily compensated. Despite the widely reported advantages in concrete properties, the addition of lactate derivatives as organic precursors have been found to have a detrimental effect on slag rich cements such as CEMIII/B, [78]. This manifests as a significant drawback in the current commercial upscaling of lactate based bacterial self healing systems, primarily as slag rich cements are widely used especially in countries like the Netherlands

In terms of application, the direct addition of the bacteria based healing agents proved disadvantageous, as the lifetime of the spores were limited to upto 4 months at maximum [71]. For enhancing the lifetime and functionality in time, encapsulation of the two-component bacterial healing agent was proposed by various authors. [79] suggested a method of encapsulation by lightweight aggregates (LWA) by bacterial solution and then their encapsulation in a polymer based coating for enhancing the healing efficiency. [80], [74] suggested immobilization of bacterial spores in expanded clay particles. In these studies, vacuum impregnated expanded clay particles contained healing agent upto 6% by weight. It was reported that the viability of the incorporated spores now increased to 6 months. [66] reported the maximum crack width that could be fully healed

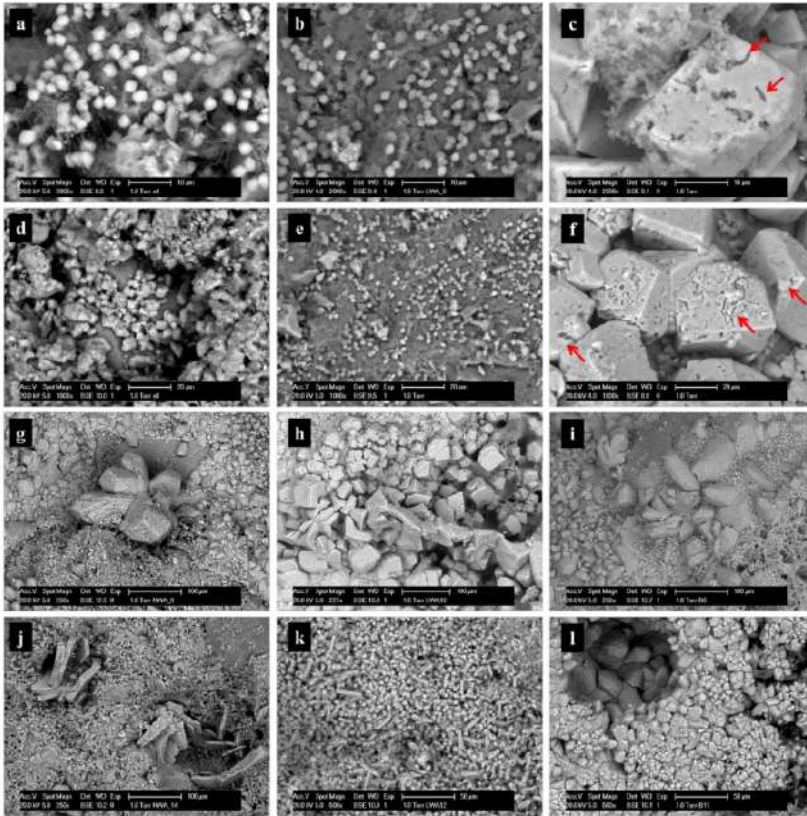


Figure 2.15: ESEM images of precipitates that were found on the surface of the crack after healing treatments a. REF specimen, b. CTRL specimen, c. B specimen submerged in water for 28 days; d. REF specimen, e. CTRL specimen, f. B specimen subjected to wet-dry cycles for 56 days; g. REF specimen, h. CTRL specimen, i. B specimen submerged in water for 28 days; j. REF specimen, k. CTRL specimen, l. B specimen subjected to wet-dry cycles for 56 day. [77]

with this encapsulation was 0.46 mm for compared to 0.18 mm healed autogenously by control specimens. However, [57] later reported that the replacement of sand and gravel by expanded clay has negative consequences for the strength of concrete composites. Modifications for practical upscaling of the LWA mechanism were proposed by [81] via pre-wetted light weight aggregates that could function as internal nutrient reservoirs. This was also studied by [82] as a promising approach to promote self-healing, specially over diatomaceous earth that were earlier suggested but found to be disadvantageous for delayed setting time. Later in 2016, [77] investigated the effect of the LWA encapsulated bacterial healing agent systems in two regimes: water immersion and wet-dry cycles, through water permeability studies. They found that the compressive strength is not negatively affected in the wet-dry regime despite the presence of LWA. The study found that the lightweight mortar incorporating bacteria-based healing demonstrates enhance crack sealing when administered in a wet-dry regime. In 2018, [83] further validated the

feasibility of aggregate replacement with expanded clay impregnated with bacteria, in recovery of strength in concrete. Besides LWA encapsulation, [84] demonstrated successful application of the bacterial healing agents embedded in polylactic acid particles.

There exists other possible ways to encapsulate bacterial healing agents, such as polymeric capsules, nanomaterials, diatomaceous earth, hydrogels, waste-derived biochar and powder compaction. However, as recently noted and successfully applied by [85] in their master thesis, other than powder compaction that facilitates composition of 'entirely usable' ingredients, the remaining approaches for encapsulation are either too laborious to prepare for large scale applications, or influences concrete properties in a negative manner.

2.5. FUTURE OF SELF-HEALING IN CONCRETE

The preceding review, although not exhaustive as far the magnitude of research literature in the domain is concerned, helps shed light on the various approaches to self-healing systems and their limitations. A perennial challenge posed to the field of experimental cementitious materials research, surrounds the topic of field application. The transfer of laboratory research successes to on field applications is often not seamless, and involves numerous constraints with regard to mass use of materials and potential discrepancies in functional behavior when applied in large scales, material regulations and standards of use, environmental exposure conditions that could be vastly different from laboratory conditions, and so on. Some of these constraints hold true with regard to self-healing systems as well.

Autogenous self-healing, although the most environmentally safe and requires zero human intervention, can only be relied upon for closing small cracks. On the other hand, most autonomous systems involve the use of encapsulations, the production and preparation of which often entail laborious and expensive activities. Microbial self-healing systems involving aerobic bacteria shows promise of being used commercially. A couple of projects demonstrate feasibility of its use as a repair material and for big scale commercial constructions [86], [78]. These studies indicate long-term stability of bacterial self healing systems. However, despite the reported feasibility of such applications, the current aerobic bacterial self-healing systems suffer from incompatibility of its lactate based precursor in slag rich cements. Overcoming this drawback appears promising with the progress of ongoing investigations, including the current study, on alkanolate based derivatives that can potentially act as substitutes. If the efficiency of these systems in real environmental conditions, such as marine environments, freezing and carbonation exposure, etc can be proven, then upscaling of this technology in all cementitious constructions could be very well feasible in the future.

3

METHODOLOGY

This chapter presents the experimental and analyses methodology that were adopted for answering the 6 research questions. It is divided into two sections. The first presents the experimental program, that involves material and sample preparation, test methodologies and steps undertaken for investigating research question 1, 2, 3, 5 and 6. The second section addresses the methodology followed for assessing the environmental and economical effects of using the newly proposed healing agent in concrete. This is for investigating the research question 4.

3.1. EXPERIMENTAL PROGRAM

3.1.1. MATERIALS

BINDERS AND MIX DESIGN

Ordinary Portland Cement (CEM I, 42.5N, ENCI, Rotterdam, the Netherlands) and Blast Furnace Slag Cement with 65-75% GGBS content (CEMIII/B, 42.5N, ENCI, Rotterdam, the Netherlands), were employed for all tests of the study. For tests involving mortars, a composition of cement:sand:water of 1:3:0.5 (by mass) was made using siliceous sand of size range 0-2mm, as specified in EN 197-1. For pastes, the water cement ratio was kept at 0.5. Healing agent content in all compositions was kept 2.6% by mass of cement.

SELF HEALING AGENT

The healing agent was composed of spores derived from *Bacillus Cohnii*, an alkaliphilic bacterium, yeast extract as growth nutrients, and mineral precursors which are either calcium lactate (PDLA and B) or alkanolate derivatives (PHBV H42 and PHBV H44). The abbreviations used for each are shown in table 3.1. The composition by mass of the healing agent was in the following order: 0.4% spores, 2% yeast extract and 97.6% mineral precursor. For checking the compatibility, functional properties and healing efficiency tests, two separate batches of the new precursor are used (PHA-1, PHA-2). These two variants conform to two separate production batches of PHA-rich biomass from the pilot

plant (Orgaworld/Paques, Lelystad, the Netherlands). Two batches are checked for testing possible variation in performance results. Besides, in addition to the proposed new healing precursor, two commercially available lactate derived variants (Basilisk, Delft, the Netherlands), PLA-1 and PLA-2 were also tested, to compare their behavior with the new healing agent.

#	SH Precursor type	Variants	Abbreviations used
1	Calcium Lactate Derivatives	PDLA B4bb2	PLA-1 PLA-2
2	Alkanoate Derivatives	H44 H42	PHA-1 PHA-2

Table 3.1: Healing agents used in the study

3.1.2. SAMPLE PREPARATION

HEALING AGENT

To form the healing agent, the contents as described in previous section were weighed, mixed and melted at 100 C to fuse into a single entity. This was then rolled into a wafer thin sheet of approximately 1mm thickness. Upon cooling of these wafers to room temperature, they were ground in a grinding machine and sieved to obtain particles of the size range 0.5 to 1mm. This was repeated till the required amount of healing agent was formed to conduct the experiments.

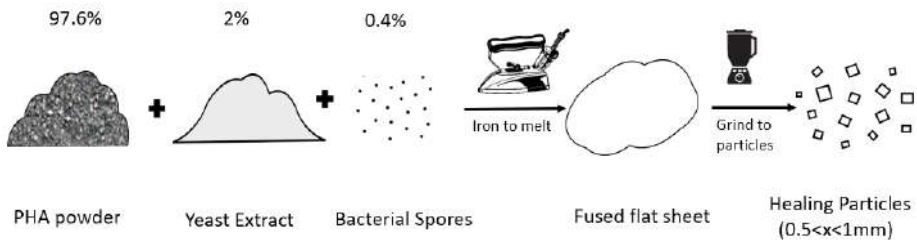


Figure 3.1: Schematic of the preparation steps involved in forming the healing agent.

PASTES

Pastes of above mentioned mix designs were mixed at w/c ratio of 0.5, for hydration and fresh state property tests of flow table test and Vicat setting time test.

MORTARS

Mortars conforming to mix design cement:sand:water of 1:3:0.5 (by mass) and with healing agent dosage of 2.6%, were made for varying tests, in three specific shapes and sizes

as given below. Each batch of mortars were mixed and cast in the same manner, conforming to standard NEN-EN1015-2. They were then demoulded after 4 days of hardening and subsequently cured at a fog room at conditions of 100%RH and 27 degrees C, for 28 or 70 days as per test requirements.

1. Cube: 4x4x4cm cubes were prepared for testing compressive strength tests. They were mixed and cast in iron moulds. 3 cube samples of each mix design set were cast, resulting in a total of 30 cubes.
2. Cylinder: For water permeability test, cylinders of size 33.5mm diameter and 60mm height were cast in plastic moulds containing spacers running through the height of the mould. The hardened cylinder after 24hrs, contained a groove along two opposite edges of size 2mm width and 3 mm depth, such that they created a dent of the above size, along the diametrically opposite edges of the hardened cylinder. At 28 days after casting and curing, these cylinders were cracked across the groove, by administering them under a hydraulic testing machine. After splitting, two plastic spacers were fitted at the groove sites in order to retain the crack width across the diameter at approximately 0.4mm - 0.8mm. This assembly was then tightly bound with tape, primarily to hold the spacers in the grooves in place. Thereafter, the cylinders with induced cracks were again subjected to curing at the fog room. 6 mortar cylinders of each mix design were cast, resulting in a total of 60 cylinders.
3. Prisms: For testing the degradation mechanisms, prisms of dimensions 16x4x4cm were cast for convenience. Two prisms were cast per mix design, resulting in a total of 16 prisms. Thereafter, they were naturally carbonated under conditions for 11 months, at a mean monthly relative humidity of 84% and 0.03-0.04% atmospheric CO₂ content [1], [2]. At the time of testing, each prism was sawed as follows: 1x prism of size 8x4cm, and 2x cubes of 4x4cm. All these were used for different purposes as discussed in section 3.3.

POLISHED SECTIONING

For conducting ESEM analyses, polished sections were prepared. To do this, first the cylinders with the healed cracks at 70 days, were sawed in halves along the perpendicular of the originally induced crack direction. The generated halves of the cylinder now contains a crack length across its exposed surface that can be studied. These are then impregnated with epoxy and polished to yield a smooth surface for ESEM analysis.

HYDRATION STOPPAGE OF POWDER SPECIMEN

For conducting the characterization tests of TGA and XRD to identify carbonated phases, a powder specimen of the same was produced. This was done by first identifying the potential carbonated edge of each sample with a pH test as is described in section[3.1.3.4]. By using a hammer and chisel, fragments of the mortar edge that is believed to be carbonated, are broken off. When about 5g of fragments are collected, they are first crushed into fine powder with a mortar and pestle. The aim thereafter, is to stop their further hydration by removing their free water so as to preserve the hydrates of the sample in

that specific state. Hydration stoppage is one of the most important parameters that can affect TGA and XRD analyses. In this study, the grinding of sample and hydration stoppage of the ground material was conducted with solvent exchange method according to [3]. A 3 step solvent exchange method with isopropanol is reported to be a relatively more compatible method for studies involving carbonate phases and portlandite, as is the case with current investigation. The prepared samples were then stored for a week inside a desiccator before testing.

3

3.1.3. METHODOLOGY

This section presents the tests and procedures adopted for testing the specified research questions.

COMPATIBILITY TEST VIA HYDRATION

Hydration is often used as a means to measure compatibility of new additions in cementitious systems. When water is added to cement mix, the clinker components in the cement undergo exothermic reactions to produce hydration products like CSH, CH, Ettringite and Monosulphate. Each mineral clinker undergoes hydration distinctly and emit different amounts of heat. The rate of heat release is often proportional to the rate of production of hydration products. Each hydration product impacts various fresh and hardened state properties of the cementitious mixture. By studying and comparing the heat release curves of a traditional mix design and that of a mix design containing healing agents, one can predict if the subsequent fresh and hardened state behavior of the later will alter remarkably from the former. If the change in the heat release trend is imperceptible, then the addition of healing agent can be considered to be compatible in the cementitious system.

An indication of the rate at which the clinker minerals are reacting with water, can be made by monitoring the rate at which heat is evolved using a technique called *isothermal calorimetry*. In traditional OPC, the heat release follows 4 distinct phases:

- Stage I: **Dissolution** of C3S and C3A, leading to rapid heat production and formation of the C3S gel. Dissolution of these clinkers into Ca and OH increases the pH of the solution. This is identified in a graph by a sharp peak at the initial hours of testing.
- Stage II: A relatively **dormant** stage is reached after extremely exothermic reaction at the first stage. This is the stage when the cement mix is suitable to be transported to casting site. This is also called the *induction* period.
- Stage III: The third stage is called **acceleration**, where the reaction again picks up speed. This corresponds to the main period of hydration, during which time concrete strengths increases. In a graph, this is identified by a rising slope forming a peak that is often smaller than the one produced in the first stage.
- Stage IV: Thereafter, **deceleration and diffusion** takes place which slows down the reaction. In the heat release curves, this is demonstrated by a gradual decline in

the slope. This signifies continued hydration upon water availability, albeit at a much slower rate.

In a traditional slag cement mix, the third stage is comprised of 2 peaks, the second representing slag. In this study, hydration via isothermal calorimetry was studied to check evolution of heat energy of PHA with both cement types. It was conducted in accordance with ASTM C1702 – 17.



Figure 3.2: A twin type eight channel TAM Air calorimeter with 20ml glass ampoules [4]

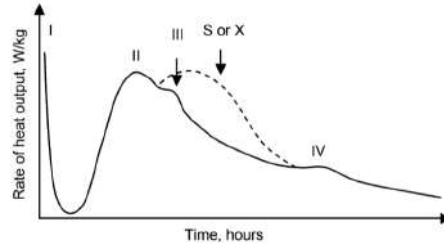


Figure 3.3: Typical isothermal conduction calorimetry curve for the hydration of ordinary Portland cement and blastfurnace slag blended cement. [5]

Experiment The effect of healing agent on cement hydration was checked via isothermal calorimetry. For this, cement pastes containing 5g cement, 2.5g water, and 0.133g healing agent, were stirred for 5 minutes and filled in calorimeter glass ampoules. These were then inserted into a twin type (sample and reference), eight channel calorimeter (TAM Air3114/3236, Thermometric AB, Sollentuna, Sweden), operating at 600mW and in room conditions of 20 degree C and 50% RH. Test was conducted over three days.

FUNCTIONAL PROPERTIES TESTS

Concrete functional properties are those that determine its service-life behavior. There are a number of fresh and hardened state properties that serve as a yardstick to measure the potential performance of cementitious composites. Apart from the traditional ingredients of concrete composites, whenever new additions like healing agents or admixtures are added to the mix, there is chance that these properties are altered by possible introduction of new chemistry by the additives. The extent to which the properties might be altered depends on the chemical and physical influence or compatibility of the new additives. If the changes in these properties are minor to none, the inclusion of additives can be considered to be compatible. In this study, tests on two mostly studied fresh state properties and one mechanical property has been carried out, to check the influence of the proposed healing agent. These tests have been conducted on mortars as they are representative of concrete composites to a substantial degree. The mix designs used for the purpose are shown in table 3.2.

Experiments

Mix Design Names #	Binder type	HA precursor involved
1. C1Control	CEM I	-
2. C1PLA-1	CEM I	PLA variant 1: B
3. C1PLA-2	CEM I	PLA variant 2: PDLA
4. C1PHA-1	CEM I	PHA variant 1: H44
5. C1PHA-2	CEM I	PHA variant 2: H42
6. 3BControl	CEMIII/B	-
7. 3BPLA-1	CEMIII/B	PLA variant 1: B
8. 3BPLA-2	CEMIII/B	PLA variant 2: PDLA
9. 3BPHA-1	CEMIII/B	PHA variant 1: H44
10. 3BPHA-2	CEMIII/B	PHA variant 2: H42

Table 3.2: Mix design variations and abbreviations used for the compatibility studies. The w/c ratio was kept constant at 0.5 for all tests. For mortars, the cement:sand:water ratio was 1:3:0.5 by mass.

1. Workability: Flow table test was conducted on freshly prepared mortar mixes as per EN 1015-3:1999.
2. Setting time: This was conducted on freshly made mortar paste with a Vicat apparatus, according to EN 196-3:2016.
3. Compressive test: This was conducted on hardened mortar after 28 days of curing, according to standard EN 1015-11:2019.

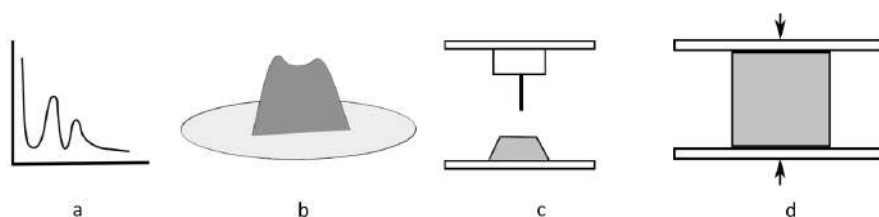


Figure 3.4: Schematic of the compatibility tests: a) Hydration curves obtained from isothermal calorimetry on paste; b) Slump formed in a flow table test for workability on fresh mortar; c) Vicat test for setting time on fresh mortar; d) Compressive strength test on hardened and cured mortar.

HEALING EFFICIENCY TESTS

Varying approaches of autonomous self-healing via bacterial precipitation on OPC have been reported to have healed cracks substantially bigger than 0.2 mm as healed by autogenous healing [6] [7] [8] [9]. Most of these reported approaches have validated their

findings based on macroscopic laboratory observations like water permeability and absorption tests, followed by microscopic analyses via ESEM and stereomicroscopy. Similar approach has been adopted in the current investigation, for studying the healing efficiency of newly proposed, alkanoate derived healing agent. According to [10], in order to validate efficient bacterial healing, (i) mineral formations on the surface of the crack, (ii) crack sealing along with reduced permeability after cracking and (iii) proof of bacterial activity should be studied. In line with this, the emphasis of this study is to analyze qualitatively and quantitatively, the water transport and durability parameters like permeability, with and without the presence of both lactate and alkanoate based healing agents. Bacterial precipitation plugs cracks, thereby densifying and refining the microstructure [11]. The extent to which the new precursor can potentially parallel previously studied precursors, and in comparison to autogenous healing in reference mortars, was investigated as follows.

Experiments The study was aimed at testing the three aforementioned criteria to validate efficient bacterial healing. These tests used cylindrical mortar specimens of dimensions 33.5mm diameter and 60mm height. The following procedures were adopted for quantifying the healing efficiency. A schematic of the steps involved and the time-line of conducting the tests is shown in figure 3.7

1. **Crack calibration:** As described in point 2 of section 3.2.3, the cylinders with grooves on diametrically opposing edges were induced with cracks through the grooves, after each set of cylinders were cured for 28 days. This was done by tensile splitting of each cylinder by placing between the compression platens of an Instron 8872 servohydraulic testing machine (Instron Corp., Canton, MA, USA). A compressive load was applied at 0.01 m.s⁻¹ until the cylinders diametrically split from groove to groove. Before subjecting the cylinders to compressive loading, the grooves on either side were inserted with steel spacers and bound with tape, for carrying the loading along the grooves. At the top and bottom surfaces of each cylinder, the crack width created were approximately 0.4 to 0.8mm. To hold these cracks in place, plastic spacers of size approximately 2mm wide and 3mm deep, were placed and bound with tape at the groove site, to prevent separation of the two cylindrical halves.
2. **Stereomicroscopy:** After crack induction, Stereomicroscopic (Leica MZ6, Nussloch Germany) images of the fresh surface cracks (0 day of healing) of both top and bottom surfaces of each cylinder, were taken for comparing with later periods of healing. Effective crack width were calculated from captured images by image analysis software *ImageJ*. This was repeated before the water permeability test on 70th day of healing.
3. **Water permeability test:** To be able to compare and quantify the permeability of cracked (un-healed) and healed specimen, water permeability test was conducted on the specimens as per the procedure developed by [11]. A representative set-up of the experiment is shown in Figure. This comprise of water column attached to a water reservoir that is placed 1m higher. After crack induction and calibration

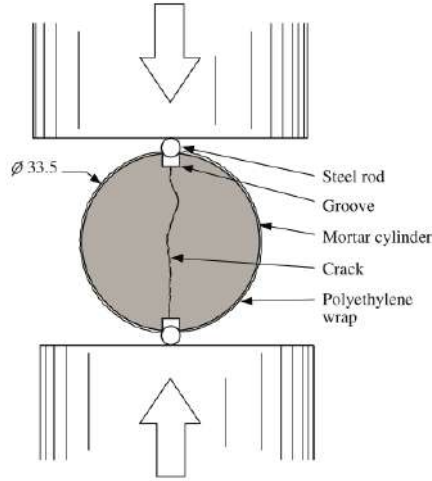


Figure 3.5: Crack induction via Instron hydraulic testing machine. [11]

in step 1, sealed specimens were attached via a fitting at the bottom of each water column. The test was initiated by releasing the taps in each reservoir, such that the released water can penetrate into the cracked specimens. The level of the water in the column was kept constant manually, ensuring a pressure of around 0.1 bar. Water flowing through the cracks was individually collected in catchment buckets and the weight of the water recorded every 5 min for a total test duration of 15 min. After this permeability test, specimens were stored under self-healing conditions in a fog room (RH>95%) for 70 days. After the healing period, optical microscope (Leica MZ6, Nussloch, Germany) images of the surface cracks were collected and compared to those before the healing period, and the water permeability test was conducted again.

4. **Analyses of crack width:** After measurement of crack width and water permeability test data were collected, the self healing capacity (SHC) of each specimen were calculated according to the following equation:

$$SHC = \left(\frac{Q_0 - Q_{70}}{Q_0} \right) * 100 \quad (3.1)$$

Where, Where Q_0 is the water flow at 0 days in m^3/s , Q_{70} is the water flow at 70 days of healing in m^3/s . The water permeability test of 0 days healing was conducted on only 3 (from here termed as SET 0) out of 6 specimens of each mix design. This is because, previous studies demonstrate potential flushing out of healing agents before their reaction. To eliminate this effect, the initial crack flow of the remaining 3 specimens of each mix design (from here termed as SET 70) were determined using Poiseulle's law:

$$Q_0 = \frac{\Delta p * l * w_{eff}}{12 * \eta * h} \quad (3.2)$$

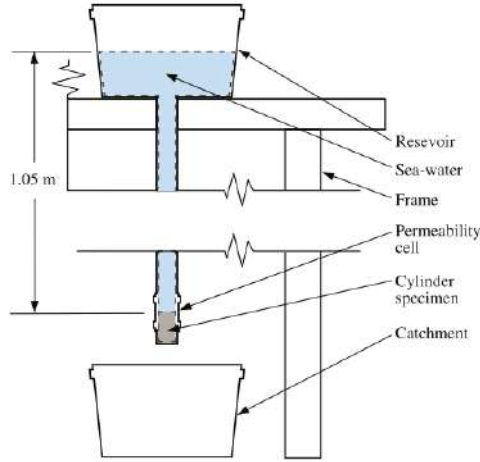


Figure 3.6: Water permeability set-up.[11]

Where Q_0 is the water flow at 0 days in m^3/s , Δp is the water pressure difference between crack inlet and outlet in Pa, l is the crack length across the surfaces of the cylindrical specimens, w_{eff} is the effective crack width, h is the height and η is the dynamic viscosity of water in Pa.s. The w_{eff} is calculated in the following way:

$$w_{eff} = \left(\frac{2 * (w_t + w_b)^2}{w_t + w_b} \right)^{\frac{1}{3}} \quad (3.3)$$

where w_t and w_b are the top and bottom average crack widths of the specimen respectively. Both these crack widths are calculated considering 10 measurements with the help of image analysis as mentioned previously.

5. **ESEM analyses:** The polished sections of the cracked specimen were scanned and images were captured at 15kV under back scatter mode (CBS).

DEGRADATION TESTS

Formation of cracks in concrete makes it susceptible to various degradation mechanisms on account of ingress of undesirable elements through these openings. Two of the most drastic deterioration mechanisms in concrete are carbonation and frost attack [12]. While both mechanisms have been comprehensively studied independently [13], [14], [15], fewer studies demonstrate their combined effect on concrete, much less on biogenic self-healing mortars. Previous investigations into these phenomena suggest that such attacks are interrelated, as damaged structures on field often show more than one form of environmental effect or loading simultaneously [16], [17]. Deeper studies by [18], [19], [1] into the pore structure in cementitious matrices, document a synergistic

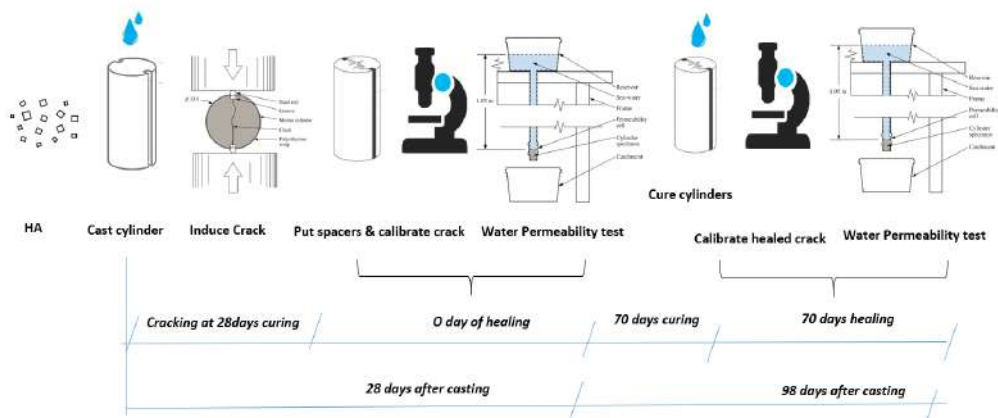


Figure 3.7: Schematic of the steps and the time-line of healing efficiency tests.

relation between damage caused by freeze thaw and pore size re-distribution owing to varying physical or chemical mechanisms such as carbonation. They suggest that the pore volume, pore radius, and pore size distribution decide the freezing point of pore solution and the amount of ice formed in pores. Hence, the subsequent extent of frost scaling is dependent on the extent of pore-reforming mechanisms like carbonation. It has been further reported that multi-damage phenomena in concrete could considerably accelerate the deterioration, and increase the complexity of the durability design and the prediction of concrete structures, especially in colder countries [14], [17]. The influence of crack-plugging bacterial precipitation on dual carbonation and frost scaling is therefore an interesting study to conduct.

Experiments This study explores the dual attack of carbonation and salt frost attack on mortars containing the newly proposed healing agent and compares them with lactate based healing agents along with reference mortars. This program involves the following tests or experiments:

- Natural (atmospheric and non-sheltered) carbonation of mortars for 11 months, at a mean monthly relative humidity of 84% and 0.03-0.04% CO₂ [20].
- pH test to check depth of carbonation on freshly split surfaces.
- TGA and XRD to identify potential carbonation phase formations.
- 10 accelerated (rapid) freeze thaw cycles on NaCl solution to check frost salt scaling and mass loss on carbonated mortars.

1. **Depth of carbonation:** 8x4cm prisms of above mix designs were split in a HTM (hydraulic testing machine) into two approximate cubes. The freshly split surface of one half was used to demarcate the carbonation front by spraying 1% phenolphthalein, wherein the carbonated area was colorless, and the non- carbonated area

was rendered shades of pink to purple. The other half was used to grind powder off the carbonated perimeter corresponding to the reading conducted on the first half. The ground powder were used for phase identification studies later. The results of the pH test on the freshly split surfaces were analyzed with *ImageJ*. 10 measurements were taken on each side to eventually arrive at an average carbonated depth per sample.

2. **TGA:** TGA was conducted in NETZSCH STA 449 F3 Jupiter, on powder samples weighing between 40-60mg, at a temperature regime of 40-1000 degree C and at a rate of 10 degree C/min. Argon was used as a purge gas, at a gas flow rate of 50mL/min. Gas flows higher than this leads to indistinct differentiation of peaks and negatively affects the weight loss region in the graph [21]. The results were analyzed using Proteus software. Indication of mass loss of CH and Calcium Carbonate phases were vital for validating carbonation.
3. **XRD:** To qualitatively examine the presence of carbonated crystals, viz. calcite, aragonite, and vaterite, powdered samples were subjected to CuK radiation inside a Philips PW 1830-XRD. These x-rays target the specimen over a range of 2Theta angles from 5 to 70 degrees. However, for the purpose of this study, data analyzing was conducted in the range from 20 to 45 degrees, as this range provides maximum peak information for specified crystals. Identification was conducted both with an open-source search-match software that is equipped with the Crystallography Open Database (COD), and manually from published work by [21], [22], [23].
4. **Frost scaling and mass loss:** Sawed cubes of all mix designs were submerged in a 3% NaCl solution as a freezing medium, to simulate deicing salt frost attack. Previous studies demonstrate 3% NaCl concentration creates maximum surface damage compared to the other solute concentrations [24]. Before exposing to freezing medium, the cubes were tightly sealed with thick plastic tape on all sides, leaving a height 3mm from the bottom surface. This was done to limit damage only to the exposed side. The sawed surface of each cube was selected for exposure to freezing medium, to eliminate the effect of inhomogeneity that can potentially bring about a wide spread in results [25]. A relatively harsh freeze-thaw regime of 20hrs freezing at -20 degree C and 4hrs thawing at 25 degrees C, was selected to simulate maximum damage. A total of 10 freeze-thaw cycles were conducted. Scaled mass were collected, dried and weighed at the end of 1st, 3rd, 7th and 10th cycles.

3.2. ENVIRONMENTAL AND ECONOMICAL ASSESSMENT

The novel alkanolate based precursor material proposed for bacterial self-healing is designed to be derived from municipal and industrial waste-streams. If tested and proved compatible for use with CEMI and CEMIII/B composites, and if it can aid in sealing cracks of width beyond 0.2mm, it can be effectively used as self-healing agent in real-life structures that are usually made of reinforced concrete.

Cracks form in concrete, owing to a variety of chemical and physical processes occurring during its lifetime such as shrinkage, tension, shear or imposed deformation.

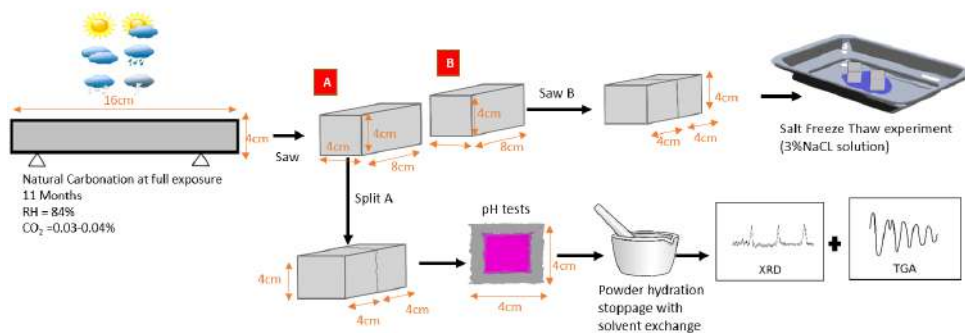


Figure 3.8: Schematic of the steps involved in the degradation studies. This is representative of each of the 8 prisms cast per cement type. Parts 'A' of the prism were used for carbonation studies, and parts 'B' were used for salt-frost attack studies.

Usually these begin as small, fine cracks that if left unrestrained, develops into wider, through-cracks. Reinforcement in the form of steel rebars are therefore applied in concrete constructions to control and to postpone the occurrence of through-cracks upon prolonged loading [26]. This effect of applying reinforcement in concrete is quantified as the *Reinforcement Ratio*(RR) on the basis of an *allowable* crack-width and the area of concrete involved per construction element. The RR indicates the amount of steel reinforcement to be provided in a structural element in order to restrain cracks beyond a particular width. From the perspective of the current investigation, it is quite interesting to study and relate RR with self-healing as both up to an extent, serve the similar purpose of restraining crack widths, albeit in fundamentally different ways.

As per the current study and based on pilot investigations, the novel precursor is hypothesised to aid in healing cracks of widths at least upto 0.4mm. If this is true, then its application in a real structure will imply that a crack width of at least 0.4mm is allowable, as this can be suitably self-healed. So the reinforcement that is now required in such a structure will only need to resist cracks beyond 0.4mm, as cracks up to this limit "will take care of themselves". In other words, a lower RR can now be applied when the self-healing agent is applied in constructions. As steel is associated with substantial environmental and economic expenses, a reduction in the quantity of required steel in a construction suggests savings on both fronts. This study analyses how much of environmental and economical savings can be possibly accomplished with the use of self-healing agent in a reinforced construction. The succeeding sections shed light on the materials considered for the analyses, the methodology adopted from analogous researches, and the assumptions considered during the calculations.

3.2.1. MATERIALS

BINDERS AND MIX DESIGN

The same binder specifications are considered for these analyses, as were mentioned in section 3.1.1.1 for experimental program. Also, just as previous experimental analy-

ses, both CEMI and CEMIII/B composites are considered for these assessments as well. However, since a study of reinforced concrete composites is considered for this part, the concrete mix design was considered in this proportion - cement : fine aggregate : coarse aggregate : water = 1 : 2 : 3 : 0.5. Table 3.3 provides the 4 mix designs that are considered for this study:

REINFORCEMENT

To arrive at an estimate of a possible reduction of reinforcement ratio (RR) upon application of self-healing, the following data are collected for comparison between composite mix designs:

- The maximum reinforcement ratio required for a no-crack or negligible crack scenario corresponding to a composite without self-healing agent.
- The reinforcement ratio required when a 0.4mm crack is allowable, corresponding to a composite containing self-healing agent.

The required RR according to standards and research literature appears to vary considerably. For instance, the maximum RR that can be applied to ensure the least or negligible crack width in the structure according to the NEN-EN 1992-1-1 is 4%, but according to the GTB 2010 which is based on the Eurocode, it is 2.13%. Similarly, there is little consensus on the amount of RR that can be provided if a crack width of 0.4mm is allowable. The DIN1045 standard provides the most realistic data on the matter and is therefore adopted for this study. According to it, if crack-width of at least 0.4mm is allowable, then providing RR of 0.7% is sufficient. In summation, RR of 2.13% is considered for composite mix designs without self-healing agent, and 0.7% for those with self-healing agent.

Mix Design	Binder	HA%	RR %
1	CEMI	0	2.13
2	CEMI	2.6	0.7
3	CEMIII/B	0	2.13
4	CEMIII/B	2.6	0.7

Table 3.3: The mix designs considered for the environmental and economic analyses

3.2.2. METHODOLOGY FOR ENVIRONMENT ASSESSMENT

In this section, the methodology adopted for assessing the environmental impact of using lower steel upon healing agent addition in both CEMI and CEMIII/B composites is presented. An environment assessment was done by calculating the ECI (Environmental Cost Indicator) values of the raw materials used in 4 mix designs, against 11 environment impact categories as laid down in the *Bouwbesluit 2012- Bepalingsmethode*, the Dutch procedure for calculating environmental impact of buildings and civil engineering constructions. The ECI costs, expressed in Euro, represent the costs required to bring the environmental impacts of a product of process to an acceptable 'sustainable' level. By comparing the total ECI of all mix designs, the environmental effect of using the healing

agent can be interpreted. The hypothesis of this study is that a reduction of negative environment impacts will occur when healing agent is used, as consequently a lower steel amount is required in the same volume of concrete. The following procedure is adopted to study the environmental impact of applying healing agent in reinforced concrete, in terms of ECI.

The ECI calculation of any product is a part of its Life Cycle Assessment (LCA). According to the ISO 14040 standard, the LCA requires four specific steps depicted in the figure below. This approach of the current study on the lines of ISO 14040 assessment

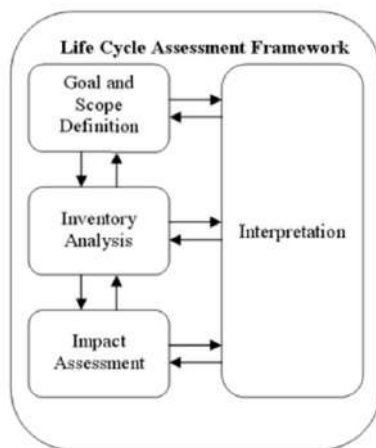


Figure 3.9: Schematic drawing of the 4 required phases of an LCA procedure[27]

framework is as follows:

1. *Goal and Scope definition*: Determine the functional unit and system boundary. For this study, the aim is to compare the cradle-to-gate environmental impact of 4 mix designs in relation to whether or not they use the newly proposed healing agent. The functional unit for all four mix designs is defined as one cubic meter (1m^3) of reinforced concrete, that is designed for a service life of 50 years, in exposure class XC1. The scope is to assess the ECI based on 11 impact categories of all raw materials relevant to producing a cubic metre of concrete. The system boundary used in a study defines which processes and products are included in the study and which not. In this study, only the raw materials involved in the mix design are studied, while the transportation and energy costs are left out of scope primarily because of data availability issues.
2. *Inventory Analysis*: This involves the compilation and quantification of all inputs and outputs throughout the life-cycle of each mix design. The inputs in this case are the raw materials that are identified in the system boundary. The corresponding emissions (output) due to production of each material are identified from databases

that are called the Life Cycle Inventory (LCI). Countries usually have their own national database, but the European Ecoinvent database is generally adopted for research representing a more generic overview of the European situation. For this study, the data derived from Ecoinvent 3.01 and used by related studies, are adopted.

Nr.	Impact category	Abbreviation	Unit	Factor [Euro/kg]
1	Abiotic Depletion, fuels	ADP1	kg Sb eq	0.16
2	Abiotic Depletion, minerals	ADP2	kg Sb eq	0.16
3	Acidifying Pollutants	AP	kg SO ₂ eq	4
4	Eutrophication Potential	EP	kg PO ₄ eq	9
5	Freshwater Aquatic Eco-Toxicity Potential	FAETP	kg 1,4-Dichlorobenzene eq	0.03
6	Global Warming Potential (100 years)	GWP 100 Y	kg CO ₂ eq	0.05
7	Human Toxicity	HTP	kg 1,4-Dichlorobenzene eq	0.09
8	Marine Aquatic Eco-Toxicity Potential	MAETP	kg 1,4-Dichlorobenzene eq	0.0001
9	Ozone Depletion Potential	ODP	kg CFC11 eq	30
10	Photochemical Ozone Creation Potential	POCP	kg Ethylene eq	2
11	Terrestrial Eco-Toxicity Potential	TETP	kg 1,4-Dichlorobenzene eq	0.06

Table 3.4: 11 impact categories, their definitions and their shadow prices[28]

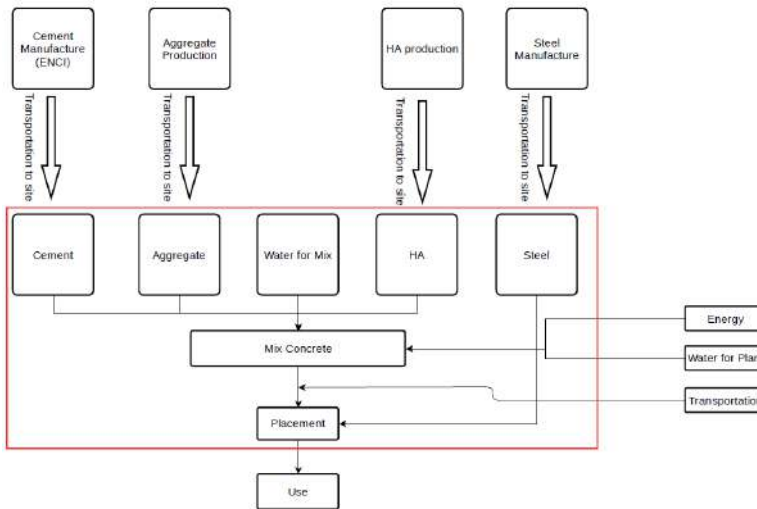


Figure 3.10: System Boundary for the study depicted by the red border.

3. *Impact Assessment:* In this step, all the LCI data collected in the previous step is tabulated and a conversion price is assigned to each output to establish a monetary value. In this study, MS-Excel is used to tabulate the inputs and outputs along with the associated shadow prices or conversion factors from [28], to interpret the output in terms of Euros. A final monetary value based on 11 impact categories is calculated for every mix design and the significance of the used raw material is evaluated based on the result. This is shown in table 3.4

4. *Interpretation:* The reinforced concrete mix designs are compared in terms of all environment impact categories. The best options regarding sustainability in the industry are then highlighted.

3.2.3. METHODOLOGY FOR ECONOMIC ASSESSMENT

This comprise of a straight-forward and conservative calculation of the approximate commercial value of each four mix-designs. For this, market values of the raw materials are drawn from available literature and online resources. This is done primarily to compare and highlight economic changes that can be possibly influenced upon adding a self-healing agent to the mix.

3.2.4. ASSUMPTIONS AND CONSIDERATIONS

Numerous assumptions were made while calculating an approximation of the above stated environment and economic cost reductions. Some of these assumptions had to made owing to a shortage of reliable information based on the environmental emissions of certain processes like transportation, energy and labour. Following were the assumptions considered during this part of the study:

1. Each mix produces a composite of 1 m³.
2. All mix designs are assumed capable of producing concretes of equivalent mechanical performance and durability. It is for this reason that technical performances examined in the experimental part of the study, have not been considered for these analyses.
3. It is assumed that 100% healing efficiency is assured upon using the proposed healing agent.
4. Concrete production processes are uniform for each mix design.
5. For the calculation of both environmental and economic costs, the proportion of PHA is taken as 2.6% of the weight of cement used in the 1 cubic meter composite (functional unit). This proportion is kept consistent with the experimental research for the larger study.
6. For calculation of ECI of the reinforced composites, only the production emission values of the raw materials are considered. The other factors like transportation and energy are conservatively assumed to be constant for all mix designs. So the variables are only the raw materials used.
7. To find the ECI of the healing agent, only the ECI of the PHA precursor is studied. This is because in the production of the healing agent, precursor is present in maximum proportion (97.6%). Hence, the ECI of the precursor is deemed representative for the whole healing agent. As the amount of spores and yeast extract required for the production of 1m³ concrete is substantially small, their environmental impact were excluded from the current assessment.

8. To arrive at a probable market price of the novel PHA based healing agent, the commercial cost of PHA as a precursor material, the market price of yeast extract, and bacterial spores of species *Bacillus* are considered from available literature. The associated energy, transportation and labour costs are neglected, due to unavailability of consistent data.

4

RESULTS

This chapter presents the results for the experimental program and the environmental and economic assessment. Like the preceding chapter, this is broadly sectioned into 2 parts: the experimental analysis and the environmental and economical assessment. Within the experimental analysis, results of experiments conducted on checking the compatibility with regard to heat of hydration, workability, setting times, and compressive strength, are presented. This is followed by experimental results of healing efficiency and degradation mechanism influences. In the next section, environmental cost assessment and a comparative evaluation of commercial prices of the bacterial and non bacterial based composites are provided.

4.1. EXPERIMENTAL ANALYSIS

4.1.1. COMPATIBILITY ANALYSIS WITH HYDRATION

The four stages of heat release as explained in Chapter 3, section 3.3.1, could be observed for the corresponding mix designs. In CEM I, energy released by PHA samples in the dormant stage is close to that released by control [Figure 4.1]. In the acceleration stage, rate of energy release has considerably reduced in PHA samples compared to PLA. They seem to peak later (at around 27 hrs), analogous to control pastes, although PHA-1 indicates a slightly higher energy release. PLA pastes reach acceleration and deceleration stages sooner than PHA and control, and with greater heat evolution as shown by their considerably higher peaks than the rest of the samples. They also demonstrate three defined peaks, 2 of them after the induction which cannot be observed in either control sample. This feature is also visible for one of two PHA variants (PHA-2 indicated by the red line). The 2 PHA curves depict different amount heat production compared to the CEMI curves, although the difference of either curves with that of CEMI's is limited. Further, heat flow for deceleration stage for PHA (approximately between 30-50hrs) is much higher than PLA, signifying continuation of hydration. In CEMIII/B pastes [figure 4.2], two well defined peaks can be observed for all the samples barring only one of the PLA samples (PLA-1) that show a single peak. These peaks suggest hydration of clinker,

followed by that of slag components and quite representative of slag cements. The PHA curves show similar release trends as the control, albeit with slightly higher peaks, suggesting more heat release. However, just as with the CEMI based pastes, this difference is restricted.

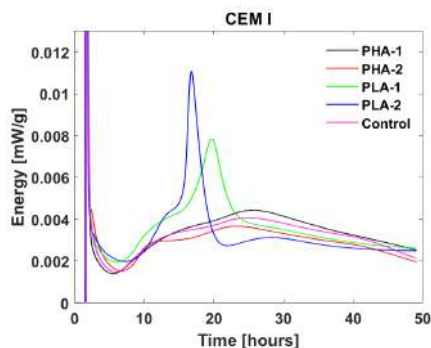


Figure 4.1: Energy evolution in CEM I

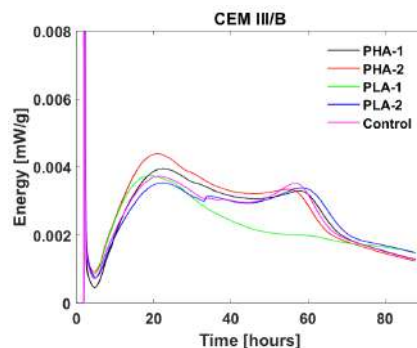


Figure 4.2: Energy evolution in CEM III/B

4.1.2. INFLUENCE ON FUNCTIONAL PROPERTIES

The results of the functional tests are shown in figures 4.3 - 4.7. In case of setting times, shown in Figures 4.3 and 4.4, both alkanolate and lactate based healing agent composites demonstrate a retarding effect on the final setting. In composites of both binder types, for the initial setting, all the healing agents based composites exhibit lesser time compared to the control. So there is an accelerating effect during the initial stages of hydration, which at least in the case of CEMI composites, is overcome during the later stages. In CEM III/B the difference of final setting times between the PLA based samples and control are rather imperceptible. The same is however not true for the PHA based samples. There is distinctly a retarding effect imparted by the PHA based healing agent, at the later stages of hydration. The heat release curves presented in figure 4.25, does show a smaller slag acceleration peak for both PHA based healing agents. This corresponds to the later retarding effect of setting. Although, compared with the corresponding retardation produced by their CEM I based counterparts w.r.t control, the amount of retardation in CEM III/B is still lower.

Compressive strength at 28 days for PHA samples appear on an average, at par with reference mortars. This is despite the supposed presence of an air void system in their matrices. In CEMI, the maximum strength is exhibited by the PLA based B sample, followed by the PHA based PHA-2. For CEM III/B cement type, the strength of alkanolate based composites, is observed to be higher than lactate based composites, and closely at par with the control, albeit with slight reductions. Figure 4.7 show workability results. For CEMI composites, the workability is higher for both bacterial based samples, but with the PHA ones indicating slightly higher figures. The figures do not appear too widespread in the case of CEM III/B composites. Nevertheless, addition of PHA based healing agents do seem to slightly enhance the workability.

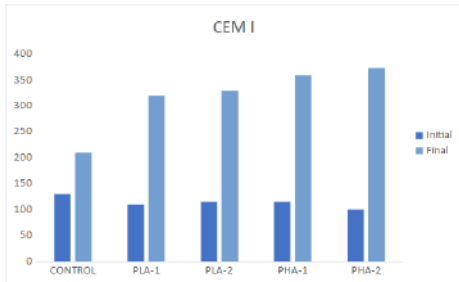


Figure 4.3: Setting times in CEM I composites

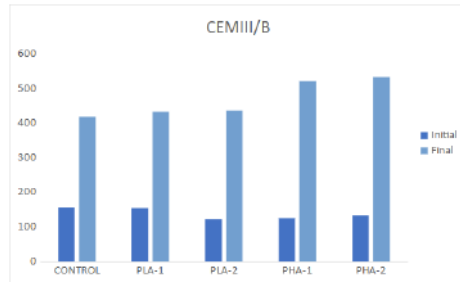


Figure 4.4: Setting times in CEM III/B composites

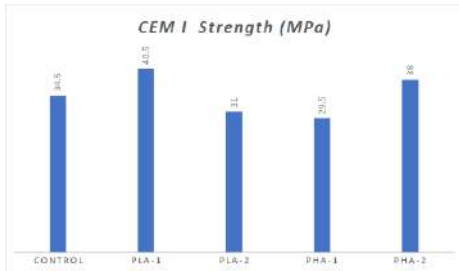


Figure 4.5: Compressive strength of CEM I composites

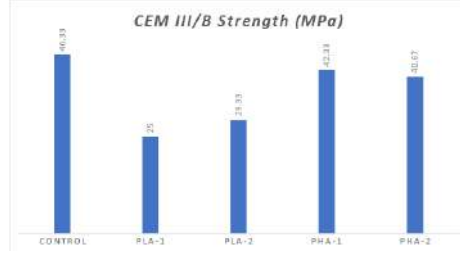


Figure 4.6: Compressive strength of CEM III/B composites

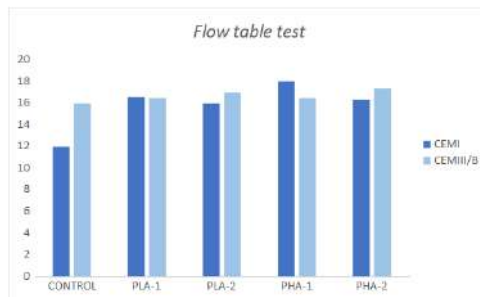


Figure 4.7: Workability results

4.1.3. INFLUENCE ON HEALING EFFICIENCY

The results for macroscopic and microscopic healing efficiency analyses are presented in Figures 4.8 - 4.28. The experimental results are categorised into three parts, in relation to the manner of execution and sequence of this investigation.

OPTICAL MICROSCOPIC ANALYSES AND QUANTIFICATION OF EFFECTIVE WIDTH

The optical microscopic test was conducted to study the crack width of the samples at 0 and 70 days of healing. Figures 4.8 to 4.12 present the comparison of the cracks before and after healing. These cracks were quantified with an image analysis software, ImageJ,

to find the reduction of crack widths after the 70 day healing period. These results are presented in a graphical form for each of the sets in figures A.9 to A.12. All the data from where the graphs were generated, are provided in the appendix.



Figure 4.8: Crack width of CEMI based control sample.



Figure 4.9: Crack width of CEMI based PLA-1 sample.

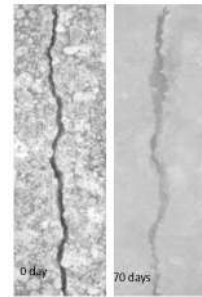


Figure 4.10: Crack width of CEMI based PLA-2 sample.



Figure 4.11: Crack width of CEMI based PHA-1 sample.



Figure 4.12: Crack width of CEMI based PHA-2 sample.

6 samples were measured for every precursor type. The images presented here are of the ones that reduced the maximum crack width over the healing period. For instance, referring to plots in Appendix A, the best performing sample among control specimens of CEM I is sample 6, as it shows the highest crack width reduction.

In figures 4.8 to 4.12, it can be observed from the stereomicroscopic images that in CEMI based samples, the most effective crack sealing occurred in PLA-1 sample. In this case, the crack was completely sealed. This was closely followed by PHA-2 sample. Other than these 2, it is fairly apparent that the remaining cracks were not fully sealed at the mouth.

Results for the effective crack width [Figures 4.18-4.23] demonstrate considerable scatter. The effective crack widths, w_{eff} , were calculated according to Equation 3.3. In CEMI, the reduction of the w_{eff} is shown lowest for PLA variant PLA-2 based composites, at 70 days. This is followed by the PHA variants PHA-1 and PHA-2 based composites,



Figure 4.13: Crack width of CEMIII/B based control sample.



Figure 4.14: Crack width of CEMIII/B based PLA-1 sample.

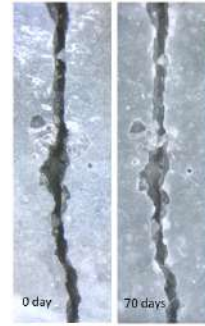


Figure 4.15: Crack width of CEMIII/B based PLA-2 sample.



Figure 4.16: Crack width of CEMIII/B based PHA-1 sample.



Figure 4.17: Crack width of CEMIII/B based PHA-2 sample.

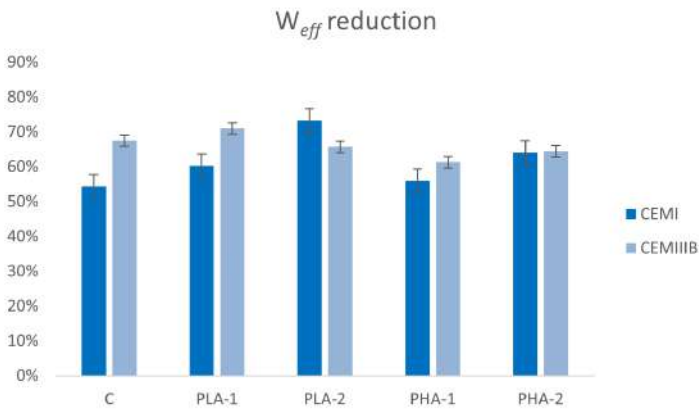


Figure 4.18: Reduction of the effective widths after 70 days of healing, as calibrated by optical microscopy.

control composites, and then the PLA variant PLA-1 based composites. From this graph,

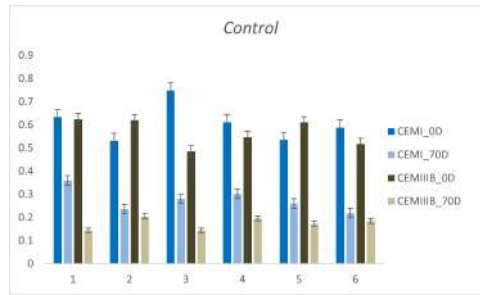


Figure 4.19: Effective widths at days 0 and 70 of healing in control specimens.

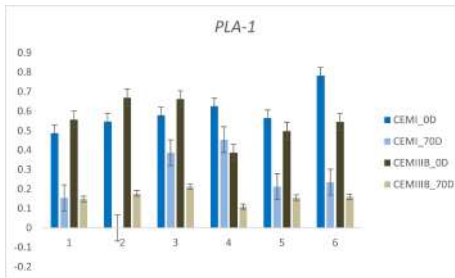


Figure 4.20: Effective widths at days 0 and 70 of healing in PLA-1 specimens.

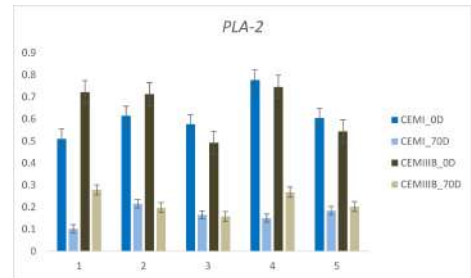


Figure 4.21: Effective widths at days 0 and 70 of healing in PLA-2 specimens.

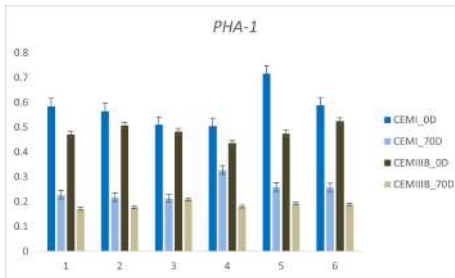


Figure 4.22: Effective widths at days 0 and 70 of healing in PHA-1 specimens.

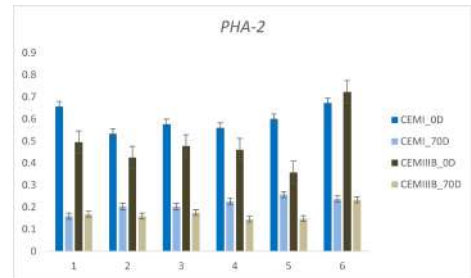


Figure 4.23: Effective widths at days 0 and 70 of healing in PHA-2 specimens.

it appears that the w_{eff} reduction resulting from self-healing of PHA is not considerably different from that resulting from autogenous healing in control samples.

In CEMIII/B, reduction of mean w_{eff} of both PHA based composites at 70 days healing is in the range of 63-67%, compared to the 58-61% reduction obtained in the case of PLA based composites. The control in this case demonstrates nearly 65% reduction of the w_{eff} . So from these observations, it appears that the performance of PHA based composites to seal the surface cracks have been analogous to that of the control.

WATER PERMEABILITY TESTS AND QUANTIFICATION OF HEALING CAPACITY

SHC was calculated at the end of 70 days of healing. It can be observed from the figures that the SHC results for the samples demonstrate much spread across all composite mix designs. In general, the scatter is lesser in the case of CEMIII/B composites. In CEMI, the least scatter is demonstrated by the PHA variant H44 based samples. This is also the group of samples whose mean SHC indicates maximum healing, at nearly 60% capacity. This is followed by that of the other PHA variant, the PHA-2 based group of samples, where the mean SHC is at about 55%. Certain samples in this group also demonstrated 100% healing capacity after 70 days healing. Comparatively, both the PLA based sample groups scored slightly lower on the mean healing capacities, and neither achieved full, 100% self-healing over 70 days. The control samples have supposedly undergone autogenous healing in the same period of time. However, the average healing capacity is considerably lower than both PLA and PHA based healing composites.



Figure 4.24: Self-healing capacity of CEMI composites.



Figure 4.25: Self-healing capacity of CEMIII/B composites.

In CEMIII/B, the SHC results are quite interesting as the PHA based healing composites exhibit considerably higher healing not only compared to control, but also to their PLA based counterparts. The mean healing capacities of both PHA variant based composites are 61-62%. The highest healing capacity is recorded by a PHA-1 based sample, at 80% healing capacity. The PLA based composites relatively show lower healing capacities, with the B-type variant demonstrating capacities even lower than autogenous healing, some reaching negative capacities as well. A negative healing is recorded when the crack is wider at 70 days than it was at 0 days of healing. PLA-2 type composites perform better than autogenous healing in general, but still poorer than either PHA type composites.

ELECTRON MICROSCOPY ANALYSES

ESEM analyses of an PHA-1 based composite for CEM III/B as shown in figure 4.26 shows evidence of likely bacterial precipitation along the crack periphery. Figure 4.27 shows precipitation in CEM I of the same batch of alkanolate based healing agent, at a depth deeper from the crack opening. It shows deposition of precipitation at locations away from the crack periphery as well. The same is also observed for PHA-2 composites as well. From previous studies on PLA based healing composites [1], [2] similar observations were made. A magnified image [figure 4.28] of these deposits revealed clusters of

hexagonal crystals that could be calcite crystals.

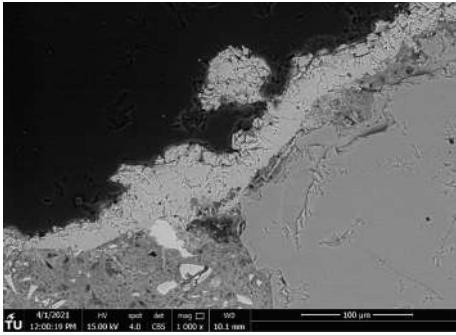


Figure 4.26: Deposition of precipitation along crack periphery

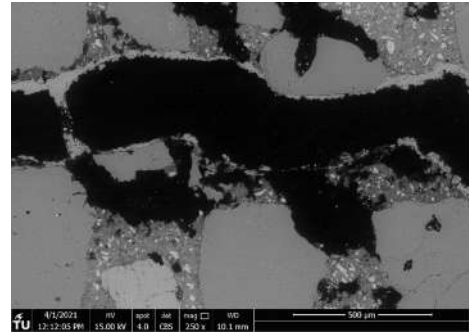


Figure 4.27: Deposition of precipitation across crack width

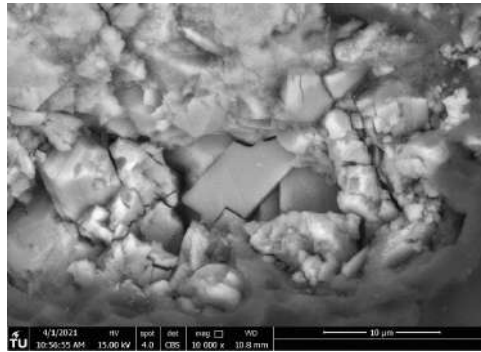


Figure 4.28: Clusters of precipitated crystals

4.1.4. INFLUENCE ON DEGRADATION CARBONATION

The characterization tests data of TGA and XRD reveals the presence of three polymorphs of CaCO_3 : the stable form of calcite and the meta-stable form of aragonite and vaterite, as can be determined from the data presented in figures 4.29 to 4.32. These occurrences are a key feature of carbonation [3], [4], [5], [6], [7] [8], [9]. The XRD data of both binder types detect the 3 polymorphs. TGA plots show weight loss shoulders between 100 and 165 °C, which are associated to the release of water present. In the CEMI composites, the 2 PLA variants PDLA and B, characterized by the red and yellow lines respectively, show a shoulder at *200 °C. This might correspond to a transformation of metastable ACC (anhydrous calcium carbonate) into stable CaCO_3 [10], [11]. This amorphous phase, which typically appears as small spheres less than 0,001mm diameter, transforms into calcite as the carbonation reaction progresses [11]. This shoulder is not seen in CEMIII/B composites. The shoulders representing loss of vaterite and calcite are not as pronounced

in CEMIII/B as in CEMI, indicating lower presence of these minerals. In other words, lower degrees of carbonation might have occurred in CEMIII/B. Loss of CH in both cement types appears most pronounced in control samples.

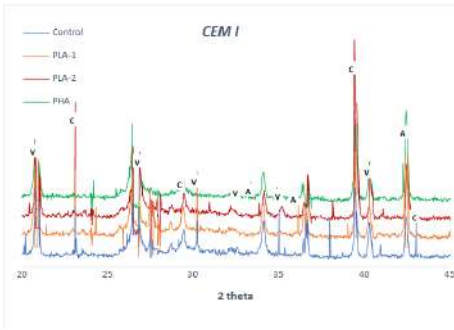


Figure 4.29: XRD data of CEM I composites

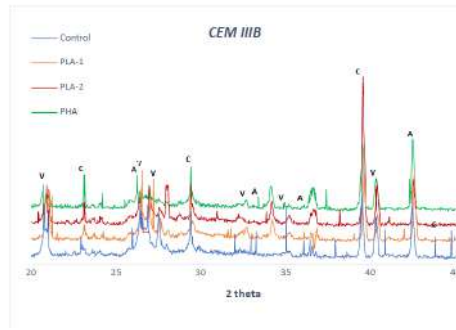


Figure 4.30: XRD data of CEMIII/B composites

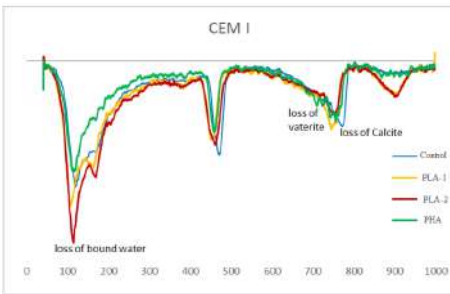


Figure 4.31: TGA data of CEM I composites

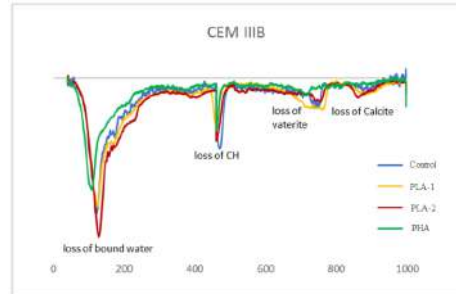


Figure 4.32: TGA data of CEM III/B composites

The results of the pH test show maximum carbonation depth on CEMIII/B control samples, followed by CEMI control samples. Presence of healing agents in general appear to lower the depth of carbonation across all composites. The average depth of carbonation observed, indicates the least damage on PHA samples, followed by PLA samples. For CEM I mortars, an approximate 64% decrease in carbonated depth could be observed on PHA samples compared to reference samples, while 44% reduction in PLA-2 and 3% reduction in B samples could be monitored. On the other hand, for CEMIII/B mortars, the recorded reduction of depth followed a similar trend, but less pronounced between the varying healing agent samples, unlike those of CEM I mortars. The PHA samples showed 44% reduction, followed by 33% decrease in B and 31% in PLA-2.

FREEZE THAW EFFECT ON CARBONATED SAMPLES

Freeze thaw test was conducted as explained previously, on carbonated samples. Scaled mass were collected, dried and weighed at the end of 1st, 3rd, 7th and 10th cycles. Mass



Figure 4.33: Observed carbonated front after pH test

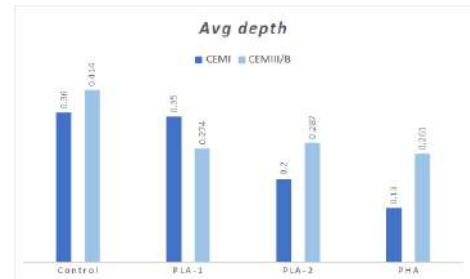


Figure 4.34: Average depth data

loss could already be observed for some samples after the 1st cycle. The total mass loss at the end of 10 cycles is shown in figure 4.35.

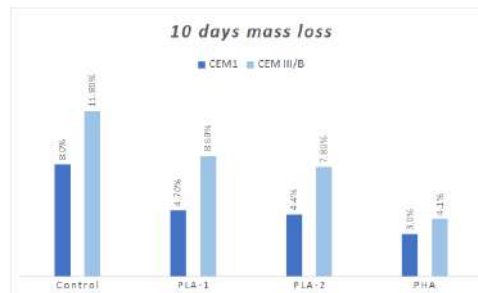


Figure 4.35: Total mass loss across both cement types after 10 cycles

It is seen that for both the cement types, PHA demonstrates the least loss, followed by PLA-2 and PLA-1. Figures 4.36 to 4.39 present the progressive mass loss over the measured timeline. It is seen that mass loss of PHA samples of both CEM I and CEM III/B, progressed the same till the 3rd cycle, after which the loss in CEM III/B rose sharply from about the 4th cycle onwards, peaking at 4.1% after the 10th cycle. However, compared to the reference samples, the mass loss of CEM III/B is still approximately 8% lower. For PLA-2, the mass loss is more gradual for both cement types, although at every stage, it exceeds that of PHA samples. For PLA-1, the mass loss curve for CEM I is more gradual than for CEM III/B. Overall, the rapid freeze and thaw cycles yield corroborative results to the carbonation. PHA samples demonstrate most resistance to salt frost attack. These comply with the fact that carbonation was also least observed in PHA based samples.



Figure 4.36: Progressive mass loss of the control mortars

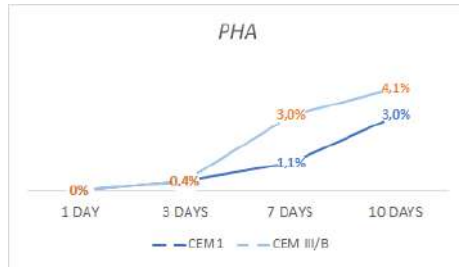


Figure 4.37: Progressive mass loss of the PHBV mortars



Figure 4.38: Progressive mass loss of the PDLA mortars



Figure 4.39: Progressive mass loss of the B mortars

4.2. ENVIRONMENTAL AND ECONOMICAL ASSESSMENT

4.2.1. ENVIRONMENTAL ASSESSMENT

Results obtained after tabulating and processing the dataset of each raw material involved in the mixes are presented here. The environment profiles were generated in MS-Excel as shown in table 4.1. The production processes of PHA can be varied and each have different emission levels. Since the PHA used in this study is derived from waste streams, the impact values of waste derived PHA has been used, as reported in [12]. In figure 4.40, the relative individual impact of the mix designs is displayed. It is apparent here that Global Warming Potential (CO₂ emission) is the most pronounced environment impact for all 4 mixes. Out of them, Mix 1 (CEMI+0%HA) demonstrates the highest impact. Categories such as Non-Fuel Abiotic Depletion (ADnf), Ozone Layer Depletion (ODP), and Fresh water ecotoxicity potential (FAETP) score considerably low on the impact relative to the the major impact categories such as GWP, AP (Acidification potential), and HT (Human Toxicity). As a result, these impacts get eliminated on the projected scale. The final ECI as shown in Figure 4.41 is visibly highest for Mix 1, followed by Mix 3. Both these mixes do not contain the healing agent. Addition of healing agent evidently, leads to a reduction of environmental costs by approximately 30% when CEMI is used as a binder, and by 38% when CEMIII/B is used.

Impact category	Material / Process Type	Abiotic D non fuel	Abiotic fuel (ADF)	De Global Warming (GWP)	Ozone Layer (ODP)	Photochemical (POCP)	Acidification (AP)	Eutrophication (EP)	Human Toxicity (HT)	Ecotoxicity (FAETP)	Ecotoxicity (MAETP)	Ecotoxicity (TETP)	ECI
Unit		kg Sb eq	kg Sb eq	kg CO ₂ eq	kg CFC-11	kg C ₂ H ₄ eq	kg SO ₂ eq	kg PO ₄ -P eq	kg 1,4-DB	kg 1,4-DB	kg 1,4-DB	kg 1,4-DB eq	
	Monetary value / impact cate	0.16	0.16	0.05	30	2	4	9	0.09	0.03	0.0001	0.06	
Raw materials:													
	Unit:												
CEM I NL	Cement	kg	6.70E-07	5.70E-04	8.20E-01	5.20E-09	2.10E-04	2.70E-03	3.60E-04	5.00E-02	6.90E-04	5.10E+00	6.80E-04
			325	3.48E-05	2.96E-02	1.33E+01	5.07E-05	1.37E-01	3.51E+00	1.05E+00	1.46E+00	6.73E-03	1.66E-01
CEM III B NL	Cement	kg	6.50E-07	8.00E-04	3.00E-01	5.20E-09	9.00E-05	1.00E-03	1.00E-04	2.70E-02	3.40E-04	7.80E+00	3.60E-04
			325	3.38E-05	4.16E-02	4.88E+00	5.07E-05	5.85E-02	1.30E+00	2.93E-01	7.90E-01	3.32E-03	2.54E-01
Sand, sea 0-4 mm NL	Aggregate Fine - pr/kg		3.40E-09	7.40E-05	1.10E-02	1.30E-09	1.00E-05	7.90E-05	1.80E-05	8.00E-03	1.30E-04	7.40E-01	2.30E-05
			660	3.59E-07	7.81E-03	3.63E-01	2.57E-05	1.32E-02	2.09E-01	1.07E-01	4.75E-01	2.57E-03	4.88E-02
Gravel, sea >4 mm NL	Aggregate Coarse -kg		3.10E-09	7.20E-05	1.10E-02	1.30E-09	1.00E-05	7.90E-05	1.80E-05	7.90E-03	1.30E-04	7.30E-01	2.00E-05
			1300	6.45E-07	1.50E-02	7.15E-01	5.07E-05	2.60E-02	4.11E-01	2.11E-01	9.24E-01	5.07E-03	9.49E-02
Tap water	Water	kg	2.60E-10	2.70E-06	3.40E-04	1.60E-11	1.10E-07	8.00E-07	1.40E-07	8.30E-05	1.30E-06	2.20E-02	1.50E-06
			160	6.66E-09	6.91E-05	2.72E-03	7.68E-08	3.52E-05	5.12E-04	2.02E-04	1.20E-03	6.24E-06	3.52E-04
Steel rebar	Reinforcement	kg	1.10E-06	1.30E-02	1.50E+00	6.00E-08	1.20E-03	5.10E-03	7.00E-04	5.50E-01	1.80E-02	5.00E+01	2.70E-02
			0.7 percent	54.95	9.67E-06	1.14E-01	4.12E+00	9.89E-05	1.32E-01	1.12E+00	3.46E-01	2.72E+00	2.97E-02
			2.13 percent	162.205	2.85E-05	3.37E-01	1.22E+01	2.92E-04	3.89E-01	3.31E+00	1.02E+00	8.03E+00	8.76E-02
PHA	Healing Agent												
	PHA	kg	0	2.18E-04	1.90E-02	1.70E-07	7.80E-04	2.40E-02	5.19E-03	8.50E-01	1.60E-01	1.29E+03	8.98E-03
			8.2	0	2.86E-04	7.79E-03	4.18E-05	1.28E-02	7.87E-01	3.83E-01	6.27E-01	3.94E-02	1.06E+00

Table 4.1: Calculation of the ECI against 11 impact categories

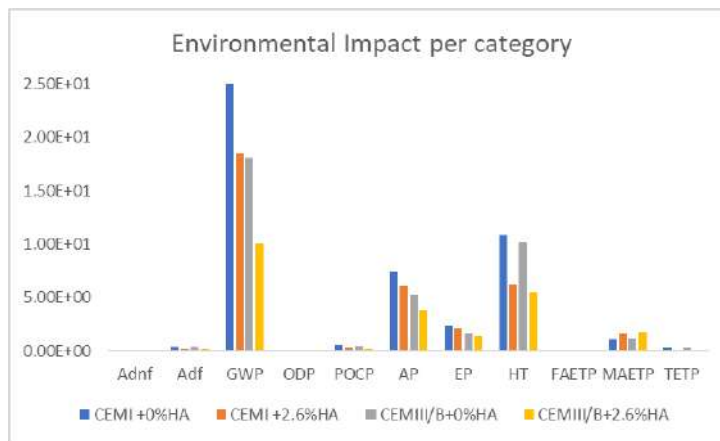


Figure 4.40: Environmental impact assessment per category. It is clear from the assessment that the GWP impact of using CEMI without the healing agents, is most damaging. The same while using the healing agent, drops significantly, implying the positive effects of using the biogenic healing agent.

4.2.2. ECONOMIC ASSESSMENT

This assessment was conducted based on commercial, market price values of the materials. Unlike the environmental prices, these prices take into account the commercial production price of the materials, and not the environmental *burden*, or cost, associated with the generation of pollutants in the production process. For economic estimations the conservative values shown in table 4.2 are drawn from available commercial database and literature. These are the prices (drawn from the)

The healing agent is comprised of PHA precursor (97.6%), yeast extract(2%), and bacterial spores(0.4%). For a 1m³ concrete composite, the quantity of each healing agent constituent and their associated costs are tabulated in table 4.3. The cost of producing bacterial spores is dependent on the specific laboratories and involved process expenses like energy. For a representative figure, the data provided in [13], for 1kg of spores,

Material	Total cost (Euros) for 1m3 concrete
CEMI concrete	100
CEMIII/B concrete	148
Steel rebars of 16mm dia (0.7% RR)	163
Steel rebars of 16mm dia (2.13% RR)	494

Table 4.2: Material costs without Healing Agent.

HA constituent	Quantity (kg)	Cost/kg (euros)	Cost for 1m3 concrete (euros)
PHA	8.2	3.4	27.88
YE	0.16	166.65	26.7
Spores	0.03	435	13
Total	8.4		68

Table 4.3: Cost of healing agent excluding labour, transportation and energy costs.

is adopted. For the PHA production cost, commercial values from the report [14] is adopted. The cost of yeast extract was found on the website [15]. Summing the respec-

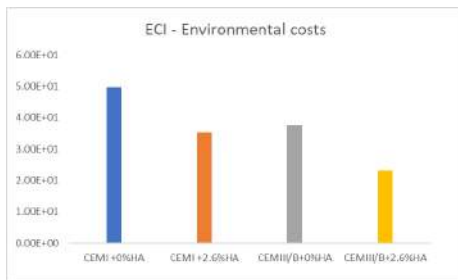


Figure 4.41: Total ECI of the 4 RC mix designs.

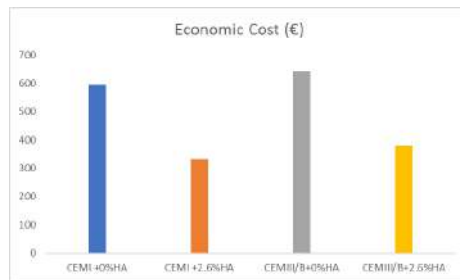


Figure 4.42: Economic costs of the mixes.

tive constituent costs of the 4 mixes yielded the results demonstrated in figure 4.42. It can be observed that using healing agent with both binder types, can lead to considerable financial savings. Out of all mixes, the lowest price is shown for Mix 2, i.e., CEMI+2.6%HA. This is because, the CEM I is commercially cheaper (though environmentally costlier) than CEMIII/B. Savings in steel owing to the use of healing agent, is therefore more pronounced in the CEMI composite. Overall, the use of healing agent leads to a 44% financial saving when CEMI binder is used, and a 41% saving when CEMIII/B binder is used. This is slightly in contrast with the savings demonstrated from the ECI calculations. However, a 3% difference in economic savings appears quite acceptable when 8% difference in environmental savings can be possible with the use of healing agent in a reinforced concrete made of CEMIII/B cement type.

5

DISCUSSION

This chapter presents a concise discussion of each result found in terms of each research question.

5.1. EXPERIMENTAL ANALYSES FOR RESEARCH QUESTIONS 1,2,3

5.1.1. COMPATIBILITY ANALYSIS WITH HYDRATION

The results of heat evolution via isothermal calorimetry indicate that the presence of the proposed new healing agent does not substantially alter the heat release of hydration. This when compared to pastes containing lactic acid based healing agents, demonstrates some notable contrast. In CEMI pastes, both the PLA variants demonstrate substantially high heat release at the acceleration stage and exhibit 2 distinct peaks after induction period that are peculiar only to them and one variant of PHA based sample (PHA-2). The former anomaly of high heat production might be associated with the presence of α -hydroxy carboxyl group in lactic acid. According to observations made by [87] on the effect of lactic acid on portland cement hydration, the presence of α -hydroxy carboxyl group acts as an accelerator for hydration. This appears to hold true for the current investigation. The latter effect of the 2 peaks visible for 3 of 4 healing agent samples, might be caused by the healing agent components. In the case of PHA based samples, although the differences in heat release in comparison to control sample, are relatively subtle, yet it might be worth noting that the two PHA variants exhibit varying behavior. The H44 has a higher accelerating peak than the control, and the PHA-2 has a lower peak. The two variants are from two different production batches. So the difference in this behavior might be attributed to the variation in constituent amounts of organic matter present in either batches, that might slightly aggravate or decelerate chemical reaction with CEM I.

In CEMIII/B, except one PLA variant (PLA-1), the rest of the curves all demonstrate comparable trends. The behavior of sample B can be also observed in [78]. Here, both the PHA based samples exhibit higher heat release than the control during the acceleration stage of clinker. PHA extraction from waste sludge is often associated with high

pH [88]. It is known that a higher pH resulting from the presence of such additives, can stimulate the dissolution of slag cements, thereby accelerating the hydration. This might be the case here as well which results in higher heat evolution. On other other hand, the same peak for PLA-2 based sample is lower than the control. Lactic acid is known to absorb Ca ions from cementitious matrix [89], [90]. Since Ca ions are very reactive, presence of more Ca ions imply faster reactions. The Ca/Si ratio of CEMIII/B is already very low, compared to OPC cements. Hence, addition of lactic acid based agents would decrease the Ca content further, which might promote a retarding effect on hydration.

Overall, the heat release of the alkanolate based pastes is closely analogous to that of the traditional, control pastes of CEMI and CEMIII/B. This implies that the addition of these healing agents do not alter remarkably the hydration characteristics of the paste in relation to control samples and therefore is expected to not drastically influence the mechanical and physical behavior of concrete.

5.1.2. INFLUENCE ON FUNCTIONAL PROPERTIES

The results of setting time can be studied along with the hydration heat release curves as they are both indicative of the early stage behavior of the respective composites. In the context of the current findings, at least for the case of initial setting times observed across the composites appear to generally correspond to the initial heat release of pastes. This is of course expected, but since both the tests are conducted on separate composites (isothermal calorimetry on pastes, and setting times on mortar), some of the behavior outcomes may sometimes differ from the expected. For instance, in the case of CEM I, from the energy evolution figure, it could be expected that the PLA-2 based composite would require the least time to set, given the high dissolution and heat release in the acceleration stage. However, from the vicat test results, the initial setting times observed for all healing agent based samples were quite comparable. The final delayed setting times also represent similar contradictions to the originally concluded remarks about the accelerating effect of PLA on OPC or CEMI. This anomaly could be the result of the presence of aggregates in the setting time samples, that could hinder the hydration reactions.

For PHA based samples in CEMI composites, the retarding effect of the final set could be linked to the probable presence of an air-entrainment system imparted by PHA. [91] reported that the biopolymer PHA can be used as a pore-forming agent in cementitious binders. For the current investigation, it might be a reason behind the retardation, since entrained air voids tend to delay setting times as was reported by [92]. This probable presence of the air void system in PHA based samples could also be the reason behind higher observed workability. A higher workability at the same w/c implies lesser water demand to reach the same relative consistency. This is quite desirable in real-life applications.

The influence of final setting retardation owing to the presence of PHA however seems diminished in the case for CEMIII/B composites. Although retardation of setting times is sometimes undesirable, especially in colder climates which anyway impedes hydration reactions, yet, a slower hydration also implies the possibility of forming a more uniformly hardened paste. In fast setting pastes, there is rapid hydration wherein the reaction products do not have time to uniformly distribute within the pores of the hydrating

paste [93]. This can also be a boon for hotter climates where the hydration tends to be extremely rapid.

The results of the compressive test at 28 days of PHA based composites are positive in both CEMI and CEMIII/B, in the sense that their presence do not drastically affect the mechanical strength compared to controls. Retarding later age hydrations and the possible formation of a more uniform microstructure might be the reason for comparable strengths, despite the alleged negative effect of an air-entrained system in concretes.

5.1.3. HEALING EFFICIENCY

The results of effective crack widths and corresponding self-healing capacities of the composites across both cement types, present a slight conflict. One would assume that a higher self-healing capacity at 70 days would suggest higher reduction of effective widths across the healing period. However, combining the observations from figures Figures 4.18-4.23 proves contrary to that premise. In CEMI, the maximum SHC is demonstrated for PHA based composites, whereas their w_{eff} are not the lowest after 70 days of healing. One way of interpreting this is to look at the formulae to obtain SHC [Equation 3.1] and w_{eff} [Equation 3.3]. The SHC depends on the water flow through the crack at both 0th and 70th days of healing. So this entirely depends on the water-permeability tests. At the same time, the w_{eff} values are based on the surface cracks observed through a stereomicroscope. One cannot interpret the full extent of healing by studying the closure of only the top and bottom surface cracks of the specimens. As suggested by the ESEM analyses later, healing products have deposited at locations away from just the surface peripheries and also at deeper levels of the cracks openings. The latter (deposition of precipitates at depths) could not be observed for PLA based samples. In PHA based samples, such depositions across crack peripheries along the depth of the crack, would impede water flow during permeability tests and result in a similar or enhanced water-tight matrix compared to PLA. In real applications, this is definitely a desirable characteristic, as water transport through the cementitious matrix paves way for numerous degradation mechanisms and is a cause of worry for most constructors. This seems to hold true in this study. In other words, the SHC at 70 days in this study for PHA is shown as independent of the corresponding observed w_{eff} .

In past studies on bacterial precipitation [10], [94], [77], [8],[95] self- *sealing* has been more commonly reported to have occurred upon addition of calcium lactate based bacterial healing agents. This is because, the conversion of calcium lactate to CaCO_3 by bacterial spores, actively require Oxygen which is readily available at the crack mouth/ surfaces [equation 2.3]. Reaction is hence unhindered at the surfaces upon availability of atmospheric Oxygen, leading to deposition of CaCO_3 , thereby sealing the cracks. At deeper reaches of the crack-widths that are away from the surfaces, oxygen concentration is not as abundant. Hence, the reaction slows at higher depths. If the crack openings are sealed, oxygen can no longer enter cracks to aid in sealing the remaining crack depth. Hence, effective *healing* of the crack is hindered, although a water-tight structure is still possible with self-sealing as well. From current study, the mechanism of the PHA based bacterial precipitation appears to be distinctly different from lactate based precipitation. The deposition in PHA appears to be uniform throughout the crack width and not only at the mouth. For a deeper understanding on this, one has to study the bacterial enzy-

matic conversion of PHA into CaCO_3 which differs from the chemical hydrolysis of PLA into CaCO_3 [20], [21], [22].

The major difference of the influence of two precursor types is observed in the case of CEMIII/B cement composites. As hypothesized in Chapter 1, the performance of the PHA based healing agent is better than that of PLA based composites. It can be validated from this study that the new healing precursor would potentially work as efficiently in low pH environments, as it does in high pH matrices.

5.1.4. INFLUENCE ON DEGRADATION

From the results of degradation presented in chapter 4, it appears that upon addition of healing agents, a distinctly better resistance against carbonation decay is feasible. This is perhaps because of the pore plugging bacterial metabolism that could make the microstructure relatively more water-tight for CO_2 transport and its eventual reaction with hydration products. The reason why PHA based samples demonstrate least damage among all, could be because of the previously mentioned entrained air-voids being present and acting as protective mechanism for the bacterial spores, facilitating better germination conditions. Use of entrained air voids as protective mechanisms for bacterial spores was studied by [96], [97]. They proved that air voids help house the microorganisms that could lead to higher precipitation in due course. It is probable that mortars containing PHA carried more active spores that led to higher metabolic conversion and hence, resulting in more dense microstructure compared to other self-healing mortars. Additionally, a symbiotic relation appear to exist between the two damage phenomena, which was also observed in other studies [98], [99], albeit without the presence of healing agents. Moreover, the presence of air void system in PHA samples as mentioned previously, could potentially offer higher resistance to frost attack according to the theory discussed by [24].

5.2. ENVIRONMENTAL AND ECONOMIC ASSESSMENT

The results obtained for this part of the assessment can aid in analysing the cost-benefit of using alkanolate based healing agent in terms of environmental and economic outlays. A comparison of the environmental impacts of four mix designs based on the production impacts of their constituent materials was conducted. It is of course true that the results in chapter 4 were arrived at after considering a select system boundary of the cradle-to-grave LCA. For a comprehensive interpretation and understanding of the environmental and economical impact, a thorough cradle-to-grave LCA should be conducted that also comprises the use phases, logistics, labour, and end-of-life aspects such as possible reduced repair frequency owing to the use of healing agent, waste generation of the constituents of the four mixes after demolition, etc. However, since the major constituent, the healing agent, on whose probable application effects the current study is based, is still under development, a thorough investigation cannot be conducted yet. So by only basing our study and interpretation on the probable impacts of producing each mix designs, it is nevertheless possible to speculate whether such an application will be feasible in real-life, on grounds of sustainability and economy.

In each mix design of the study, the variations were based entirely on the materi-

als used and not on the auxiliary processes involved in real-life situations. The material variations were made in terms of binder type, quantity of steel used, and percentage (0 or 2.6%) of healing agent in each mix. By checking the minimum combined environmental impact, and the least expensive mix, a prediction of the optimum mix type can be established that is both sustainable and economical.

As presented in chapter 4, the viable candidates for the most sustainable composite are Mix 4, followed by Mix 2. Both these contain healing agent, that in turn enable a restrictive use of steel rebars. Mix 4 is most sustainable because the presence of ground-granulated blast furnace slag in CEMIII/B type binder enables a substantial reduction of environmental impacts relative to CEMI type binder, the most reduction being observed in the category of GWP. This together with steel reduction enhance the positive effect of using healing agent in the mix. Of course, in reality, these costs will likely vary considerably if the other processes that are avoided in this assessment are also taken into consideration. This can be conducted as part of a more detailed future analysis. However, the observational distinction between the environment performance between these two mixes (Mix 2 and Mix 4) is unlikely to be contradicted by major degrees. This is because, similar results were found by [100] for mix designs based on OPC and GGBS supplemented cement types. The environmental impact of producing an organic healing agent derived from waste streams, cannot surpass that of steel. As a result, any probable environmental disadvantage emerging from the accompanying processes eliminated in this study, will be likely outweighed by the advantageous savings incurred by using the healing agent.

The proposed PHA precursor for the healing agent demonstrates a high sustainability potential when applied in the mixes. The reductions of environmental impact that was obtained after application of healing agent was considered was shown in table 5.1. Similar studies were conducted by [101] on self-healing concrete with encapsulated PU precursor, and by [102] who studied cradle-to-grave impact of SAPs (Super Absorbent Polymers) based self-healing. They compared the individual impacts of binder versus the healing agents, but did not demonstrate the impact if reinforced concrete is considered. The demonstrated reductions in these studies obtained upon using their respective healing agent will likely be affected once steel and other components of a mix design come into picture. Taking that into account, from the observations obtained in this study it can be understood that the use of currently proposed PHA based healing agent has quite positive impact on the RC mixes of both CEMI and CEMIII/B. It does warrant mentioning that in one category of toxicity (MAEP), the effect of PHA is negative. However, the overall ECI is still quite considerably reduced compared to the control mixes.

Mixes	Adnf	Adf	GWP	ODP	POCP	AP	EP	HT	FAETP	MAETP	TETP	ECI
CEMI+0%HA (Mix1)	6.43986E-05	0.389886	26.5711	0.000419	0.565027	7.438854	2.392613	10.89234	0.101968	1.120867	0.278517	49.75165
CEMI+2.6%HA (Mix2)	4.55217E-05	0.167082	18.53476	0.000268	0.320407	6.038052	2.099929	6.21052	0.083411	1.642392	0.109182	35.20605
Reductions	29%	57%	30%	36%	43%	19%	12%	43%	18%	-47%	61%	29%
CEMIII/B+0%HA (Mix 3)	6.33586E-05	0.401846	18.1211	0.000419	0.487027	5.228854	1.632113	10.21959	0.098556	1.208617	0.272277	37.67046
CEMIII/B+2.6%HA (Mix3)	4.44817E-05	0.179042	10.08476	0.000268	0.242407	3.828052	1.339429	5.53777	0.079998	1.730142	0.102942	23.12485
Reductions	30%	55%	44%	36%	50%	27%	18%	46%	19%	-43%	62%	39%

Table 5.1: Reductions observed in 11 impact categories due to addition of PHA based healing agent.

As far as the economic comparisons are concerned, as discussed in section 4.2.2 of

the preceding chapter, Mix 2 appears most economical given the reasons stated. Reiterating to the observation presented in that section, it appears tolerable if a consideration is made with respect to also the environmental costs. For a large project, a relative 8% environmental savings at the expense of using a slightly higher-priced binder would imply significant progress in terms of making our construction processes more sustainable. With respect to the concerns addressed in chapter 1 regarding enhancing the service-life of our concrete infrastructure and addressing the harmful emission levels associated with the construction sector, it is imperative that such considerations are made with respect to constituent materials in mix designs. This study only highlights the possible options to optimize a reinforced concrete mix with the help of the proposed novel alkanolate based healing agent. A future detailed process-based study of these mixes considering various loading conditions and environmental classes can help bolster the optimization.

6

CONCLUSION

Polyhydroxyalkanoates (PHA) are a group of biodegradable polymers that can be extracted from municipal waste sludges. Studies have shown that these can be enzymatically converted to Calcium Carbonates by bacterial strains such as of species *Bacillus*. Successful bacterial self healing of concrete, involving the metabolic conversion of lactates by the same bacterial species was established by [4]. Over the past decade and a half, numerous studies have validated the potential of bacterial self healing as an environmentally viable way to ensure longer service life of concrete structures. The lactic acid based precursors that has been in use for the process so far however, is found to be associated with exceptionally high production costs and incompatibility with low pH cement matrices. These ramifications weigh heavy on the otherwise viable technology of bacterial self healing. Comparatively, the prospect of using PHA as an alternative precursor, appears promising. In light of this, the current research study was an endeavour to investigate the feasibility of incorporating a PHA based precursor to aid in bacterial self healing of cementitious composites.

To understand the effect of and judge the feasibility of the new healing agent, four main research objectives or questions were formulated along with 2 supplementary questions. These were based on-

1. Investigating the compatibility of the new precursor based healing agent w.r.t its influence on hydration heat evolution and functional properties of workability, setting time and compressive strength.
2. Investigating and comparing the healing efficiency of the healing agent w.r.t autogenous healing and that by lactic acid based precursors.
3. Investigating the influence of the healing agent on commonly occurring carbonation and salt-frost attack dual-degradation mechanisms.
4. Assessing the probable environmental and economical impact of using the healing agent in reinforced concrete.

A number of experimental tests were designed to check the first three of these four major questions, while a life cycle analysis involving an Environmental Cost Indicator study, was conducted to check for the fourth question. To check for the first two research questions 2 variants of the new PHA based healing agent was considered to check the possibility of inconsistency across varying production batches of the precursor. It was found that there were discrepancies in the behavior and influence of the 2 variants, but these were negligible. As a result, for the next 2 research questions, only a single batch was considered for study.

After the tests and analyses were conducted, the results proved that the hypotheses that were made in the beginning of the study have been largely fulfilled. The following section briefly illustrates the hypotheses and the conclusions derived after studying for each research question.

6.0.1. COMPATIBILITY W.R.T HYDRATION

Hypothesis: New healing agent is potentially more compatible with low pH environments than lactate based derivatives.

Conclusion from experiment: The addition of PHA based healing agents do not alter remarkably the hydration characteristics of the paste in relation to control samples in either CEMI or CEMIII/B, and therefore is expected to not drastically influence the mechanical and physical behavior of concrete.

6.0.2. COMPATIBILITY W.R.T FUNCTIONAL PROPERTIES

Hypothesis: Although denser microstructure can be expected in CEMIII/B composites, the addition of PHA might also lead to formation of an air-entrainment network thereby leading to lowering of compressive strength. In other words, the positive effects of a possible gain in density might be offset by an air-entrainment.

Conclusion from experiments: Despite the probable presence of an air entrainment system, the PHA based composites do not drastically affect the 28th day mechanical strength compared to control specimens of both binder types. It is conjectured that this might be because of a pronounced retarding effect on final setting, which in turn might have resulted in a more uniformly formed microstructure. This could potentially offset the negative impact of an air-entrainment if present.

6.0.3. HEALING EFFICIENCY

Hypothesis: In CEMI, the healing efficiency of the new healing agent will be comparable with that of lactic acid based healing agents. In CEMIII/B the same will be better than lactic acid healing agents.

Conclusion from experiments: The healing mechanism of PHA appeared to be different from the PLA based healing agents. As opposed to self-sealing found in lactic acid based composites, the PHA based composites demonstrated higher healing at the crack depths. The overall self-healing capacity in CEMI based binders was not as varied from

the PLA based composites. In CEMIII/B indeed as hypothesized, the performance of PHA was better than PLA based composites.

6.0.4. INFLUENCE ON DEGRADATION MECHANISMS

Hypothesis: With resisting carbonation, the new healing agent will perform better in CEMIII/B cements than lactic acid derived agents. Additionally, the probable presence of air voids due to the addition of PHA in cement composites, may enhance its frost scaling resistance.

Conclusion from experiments: PHA based samples indeed demonstrated least damage in both cement types, due to carbonation and salt-frost attack.

6.0.5. ENVIRONMENTAL AND ECONOMICAL ASSESSMENT

Hypothesis: The economic and environmental costs analyses of the new HA are therefore expected to yield promising outcomes.

Conclusion from assessment: Addition of healing agent evidently, leads to a reduction of environmental costs (ECI) by approximately 30% when CEMI is used as a binder, and by 38% when CEMIII/B is used. Economically, the use of healing agent leads to a 44% financial saving when CEMI binder is used, and 41% saving when CEMIII/B binder is used.

The results of this study suggest feasibility of replacing the disadvantageous impacts of lactic acid based healing precursors with the new alkanolate based precursor. There are of course challenges with respect to large scale implementation of the new healing agent as is the case with most novel material researches. Nevertheless, the results obtained in this study can be used as a starting point for a larger discourse on the topic. For now, these results demonstrate the promising potentials of the alkanolate based precursor.

7

FUTURE SCOPE AND RECOMMENDATION

The results obtained through the course of studying for the compatibility, healing efficiency, influence on degradation mechanisms, and the potential environment and economic impact of a new alkanoate based healing precursor, demonstrate feasibility of its application in bacteria-based self healing of cement composites. Nevertheless, these same results drawn from the several experiments in this study, also open a plethora of new questions that can be investigated in future studies. From where it stands through the investigations from this study, there is definitely a scope for the new healing agent to be commercially utilized for real life applications. To bolster such possibilities, these following topics can be recommended for further understand the new healing agent:

1. The functional and mechanical behavior, healing potential and durability of the new healing agent in varying cementitious composites such as concrete and reinforced concrete.
2. The influence of varying w/c on the behavior of healing agent.
3. The consistency of the healing agent properties when large scale applications are involved.
4. The effect of a possible use of an accelerating agent along with this healing agent.
5. Better understanding of the enzymatic conversion of the healing agent by bacteria and the possibility of healing larger cracks.
6. Effect of the healing agent on longer healing periods.
7. Establish further proof of bacterial activity using more characterization studies.
8. Check for detailed understanding of the pore structure changes owing to the use of the new healing agent.

9. Check for effect on other degradation processes like Chloride induced corrosion.
10. Conduct a more inclusive, process based, and preferably cradle-to-grave life cycle analysis on the use of this healing agent in cementitious applications.

BIBLIOGRAPHY

- [1] “Procedures Required for the Assessment of Highway Structures (Final Report)”. In: (2004).
- [2] Victor C. Li and Emily Herbert. “Robust self-healing concrete for sustainable infrastructure”. In: *Journal of Advanced Concrete Technology* 10.6 (2012), pp. 207–218. ISSN: 13468014. DOI: [10.3151/jact.10.207](https://doi.org/10.3151/jact.10.207).
- [3] K van Breugel. “Is there a market for self-healing cement-based materials?” In: *1St International Conference on Self-Healing Materials* April (2007), pp. 1–9.
- [4] Henk M. Jonkers. “Self Healing Concrete: A Biological Approach”. In: *Springer Series in Materials Science* 100 (2007), pp. 195–204. ISSN: 21962812. DOI: [10.1007/978-1-4020-6250-6_9](https://doi.org/10.1007/978-1-4020-6250-6_9).
- [5] Nele De Belie et al. “A Review of Self-Healing Concrete for Damage Management of Structures”. In: *Advanced Materials Interfaces* 5.17 (2018), pp. 1–28. ISSN: 21967350. DOI: [10.1002/admi.201800074](https://doi.org/10.1002/admi.201800074).
- [6] E. Tziviloglou. “Biogenic self healing mortar”. In: *TU Delft University* (2018), p. 289. DOI: [10.4233/uuid](https://doi.org/10.4233/uuid).
- [7] Jack M. Chi, Ran Huang, and C. C. Yang. “Effects of carbonation on mechanical properties and durability of concrete using accelerated testing method”. In: *Journal of Marine Science and Technology* 10.1 (2002), pp. 14–20. ISSN: 10232796.
- [8] HM Jonkers. “Bacteria based self healing concrete”. In: *Construction and Building Materials* 152.1 (2017), pp. 1008–1014. ISSN: 09500618. DOI: [10.1016/j.conbuildmat.2017.07.040](https://doi.org/10.1016/j.conbuildmat.2017.07.040).
- [9] R. M. Mors and H. M. Jonkers. “Feasibility of lactate derivative based agent as additive for concrete for regain of crack water tightness by bacterial metabolism”. In: *Industrial Crops and Products* 106 (2017), pp. 97–104. ISSN: 09266690. DOI: [10.1016/j.indcrop.2016.10.037](https://doi.org/10.1016/j.indcrop.2016.10.037). URL: <http://dx.doi.org/10.1016/j.indcrop.2016.10.037>.
- [10] E. Tziviloglou et al. “Bacteria-based self-healing concrete to increase liquid tightness of cracks”. In: *Construction and Building Materials* 122 (2016), pp. 118–125. ISSN: 09500618. DOI: [10.1016/j.conbuildmat.2016.06.080](https://doi.org/10.1016/j.conbuildmat.2016.06.080). URL: <http://dx.doi.org/10.1016/j.conbuildmat.2016.06.080>.
- [11] Willem De Muynck et al. “Bacterial carbonate precipitation improves the durability of cementitious materials”. In: *Cement and Concrete Research* 38.7 (2008), pp. 1005–1014. ISSN: 00088846. DOI: [10.1016/j.cemconres.2008.03.005](https://doi.org/10.1016/j.cemconres.2008.03.005).
- [12] Eirini Tziviloglou et al. “Selection of nutrient used in biogenic healing agent for cementitious materials”. In: *Frontiers in Materials* 4.June (2017), pp. 1–7. ISSN: 22968016. DOI: [10.3389/fmats.2017.00015](https://doi.org/10.3389/fmats.2017.00015).

- [13] Commission European. “Environmental Factsheet : Lactic acid”. In: (2014), pp. 1–4.
- [14] Zibiao Li, Jing Yang, and Xian Jun Loh. “Polyhydroxyalkanoates: Opening doors for a sustainable future”. In: *NPG Asia Materials* 8.4 (2016), pp. 1–20. ISSN: 18844057. DOI: [10.1038/am.2016.48](https://doi.org/10.1038/am.2016.48).
- [15] A. K.H.Nor Aslan et al. “Polyhydroxyalkanoates production from waste biomass”. In: *IOP Conference Series: Earth and Environmental Science* 36.1 (2016). ISSN: 17551315. DOI: [10.1088/1755-1315/36/1/012040](https://doi.org/10.1088/1755-1315/36/1/012040).
- [16] Michaela Titz et al. “Process optimization for efficient biomediated PHA production from animal-based waste streams”. In: *Clean Technologies and Environmental Policy* 14.3 (2012), pp. 495–503. ISSN: 16189558. DOI: [10.1007/s10098-012-0464-7](https://doi.org/10.1007/s10098-012-0464-7).
- [17] D. H. Rhu et al. “Polyhydroxyalkanoate (PHA) production from waste”. In: *Water Science and Technology* 48.8 (2003), pp. 221–228. ISSN: 02731223. DOI: [10.2166/wst.2003.0472](https://doi.org/10.2166/wst.2003.0472).
- [18] Luisa S. Serafim et al. “Strategies for PHA production by mixed cultures and renewable waste materials”. In: *Applied Microbiology and Biotechnology* 81.4 (2008), pp. 615–628. ISSN: 01757598. DOI: [10.1007/s00253-008-1757-y](https://doi.org/10.1007/s00253-008-1757-y).
- [19] Michael Niaounakis. *Building and Construction Applications*. 2015, pp. 445–505. ISBN: 9780323353991. DOI: [10.1016/b978-0-323-35399-1.00010-7](https://doi.org/10.1016/b978-0-323-35399-1.00010-7).
- [20] R. A.J. Verlinden et al. “Bacterial synthesis of biodegradable polyhydroxyalkanoates”. In: *Journal of Applied Microbiology* 102.6 (2007), pp. 1437–1449. ISSN: 13645072. DOI: [10.1111/j.1365-2672.2007.03335.x](https://doi.org/10.1111/j.1365-2672.2007.03335.x).
- [21] S. Vigneswari et al. “Extracellular Polyhydroxyalkanoate Depolymerase by *Acidovorax* sp. DP5”. In: *Enzyme Research* 2015 (2015). ISSN: 20900414. DOI: [10.1155/2015/212159](https://doi.org/10.1155/2015/212159).
- [22] Michael Knoll et al. “The PHA Depolymerase Engineering Database: A systematic analysis tool for the diverse family of polyhydroxyalkanoate (PHA) depolymerases”. In: *BMC Bioinformatics* 10 (2009), pp. 1–8. ISSN: 14712105. DOI: [10.1186/1471-2105-10-89](https://doi.org/10.1186/1471-2105-10-89).
- [23] Chris M. Vermeer et al. “From waste to self-healing concrete: A proof-of-concept of a new application for polyhydroxyalkanoate”. In: *Resources, Conservation and Recycling* 164 (2021), p. 105206. ISSN: 18790658. DOI: [10.1016/j.resconrec.2020.105206](https://doi.org/10.1016/j.resconrec.2020.105206). URL: <https://doi.org/10.1016/j.resconrec.2020.105206>.
- [24] John J. Valenza and George W. Scherer. “Mechanism for salt scaling of a cementitious surface”. In: *Materials and Structures/Materiaux et Constructions* 40.3 (2007), pp. 259–268. ISSN: 13595997. DOI: [10.1617/s11527-006-9104-1](https://doi.org/10.1617/s11527-006-9104-1).
- [25] M Rooij et al. *Self-Healing Phenomena in Cement-Based Materials: State-of-the-Art Report of RILEM Technical Committee*. 2013, p. 266. ISBN: 9400766246. URL: <http://www.worldcat.org/oclc/846968087>.

- [26] Sybrand van der Zwaag. *Self-Healing Materials: An Alternative Approach to 20 Centuries of Materials Science*. Ed. by Sybrand van der Zwaag et al. 2007. ISBN: 9781402062490.
- [27] Tanvir Qureshi and Abir Al-Tabbaa. "Self-Healing Concrete and Cementitious Materials". In: *Advanced Functional Materials* (2020), pp. 1–24. DOI: [10.5772/intechopen.92349](https://doi.org/10.5772/intechopen.92349).
- [28] Kenneth R. Lauer and Floyd O. Slate. "Autogenous Healing of Cement Paste". In: *Journal Proceedings* 52 (6 1956), pp. 1083–1098.
- [29] Duff A Abrams. *Tests of bond between concrete and steel*. Tech. rep. University of Illinois at Urbana Champaign, College of Engineering, 1913.
- [30] V.J. Soroker and A.J. Denson. "Autogenous healing of concrete". In: *Zement* 25 13 (1926).
- [31] MW Loving. "Autogenous healing of concrete". In: *Bulletin* 13 (1936).
- [32] Nataliya Hearn. "Self-sealing, autogenous healing and continued hydration: What is the difference?" In: *Materials and Structures/Materiaux et Constructions* 31.8 (1998), pp. 563–567. ISSN: 13595997. DOI: [10.1007/bf02481539](https://doi.org/10.1007/bf02481539).
- [33] CA Clear. *The effects of autogenous healing upon the leakage of water through cracks in concrete*. Tech. rep. 1985.
- [34] Wieland Ramm and Michaela Biscopig. "Autogenous healing and reinforcement corrosion of water-penetrated separation cracks in reinforced concrete". In: *Nuclear Engineering and Design* 179.2 (1998), pp. 191–200. ISSN: 00295493. DOI: [10.1016/S0029-5493\(97\)00266-5](https://doi.org/10.1016/S0029-5493(97)00266-5).
- [35] Carola Edvardsen. "Water permeability and autogenous healing of cracks in concrete". In: *ACI Materials Journal* 96.4 (1999), pp. 448–454. ISSN: 0889325X. DOI: [10.14359/645](https://doi.org/10.14359/645).
- [36] Adam Neville. "Autogenous healing—a concrete miracle?" In: *Concrete international* 24.11 (2002), pp. 76–82.
- [37] Natalya Hearn and C. T. Morley. "Self-sealing property of concrete - Experimental evidence". In: *Materials and Structures/Materiaux et Constructions* 30.7 (1997), pp. 404–411. ISSN: 13595997. DOI: [10.1007/bf02498563](https://doi.org/10.1007/bf02498563).
- [38] Hans Wolf Reinhardt and Martin Jooss. "Permeability and self-healing of cracked concrete as a function of temperature and crack width". In: *Cement and Concrete Research* 33.7 (2003), pp. 981–985. ISSN: 00088846. DOI: [10.1016/S0008-8846\(02\)01099-2](https://doi.org/10.1016/S0008-8846(02)01099-2).
- [39] Stefan Jacobsen, Jacques Marchand, and Hugues Homain. "(Refereed) (Received May 2; in final form July 24.1995)". In: 25.8 (1995), pp. 1781–1790.
- [40] E. Schlangen, N. ter Heide, and K. van Breugel. "CRACK HEALING OF EARLY AGE CRACKS IN CONCRETE". In: *Measuring, Monitoring and Modeling Concrete Properties*. Ed. by MARIA S. KONSTA-GDOUTOS. Dordrecht: Springer Netherlands, 2006, pp. 273–284. ISBN: 978-1-4020-5104-3.
- [41] In: ()

- [42] Haoliang Huang. “Thermodynamics of Autogenous Self-healing in Cementitious Materials”. PhD thesis. 2014, p. 188. ISBN: 978-94-6186-397-3.
- [43] Magdalena Rajczakowska et al. “Autogenous Self-Healing: A Better Solution for Concrete”. In: *Journal of Materials in Civil Engineering* 31.9 (2019), p. 03119001. ISSN: 0899-1561. DOI: [10.1061/\(asce\)mt.1943-5533.0002764](https://doi.org/10.1061/(asce)mt.1943-5533.0002764).
- [44] L. Ferrara. “Self-healing cement-based materials: An asset for sustainable construction industry”. In: *IOP Conference Series: Materials Science and Engineering* 442.1 (2018). ISSN: 1757899X. DOI: [10.1088/1757-899X/442/1/012007](https://doi.org/10.1088/1757-899X/442/1/012007).
- [45] Lívia Souza and Abir Al-Tabbaa. “Microfluidic fabrication of microcapsules tailored for self-healing in cementitious materials”. In: *Construction and Building Materials* 184 (2018), pp. 713–722. ISSN: 09500618. DOI: [10.1016/j.conbuildmat.2018.07.005](https://doi.org/10.1016/j.conbuildmat.2018.07.005). URL: <https://doi.org/10.1016/j.conbuildmat.2018.07.005>.
- [46] MARWAN SUHAIL SUNAKH ZABANOOT. “Review of Autogenous and Autonomous Self-Healing Concrete Technologies for Marine Environments”. In: *High Performance and Optimum Design of Structures and Materials IV I* (2020), pp. 31–38. DOI: [10.2495/hpsm200041](https://doi.org/10.2495/hpsm200041).
- [47] Gupta Souradeep and Harn Wei Kua. “Encapsulation Technology and Techniques in Self-Healing Concrete”. In: *Journal of Materials in Civil Engineering* 28.12 (2016), p. 04016165. ISSN: 0899-1561. DOI: [10.1061/\(asce\)mt.1943-5533.0001687](https://doi.org/10.1061/(asce)mt.1943-5533.0001687).
- [48] Caihong Xue et al. “A review study on encapsulation-based self-healing for cementitious materials”. In: *Structural Concrete* 20.1 (2019), pp. 198–212. ISSN: 17517648. DOI: [10.1002/suco.201800177](https://doi.org/10.1002/suco.201800177).
- [49] Biqin Dong et al. “Smart releasing behavior of a chemical self-healing microcapsule in the stimulated concrete pore solution”. In: *Cement and Concrete Composites* 56 (2015), pp. 46–50. ISSN: 09589465. DOI: [10.1016/j.cemconcomp.2014.10.006](https://doi.org/10.1016/j.cemconcomp.2014.10.006). URL: <http://dx.doi.org/10.1016/j.cemconcomp.2014.10.006>.
- [50] Yangyang Zhu et al. “Preparation of pH-sensitive core-shell organic corrosion inhibitor and its release behavior in simulated concrete pore solutions”. In: *Materials and Design* 119 (2017), pp. 254–262. ISSN: 18734197. DOI: [10.1016/j.matdes.2017.01.063](https://doi.org/10.1016/j.matdes.2017.01.063).
- [51] Leyang Lv et al. “Micromechanical Properties of a New Polymeric Microcapsule for Self-Healing Cementitious Materials”. In: *Materials* 9.12 (2016). ISSN: 1996-1944. DOI: [10.3390/ma9121025](https://doi.org/10.3390/ma9121025). URL: <https://www.mdpi.com/1996-1944/9/12/1025>.
- [52] TS Qureshi, Antonis Kanellopoulos, and Abir Al-Tabbaa. “Encapsulation of expansive powder minerals within a concentric glass capsule system for self-healing concrete”. In: *Construction and Building Materials* 121 (2016), pp. 629–643.
- [53] Michelle M Pelletier et al. “Self-healing concrete with a microencapsulated healing agent”. In: *University of Rhode Island, Kingston, USA C* (2010).

- [54] A. Kanellopoulos et al. “Polymeric microcapsules with switchable mechanical properties for self-healing concrete: Synthesis, characterisation and proof of concept”. In: *Smart Materials and Structures* 26.4 (2017). ISSN: 1361665X. DOI: [10.1088/1361-665X/aa516c](https://doi.org/10.1088/1361-665X/aa516c).
- [55] Philip Van den Heede et al. “Screening Encapsulated Polymeric Healing Agents for Carbonation-Exposed Self-Healing Concrete, Service Life Extension, and Environmental Benefit”. In: *International Congress on Polymers in Concrete (ICPIC 2018)* Icpic (2018), pp. 83–89. DOI: [10.1007/978-3-319-78175-4_8](https://doi.org/10.1007/978-3-319-78175-4_8).
- [56] Philip Van den Heede et al. “Cradle-to-gate life cycle assessment of self-healing engineered cementitious composite with in-house developed (semi-)synthetic superabsorbent polymers”. In: *Cement and Concrete Composites* 94.April (2018), pp. 166–180. ISSN: 09589465. DOI: [10.1016/j.cemconcomp.2018.08.017](https://doi.org/10.1016/j.cemconcomp.2018.08.017). URL: <https://doi.org/10.1016/j.cemconcomp.2018.08.017>.
- [57] H M Jonkers. “Bacteria-based self-healing concrete”. In: (), pp. 1–5.
- [58] Kunamineni Vijay, Meena Murmu, and Shirish V. Deo. “Bacteria based self healing concrete – A review”. In: *Construction and Building Materials* 152 (2017), pp. 1008–1014. ISSN: 09500618. DOI: [10.1016/j.conbuildmat.2017.07.040](https://doi.org/10.1016/j.conbuildmat.2017.07.040). URL: <http://dx.doi.org/10.1016/j.conbuildmat.2017.07.040>.
- [59] Min Wu, Björn Johannesson, and Mette Geiker. “A review: Self-healing in cementitious materials and engineered cementitious composite as a self-healing material”. In: *Construction and Building Materials* 28.1 (2012), pp. 571–583. ISSN: 09500618. DOI: [10.1016/j.conbuildmat.2011.08.086](https://doi.org/10.1016/j.conbuildmat.2011.08.086). URL: <http://dx.doi.org/10.1016/j.conbuildmat.2011.08.086>.
- [60] U.K. Gollapudi et al. “A NEW METHOD FOR CONTROLLING LEACHING THROUGH PERMEABLE CHANNELS U.K.” In: *Chemosphere* 30.4 (1995), pp. 695–705. DOI: [https://doi.org/10.1016/0045-6535\(94\)00435-W](https://doi.org/10.1016/0045-6535(94)00435-W).
- [61] Sookie S. Bang, Johnna K. Galinat, and V. Ramakrishnan. “Calcite precipitation induced by polyurethane-immobilized *Bacillus pasteurii*”. In: *Enzyme and Microbial Technology* 28.4-5 (2001), pp. 404–409. ISSN: 01410229. DOI: [10.1016/S0141-0229\(00\)00348-3](https://doi.org/10.1016/S0141-0229(00)00348-3).
- [62] De Muynck, Willem and DE GRAEF, B and De Belie, Nele and DICK, J and DE WINDT, W and Verstraete, Willy. “Microbial ureolytic calcium carbonate precipitation for remediation of concrete surfaces”. und. In: *Concrete Repair, Rehabilitation and Retrofitting (ICRRR)*. Taylor Francis, 2005. ISBN: 0-415-39655-7.
- [63] Santhosh K. Ramachandran, V. Ramakrishnan, and Sookie S. Bang. “Remediation of Concrete Using Microorganisms”. und. In: *ACI Materials Journal* (2001). DOI: [10.14359/10154](https://doi.org/10.14359/10154).
- [64] Jan Dick et al. “Bio-deposition of a calcium carbonate layer on degraded limestone by *Bacillus* species”. In: *Biodegradation* 17.4 (2006), pp. 357–367. ISSN: 09239820. DOI: [10.1007/s10532-005-9006-x](https://doi.org/10.1007/s10532-005-9006-x).
- [65] Kim Van Tittelboom and Nele De Belie. *Self-healing in cementitious materials-a review*. Vol. 6. 6. 2013, pp. 2182–2217. ISBN: 3292645522. DOI: [10.3390/ma6062182](https://doi.org/10.3390/ma6062182).

- [66] Willem De Muynck, Nele De Belie, and Willy Verstraete. "Microbial carbonate precipitation in construction materials: A review". In: *Ecological Engineering* 36.2 (2010). Special Issue: BioGeoCivil Engineering, pp. 118–136. ISSN: 0925-8574. DOI: <https://doi.org/10.1016/j.ecoleng.2009.02.006>. URL: <https://www.sciencedirect.com/science/article/pii/S092585740900113X>.
- [67] Adrienne J Phillips et al. "Engineered applications of ureolytic biomineralization: a review". In: *Biofouling* 29.6 (2013), pp. 715–733.
- [68] Sumit Joshi et al. "Protection of concrete structures under sulfate environments by using calcifying bacteria". In: *Construction and Building Materials* 209 (2019), pp. 156–166.
- [69] Kunamineni Vijay, Meena Murmu, and Shirish V. Deo. "Bacteria based self healing concrete – A review". In: *Construction and Building Materials* 152 (2017), pp. 1008–1014. ISSN: 09500618. DOI: [10.1016/j.conbuildmat.2017.07.040](https://doi.org/10.1016/j.conbuildmat.2017.07.040). URL: <http://dx.doi.org/10.1016/j.conbuildmat.2017.07.040>.
- [70] Yousef Al-Salloum et al. "Bio-induction and bioremediation of cementitious composites using microbial mineral precipitation – A review". In: *Construction and Building Materials* 154 (2017), pp. 857–876. ISSN: 0950-0618. DOI: <https://doi.org/10.1016/j.conbuildmat.2017.07.203>. URL: <https://www.sciencedirect.com/science/article/pii/S0950061817315568>.
- [71] Henk M. Jonkers et al. "Application of bacteria as self-healing agent for the development of sustainable concrete". In: *Ecological Engineering* 36.2 (2010), pp. 230–235. ISSN: 09258574. DOI: [10.1016/j.ecoleng.2008.12.036](https://doi.org/10.1016/j.ecoleng.2008.12.036).
- [72] Renée M Mors and Henk M Jonkers. "Bacteria-based self-healing concrete – an introduction". In: (), pp. 32–39.
- [73] Henk M. Jonkers and Erik Schlangen. "Development of a bacteria-based self healing concrete". In: *Proceedings of the International FIB Symposium 2008 - Tailor Made Concrete Structures: New Solutions for our Society* (2008), p. 109. DOI: [10.1201/9781439828410.ch72](https://doi.org/10.1201/9781439828410.ch72).
- [74] Virginie Wiktor and Henk M. Jonkers. "Quantification of crack-healing in novel bacteria-based self-healing concrete". In: *Cement and Concrete Composites* 33.7 (2011), pp. 763–770. ISSN: 09589465. DOI: [10.1016/j.cemconcomp.2011.03.012](https://doi.org/10.1016/j.cemconcomp.2011.03.012). URL: <http://dx.doi.org/10.1016/j.cemconcomp.2011.03.012>.
- [75] D. Palin, V. Wiktor, and H. M. Jonkers. "Towards cost efficient bacteria based self-healing marine concrete". In: *Concrete Solutions - Proceedings of Concrete Solutions, 5th International Conference on Concrete Repair* July 2016 (2014), pp. 105–108. DOI: [10.1201/b17394-17](https://doi.org/10.1201/b17394-17).
- [76] Damian Palin et al. "A BACTERIA-BASED AGENT FOR REALIZING COST-EFFECTIVE SELF-HEALING CONCRETE IN LOW TEMPERATURE MARINE ENVIRONMENTS". In: *Microorganisms-Cementitious Materials Interactions*. 2018.

- [77] E. Tziviloglou et al. “Bacteria-based self-healing concrete to increase liquid tightness of cracks”. In: *Construction and Building Materials* 122 (2016), pp. 118–125. ISSN: 09500618. DOI: [10.1016/j.conbuildmat.2016.06.080](https://doi.org/10.1016/j.conbuildmat.2016.06.080). URL: <http://dx.doi.org/10.1016/j.conbuildmat.2016.06.080>.
- [78] Renee Mors and Henk Jonkers. “Effect on concrete surface water absorption upon addition of lactate derived agent”. In: *Coatings* 7.4 (2017). ISSN: 20796412. DOI: [10.3390/coatings7040051](https://doi.org/10.3390/coatings7040051).
- [79] Willem De Muynck et al. “Bacterial carbonate precipitation improves the durability of cementitious materials”. In: *Cement and Concrete Research* 38.7 (2008), pp. 1005–1014. ISSN: 0008-8846. DOI: <https://doi.org/10.1016/j.cemconres.2008.03.005>. URL: <https://www.sciencedirect.com/science/article/pii/S0008884608000598>.
- [80] V A C Wiktor and H M Jonkers. “Assessment of the crack healing capacity in bacteria-based self-healing concrete.” In: *In of the 3rd Inte* 2011 SRC.June (2011), pp. 32116–32124.
- [81] R M Mors and H M Jonkers. “Practical approach for production of bacteria-based agent-contained light weight aggregates to make concrete self-healing”. In: *Ic-shm* (2013), pp. 240–243.
- [82] Zeynep Başaran Bundur, Mary Jo Kirisits, and Raissa Douglas Ferron. “Use of pre-wetted lightweight fine expanded shale aggregates as internal nutrient reservoirs for microorganisms in bio-mineralized mortar”. In: *Cement and Concrete Composites* 84 (2017), pp. 167–174. ISSN: 0958-9465. DOI: <https://doi.org/10.1016/j.cemconcomp.2017.09.003>. URL: <https://www.sciencedirect.com/science/article/pii/S0958946516301780>.
- [83] S. S. Lucas et al. “Study of self-healing properties in concrete with bacteria encapsulated in expanded clay”. In: *Science and Technology of Materials* 30 (2018), pp. 93–98. ISSN: 26036363. DOI: [10.1016/j.stmat.2018.11.006](https://doi.org/10.1016/j.stmat.2018.11.006).
- [84] Author Martin Megalla. “Bacteria based self - healing concrete Master thesis”. In: ().
- [85] Rahul Roy. “Bacteria-based self-healing mortar with bio-plastic healing agents Comparative analysis on quantification and characterization of self-healing by”. In: January (2021). DOI: [10.13140/RG.2.2.12850.63687](https://doi.org/10.13140/RG.2.2.12850.63687).
- [86] V. Wiktor and H. M. Jonkers. “Field performance of bacteria-based repair system: Pilot study in a parking garage”. In: *Case Studies in Construction Materials* 2 (2015), pp. 11–17. ISSN: 22145095. DOI: [10.1016/j.cscm.2014.12.004](https://doi.org/10.1016/j.cscm.2014.12.004). URL: <http://dx.doi.org/10.1016/j.cscm.2014.12.004>.
- [87] N. B. Singh, S. Prabha, and A. K. Singh. “Effect of lactic acid on the hydration of portland cement”. In: *Cement and Concrete Research* 16.4 (1986), pp. 545–553. ISSN: 00088846. DOI: [10.1016/0008-8846\(86\)90092-X](https://doi.org/10.1016/0008-8846(86)90092-X).

- [88] Marianna Villano et al. "Effect of pH on the production of bacterial polyhydroxyalkanoates by mixed cultures enriched under periodic feeding". In: *Process Biochemistry* 45.5 (2010), pp. 714–723. ISSN: 13595113. DOI: [10.1016/j.procbio.2010.01.008](https://doi.org/10.1016/j.procbio.2010.01.008). URL: <http://dx.doi.org/10.1016/j.procbio.2010.01.008>.
- [89] Elke Gruyaert et al. "Investigation of the influence of blast-furnace slag on the resistance of concrete against organic acid or sulphate attack by means of accelerated degradation tests". In: *Cement and Concrete Research* 42.1 (2012), pp. 173–185. ISSN: 00088846. DOI: [10.1016/j.cemconres.2011.09.009](https://doi.org/10.1016/j.cemconres.2011.09.009). URL: <http://dx.doi.org/10.1016/j.cemconres.2011.09.009>.
- [90] E. Gruyaert et al. "Capsules with evolving brittleness to resist the preparation of self-healing concrete". In: *Materiales de Construccion* 66.323 (2016). ISSN: 19883226. DOI: [10.3989/mc.2016.07115](https://doi.org/10.3989/mc.2016.07115).
- [91] Michael Niaounakis. *BIOPOLYMERS: APPLICATIONS AND TRENDS*. 2015. ISBN: 978-0-323-35399-1.
- [92] G. Lomboy and K. Wang. "Effects of Strength, Permeability, and Air Void Parameters on Freezing-Thawing Resistance of Concrete with and Without Air Entrainment". In: *Journal of ASTM International* 6 (2009), pp. 1–14. ISSN: 1546-962X. URL: <https://doi.org/10.1520/JAI102454>.
- [93] P.K. Mehta and P.J.M. Monteiro. *Concrete: Microstructure, Properties, and Materials*. McGraw-Hill Education, 2013. ISBN: 9780071797887. URL: <https://books.google.nl/books?id=c-9JAgAAQBAJ>.
- [94] Nasiru Zakari Muhammad et al. "Tests and methods of evaluating the self-healing efficiency of concrete: A review". In: *Construction and Building Materials* 112 (2016), pp. 1123–1132. ISSN: 09500618. DOI: [10.1016/j.conbuildmat.2016.03.017](https://doi.org/10.1016/j.conbuildmat.2016.03.017). URL: <http://dx.doi.org/10.1016/j.conbuildmat.2016.03.017>.
- [95] Chigozirim Goodnews Iheanyichukwu, Sadiq A. Umar, and Prince Chibuikwe Ekwueme. "A Review on Self-Healing Concrete Using Bacteria". In: *Sustainable Structures and Materials, An International Journal* 1.1 (2018), pp. 12–20. URL: <http://ssmij.org/index.php/ssm/article/view/5>.
- [96] Zeynep Başaran Bundur et al. "Impact of air entraining admixtures on biogenic calcium carbonate precipitation and bacterial viability". In: *Cement and Concrete Research* 98. April (2017), pp. 44–49. ISSN: 00088846. DOI: [10.1016/j.cemconres.2017.04.005](https://doi.org/10.1016/j.cemconres.2017.04.005).
- [97] Claudia Stuckrath et al. "Quantification of chemical and biological calcium carbonate precipitation: Performance of self-healing in reinforced mortar containing chemical admixtures". In: *Cement and Concrete Composites* 50 (2014), pp. 10–15. ISSN: 09589465. DOI: [10.1016/j.cemconcomp.2014.02.005](https://doi.org/10.1016/j.cemconcomp.2014.02.005). URL: <http://dx.doi.org/10.1016/j.cemconcomp.2014.02.005>.
- [98] Hugo Eguez Alava. *Durability of Concrete under Combined Attack. Frost Salt Scaling in Carbonated Concrete and Chloride Ingress in Mechanically Loaded Concrete*. February. 2017. ISBN: 9789463550314.

- [99] Philip Van Den Heede, Mieke De Schepper, and Nele De Belie. “Accelerated and natural carbonation of concrete with high volumes of fly ash: Chemical, mineralogical and microstructural effects”. In: *Royal Society Open Science* 6.1 (2019). ISSN: 20545703. DOI: [10.1098/rsos.181665](https://doi.org/10.1098/rsos.181665).
- [100] Michael W. Tait and Wai M. Cheung. “A comparative cradle-to-gate life cycle assessment of three concrete mix designs”. In: *International Journal of Life Cycle Assessment* 21.6 (2016), pp. 847–860. ISSN: 16147502. DOI: [10.1007/s11367-016-1045-5](https://doi.org/10.1007/s11367-016-1045-5). URL: <http://dx.doi.org/10.1007/s11367-016-1045-5>.
- [101] Bjorn Van Belleghem et al. “Quantification of the service life extension and environmental benefit of Chloride Exposed Self-Healing Concrete”. In: *Materials* 10.1 (2017). ISSN: 19961944. DOI: [10.3390/ma10010005](https://doi.org/10.3390/ma10010005).
- [102] P. Van Den Heede and N. De Belie. “Environmental impact and life cycle assessment (LCA) of traditional and ‘green’ concretes: Literature review and theoretical calculations”. In: *Cement and Concrete Composites* 34.4 (2012), pp. 431–442. ISSN: 09589465. DOI: [10.1016/j.cemconcomp.2012.01.004](https://doi.org/10.1016/j.cemconcomp.2012.01.004). URL: <http://dx.doi.org/10.1016/j.cemconcomp.2012.01.004>.

A

APPENDIX

A.1. WORKABILITY :FLOW TABLE PHOTOGRAPHS

Figures A.1-A.4 present the flow table photographs of the CEMI specimen.



Figure A.1: CEMI PLA-1



Figure A.2: CEMI PLA-2



Figure A.3: CEMI PHA-1



Figure A.4: CEMI PHA-2

Figures A.5-A.8 present the flow table photographs of the CEMIII/B specimen.



Figure A.5: CEMIII/B PLA-1



Figure A.6: CEMIII/B PLA-2



Figure A.7: CEMIII/B PHA-1



Figure A.8: CEMIII/B PHA-2

A.2. HEALING EFFICIENCY

A.2.1. STEREOMICROSCOPY AND WATER PERMEABILITY

Figures A.9-A.13 present the crack width reduction for CEMI and CEMIII/B specimens, observed by image analyses of stereomicroscopic photographs.

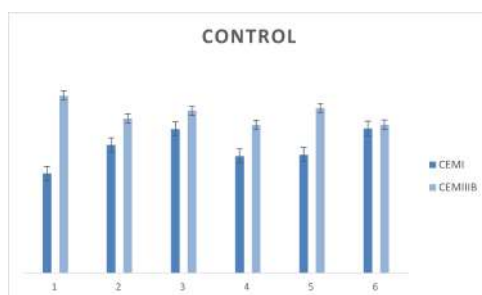


Figure A.9: Control

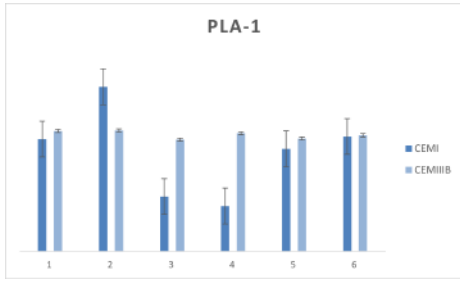


Figure A.10: PLA1

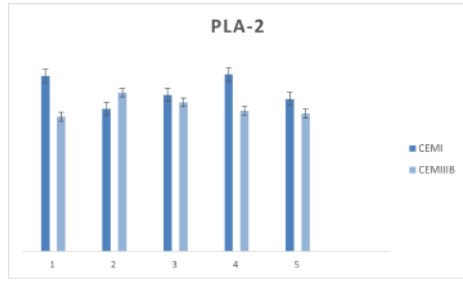


Figure A.11: PLA2

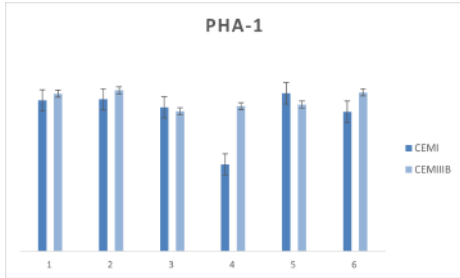


Figure A.12: PHA1

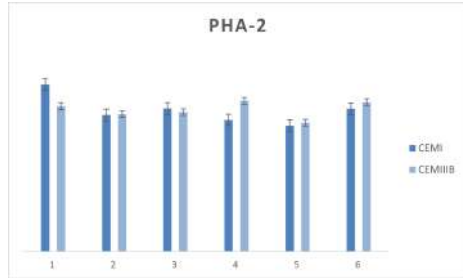


Figure A.13: PHA2

Figures A.14-A.23 present the tables used for computing healing efficiency for CEMI specimen.

Control-1		Control-2		Control-3		Control-4		Control-5		Control-6	
crack up	crack low										
0.448	0.714	0.546	0.588	0.609	0.588	0.525	0.525	0.441	0.588	0.378	0.903
1.031	0.63	0.399	0.63	1.05	0.777	0.756	0.735	0.651	0.567	0.42	0.819
1.099	0.651	0.441	0.672	0.756	0.84	0.672	0.672	0.483	0.672	0.336	0.777
0.74	0.525	0.567	0.651	0.756	0.735	0.63	0.588	0.567	0.588	0.336	0.567
0.628	0.63	0.189	0.588	0.84	0.63	0.546	0.672	0.63	0.735	0.462	1.029
0.717	0.63	0.399	0.567	0.714	0.672	0.546	0.502	0.483	0.42	0.42	0.861
0.695	0.546	0.441	0.588	1.239	0.525	0.819	0.525	0.441	0.567	0.42	0.798
0.359	0.588	0.483	0.903	0.735	0.987	0.483	0.609	0.378	0.651	0.525	0.903
0.471	0.567	0.609	0.819	0.588	0.714	0.567	0.504	0.401	0.588	0.525	0.798
0.404	0.609	0.42	0.336	0.84	0.441	0.798	0.567	0.336	0.609	0.42	1.05
AVG	AVG										
0.6592	0.609	0.4494	0.6342	0.8127	0.6909	0.6342	0.5899	0.4811	0.5985	0.4242	0.8505
L_{top}	L_{dw}										
W_{eff}	0.633437	W_{eff}	0.531243	W_{eff}	0.748508	W_{eff}	0.611515	W_{eff}	0.535536	W_{eff}	0.588894

Figure A.14: CEMI Control 0 day

A

Control-1		Control-2		Control-3		Control-4		Control-5		Control-6	
crack up	crack low	crack up	crack low	crack up	crack low						
0.609	0.469	0.07	0.398	0.281	0	0.398	0.375	0.258	0.443	0	0.469
0.422	0.364	0.258	0.141	0.328	0	0.281	0.404	0.258	0.351	0	0.211
0.445	0.398	0.258	0.375	0.187	0.211	0.398	0.117	0.539	0.351	0.164	0.548
0.375	0.469	0.211	0.141	0.258	0.305	0.328	0.422	0.328	0.515	0.141	0.328
0.492	0	0.305	0.389	0.586	0.187	0.328	0.164	0.234	0.398	0.099	0.117
0.234	0.63	0.211	0	0.234	0.141	0.305	0.398	0.281	0	0.281	0.211
0.469	0	0.258	0	0.633	0.211	0.258	0.351	0.281	0.141	0.305	0.258
0.375	0.351	0.281	0.117	0.328	0.584	0.351	0.281	0.094	0	0.211	0.305
0.398	0.328	0.305	0.398	0.281	0.211	0.211	0.094	0.161	0.234	0.258	0.211
0.047	0.351	0.281	0.328	0.117	0.609	0.375	0.211	0.141	0.211	0.234	0.258
AVG	AVG	AVG	AVG	AVG	AVG	AVG	AVG	AVG	AVG	AVG	AVG
0.3866	0.336	0.2438	0.2287	0.3233	0.2459	0.3233	0.2817	0.2575	0.2644	0.1693	0.2916
L,top	L,dw	L,top	L,dw	L,top	L,dw	L,top	L,dw	L,top	L,dw	L,top	L,dw
W,eff	0.360118	W,eff	0.236089	W,eff	0.281081	W,eff	0.301546	W,eff	0.26092	W,eff	0.219501

Figure A.15: CEMI Control 70 days

PLA1-1		PLA1-2		PLA1-3		PLA1-4		PLA1-5		PLA1-6	
crack up	crack low	crack up	crack low	crack up	crack low	crack up	crack low	crack up	crack low	crack up	crack low
0.449	0.505	0.406	0.411	0.579	1.415	0.336	0.486	0.491	0.357	0.525	0.777
0.407	0.47	0.476	0.551	0.626	0.588	0.448	0.738	0.576	0.735	0.505	0.777
0.421	0.604	0.434	0.7	0.224	0.728	0.525	1.289	0.491	0.63	0.4	0.777
0.534	0.515	0.49	0.523	0.3545	0.63	0.476	0.71	0.512	0.63	0.609	0.756
0.435	0.402	0.448	0.607	0.375	0.644	0.497	0.719	0.553	0.672	0.484	0.798
0.393	0.477	0.378	0.532	0.448	1.653	0.714	0.57	0.533	0.525	0.693	1.723
0.449	0.58	0.462	0.691	0.439	0.756	0.833	0.663	0.597	0.504	0.421	1.176
0.533	0.664	0.448	1.083	0.43	0.658	0.532	0.775	0.704	0.756	0.63	1.134
0.561	0.468	0.672	0.588	0.355	0.476	0.441	0.616	0.619	0.399	1.828	0.819
0.449	0.477	0.56	0.626	0.43	0.63	0.644	0.7	0.533	0.483	0.462	0.714
AVG	AVG	AVG	AVG	AVG	AVG	AVG	AVG	AVG	AVG	AVG	AVG
0.4631	0.5162	0.4774	0.6312	0.42605	0.8178	0.5446	0.7266	0.5611	0.5691	0.6557	0.9451
L,top	L,dw	L,top	L,dw	L,top	L,dw	L,top	L,dw	L,top	L,dw	L,top	L,dw
W,eff	0.48869	W,eff	0.547165	W,eff	0.580086	W,eff	0.626884	W,eff	0.565081	W,eff	0.782864

Figure A.16: CEMI PLA1 0 day

PLA1-1		PLA1-2		PLA1-3		PLA1-4		PLA1-5		PLA1-6	
crack up	crack low	crack up	crack low	crack up	crack low	crack up	crack low	crack up	crack low	crack up	crack low
0	0.539	0	0.258	0.281	0.67	0.328	0.445	0	0.299	0	0.281
0	0.422	0	0.445	0.334	0.67	0.422	0.478	0.264	0.211	0.212	0.636
0	0.164	0	0.422	0.369	0.164	0.469	0.328	0.316	0	0.228	0.281
0	0.492	0	0.539	0.334	0.515	0.445	0.656	0.281	0	0.264	0.351
0	0.351	0	0.422	0.334	0.492	0.398	0.562	0.351	0.51	0	0.668
0	0.07	0	0.445	0.422	0.679	0.539	0.234	0.211	0.053	0	0.442
0.246	0.398	0	0.375	0.281	0.492	0.305	0.515	0	0.193	0	0.351
0.249	0.375	0	0.389	0.193	0.164	0.351	0.679	0.404	0.288	0.422	0.158
0.07	0.328	0	0.492	0.281	0.679	0.445	0.539	0	0.58	0.281	0.299
0.246	0.351	0	0.445	0.088	0.75	0.375	0.633	0	0.351	0.211	0.15
AVG	AVG	AVG	AVG	AVG	AVG	AVG	AVG	AVG	AVG	AVG	AVG
0.0811	0.349	0	0.4232	0.2917	0.5275	0.4077	0.5069	0.1827	0.2485	0.1618	0.3617
L,top	L,dw	L,top	L,dw	L,top	L,dw	L,top	L,dw	L,top	L,dw	L,top	L,dw
W,eff	0.155019	W,eff	0	W,eff	0.386651	W,eff	0.453706	W,eff	0.21224	W,eff	0.235644

Figure A.17: CEMI PLA1 70 days



PLA2-1		PLA2-2		PLA2-3		PLA2-4		PLA2-5	
crack up	crack low								
0.315	0.672	0.714	0.462	0.525	1.155	0.546	0.714	0.609	0.903
0.399	0.462	0.525	0.483	0.462	0.735	0.483	0.525	0.63	0.777
0.168	0.735	0.546	0.693	0.567	0.714	0.63	0.651	0.546	0.609
0.441	0.546	1.366	0.546	0.588	0.462	0.819	1.828	0.525	0.546
0.42	0.756	0.714	0.588	0.546	0.441	1.332	0.756	0.546	0.231
0.504	0.882	0.546	0.42	0.42	0.672	1.723	0.714	0.714	0.609
0.525	0.798	0.63	0.588	0.462	0.693	0.882	0.63	0.525	0.567
0.462	0.462	0.819	0.672	0.672	0.861	0.462	0.546	0.758	0.756
0.42	0.63	0.441	0.504	0.525	0.357	0.84	0.378	0.567	0.693
0.441	0.525	0.504	0.609	0.378	0.399	0.777	0.399	0.441	0.546
AVG	AVG								
0.4095	0.6468	0.6805	0.5565	0.5145	0.6489	0.8494	0.7141	0.5859	0.6237
L_{top}	L_{dw}								
W_{eff}	0.510227	W_{eff}	0.61435	W_{eff}	0.576513	W_{eff}	0.777842	W_{eff}	0.604406

Figure A.18: CEMI PLA2 0 day

PLA2-1		PLA2-2		PLA2-3		PLA2-4		PLA2-5	
crack up	crack low								
0	0.164	0.378	0.258	0.187	0.305	0.211	0.264	0.187	0
0.164	0.211	0.281	0.164	0.398	0.211	0.398	0.123	0.094	0.439
0	0.328	0.047	0.187	0.117	0	0.211	0.228	0.259	0.264
0	0.305	0.258	0.187	0.351	0	0	0.158	0.094	0.264
0	0.141	0.281	0.164	0.234	0	0	0.158	0.164	0.176
0	0.117	0.211	0.281	0	0	0	0.105	0.164	0.492
0	0.117	0.141	0.281	0	0.281	0.305	0.141	0.141	0.422
0	0.141	0.141	0.234	0.258	0.305	0.211	0.035	0.094	0.387
0.239	0.164	0.187	0.211	0.141	0.164	0.234	0.053	0.07	0.088
0.234	0.117	0.164	0.258	0.141	0.234	0.117	0.088	0.07	0.123
AVG	AVG								
0.0637	0.1805	0.2089	0.2225	0.1827	0.15	0.1687	0.1353	0.1337	0.2655
L_{top}	L_{dw}								
W_{eff}	0.102685	W_{eff}	0.215557	W_{eff}	0.165277	W_{eff}	0.150774	W_{eff}	0.184818

Figure A.19: CEMI PLA2 70 days

PHA1-1		PHA1-2		PHA1-3		PHA1-4		PHA1-5		PHA1-6	
crack up	crack low										
0.482	0.588	0.462	0.882	0.504	0.42	0.532	0.588	0.714	0.672	0.546	0.476
0.462	0.588	0.441	0.399	0.617	0.63	0.448	0.462	0.777	1.155	0.567	0.392
0.924	0.504	0.588	0.693	0.7	0.399	0.476	0.693	0.588	0.525	0.588	0.476
0.588	0.532	0.567	0.42	0.616	0.546	0.532	0.966	0.798	0.588	0.672	0.476
0.63	0.784	0.463	0.567	0.784	0.526	0.504	0.504	0.798	0.693	0.525	0.672
0.504	0.504	0.378	0.399	0.532	0.609	0.532	0.588	0.672	0.546	0.63	0.644
0.567	0.504	0.63	0.63	0.672	0.441	0.728	0.504	0.777	0.714	0.798	0.504
0.378	0.56	0.525	0.63	0.504	0.399	0.7	0.777	0.819	0.546	0.777	0.505
0.588	0.672	0.756	0.504	0.308	0.462	0.756	0.336	0.672	0.714	0.819	0.616
0.609	0.728	0.693	0.672	0.532	0.315	0.644	0.42	0.798	0.777	0.546	0.616
AVG	AVG										
0.5732	0.5964	0.5503	0.5796	0.5503	0.4747	0.5852	0.4391	0.7413	0.693	0.6468	0.5377
L_{top}	L_{dw}										
W_{eff}	0.584647	W_{eff}	0.564697	W_{eff}	0.51064	W_{eff}	0.50518	W_{eff}	0.716608	W_{eff}	0.588896

Figure A.20: CEMI PHA1 0 day

A

PHA1-1		PHA1-2		PHA1-3		PHA1-4		PHA1-5		PHA1-6	
crack up	crack low										
0.234	0.305	0	0.192	0.234	0.328	0.093	0.123	0.351	0.211	0.404	0.141
0.258	0	0	0.422	0.281	0.211	0.164	0	0.375	0.018	0.246	0.164
0.351	0	0	0.228	0.258	0.445	0.234	0	0.258	0.254	0.193	0.211
0.234	0.375	0	0.176	0.328	0.305	0.187	0.281	0.258	0.211	0.299	0.281
0.305	0.094	0	0.228	0.258	0.234	0.258	0.228	0.398	0.211	0.211	0.164
0.211	0.422	0.422	0.299	0.259	0.187	0.211	0.176	0.328	0.246	0.193	0.234
0.258	0.187	0.334	0.211	0.211	0.422	0.258	0.264	0.351	0.228	0.404	0.234
0.398	0.234	0.316	0.123	0.258	0	0.562	0.176	0.351	0.176	0.281	0.398
0.234	0.211	0.439	0.246	0.351	0	0.328	0.246	0.375	0.246	0.299	0.164
0.187	0.141	0.526	0.211	0.258	0.117	0.211	0.158	0.141	0.334	0.211	0.422
AVG	AVG										
0.267	0.1969	0.2037	0.2336	0.2037	0.2249	0.2506	0.4391	0.3186	0.2135	0.2741	0.2413
L_{top}	L_{dw}										
W_{eff}	0.228405	W_{eff}	0.217968	W_{eff}	0.21395	W_{eff}	0.327456	W_{eff}	0.259084	W_{eff}	0.257004

Figure A.21: CEMI PHA1 70 days

PHA2-1		PHA2-2		PHA2-3		PHA2-4		PHA2-5		PHA2-6	
crack up	crack low										
0.63	0.273	0.294	0.483	0.567	1.429	0.651	0.525	0.504	0.462	0.609	0.483
0.987	0.819	0.693	0.504	0.378	0.42	0.861	0.525	0.252	0.903	0.609	0.483
0.484	0.588	0.84	0.63	0.63	0.357	0.693	0.525	0.672	0.609	0.777	0.378
0.736	1.134	0.567	0.42	0.546	0.42	0.567	0.483	0.651	0.651	0.63	0.483
0.63	1.45	0.441	0.609	0.441	0.567	0.525	0.63	0.568	0.504	0.714	0.462
0.754	0.651	0.63	0.525	0.483	0.294	0.651	0.546	0.483	0.652	0.588	0.504
0.42	0.714	0.399	0.693	0.462	0.504	0.63	0.462	0.588	0.924	0.756	1.303
0.609	0.567	0.504	0.462	0.483	0.485	0.504	0.357	0.819	0.756	0.609	1.891
0.589	0.504	0.567	0.546	0.504	1.05	0.798	0.569	0.483	0.546	0.693	0.63
0.273	0.441	0.546	0.336	0.378	1.37	0.346	0.294	0.546	0.483	0.546	0.315
AVG	AVG										
0.6072	0.7141	0.5481	0.5208	0.4872	0.6896	0.6426	0.4915	0.5566	0.649	0.6531	0.6932
L_{top}	L_{dw}										
W_{eff}	0.657764	W_{eff}	0.534218	W_{eff}	0.576738	W_{eff}	0.560379	W_{eff}	0.600437	W_{eff}	0.672752

Figure A.22: CEMI PHA2 0 day

PHA2-1		PHA2-2		PHA2-3		PHA2-4		PHA2-5		PHA2-6	
crack up	crack low										
0	0.141	0.258	0.234	0.228	0.305	0.305	0.211	0.258	0.281	0.305	0
0	0.187	0.187	0	0.098	0.117	0.187	0.234	0.281	0.351	0.351	0
0	0.422	0.187	0	0.137	0.211	0.53	0.281	0.164	0.398	0.492	0
0.228	0.117	0.351	0.117	0.392	0.187	0.258	0.211	0.398	0.328	0.281	0.258
0.492	0.033	0.422	0.258	0.372	0.187	0.398	0.117	0.117	0.07	0.351	0.117
0.334	0.187	0.375	0.258	0.157	0.023	0.258	0.234	0.187	0.047	0.351	0.351
0.246	0.281	0.07	0.187	0.392	0.187	0.422	0.258	0.164	0.234	0.375	0.375
0.088	0.117	0.258	0.281	0.176	0.211	0.324	0	0.351	0.187	0.398	0.141
0	0.164	0.234	0.141	0.274	0.164	0.392	0	0.351	0.445	0.281	0.351
0	0.187	0.211	0.164	0.196	0.117	0.398	0	0.234	0.305	0.281	0.094
AVG	AVG										
0.1388	0.1836	0.2553	0.164	0.2422	0.1709	0.3472	0.1546	0.2505	0.2646	0.3466	0.1687
L_{top}	L_{dw}										
W_{eff}	0.159118	W_{eff}	0.20297	W_{eff}	0.202427	W_{eff}	0.22561	W_{eff}	0.257421	W_{eff}	0.236748

Figure A.23: CEMI PHA2 70 days



Figures A.24-A.33 present the tables used for computing healing efficiency for CEMIII/B specimen.

Control-1		Control-2		Control-3		Control-4		Control-5		Control-6	
crack up	crack low	crack up	crack low	crack up	crack low	crack up	crack low	crack up	crack low	crack up	crack low
0.603	0.344	0.387	0.430	0.538	0.43	0.538	0.56	0.603	1.377	0.474	0.839
1.313	0.459	0.646	0.538	0.624	0.344	0.366	0.474	0.517	0.624	0.366	0.603
2.002	0.416	0.667	0.474	0.538	0.43	0.624	0.603	0.624	0.454	0.538	0.538
0.796	0.545	0.775	0.387	0.496	0.409	0.495	0.56	0.517	0.646	0.495	0.495
0.828	0.43	0.689	1.184	0.495	0.474	0.624	0.646	0.517	0.582	0.452	0.538
0.603	0.373	0.624	0.882	0.538	0.517	0.603	0.538	0.517	0.538	0.452	0.603
0.474	0.43	0.646	0.538	0.495	0.388	0.604	0.43	0.538	0.689	0.517	0.667
1.356	0.488	0.667	0.538	0.538	0.474	0.495	0.581	0.56	0.624	0.495	0.56
0.56	0.517	0.581	0.517	0.517	0.301	0.581	0.43	0.56	0.839	0.43	0.495
0.624	0.445	0.667	0.581	0.71	0.56	0.71	0.495	0.474	0.56	0.409	0.495
AVG	AVG	AVG	AVG	AVG	AVG	AVG	AVG	AVG	AVG	AVG	AVG
0.9159	0.4447	0.6349	0.6069	0.5489	0.4327	0.564	0.5317	0.5427	0.6933	0.4628	0.8833
L,top	L,dw	L,top	L,dw	L,top	L,dw	L,top	L,dw	L,top	L,dw	L,top	L,dw
W,eff	0.624755	W,eff	0.62069	W,eff	0.486204	W,eff	0.547533	W,eff	0.611868	W,eff	0.518413

Figure A.24: CEMIII/B Control 0 day

Control-1		Control-2		Control-3		Control-4		Control-5		Control-6	
crack up	crack low	crack up	crack low	crack up	crack low	crack up	crack low	crack up	crack low	crack up	crack low
0.117	0.141	0.187	0.158	0.246	0.158	0.158	0.228	0.264	0.211	0.176	0.264
0.164	0.264	0.234	0.246	0.141	0.176	0.141	0.158	0.123	0.193	0.211	0.228
0.117	0.193	0.539	0.246	0.316	0.141	0.193	0.158	0.193	0.299	0.07	0.176
0.281	0.141	0.281	0.158	0.176	0.123	0.334	0.264	0.404	0.158	0.211	0.176
0.117	0.123	0.164	0.228	0.123	0.105	0.158	0.123	0.141	0.105	0.158	0.141
0.141	0.141	0.117	0.088	0.246	0.141	0.299	0.176	0.123	0.176	0.228	0.193
0.117	0.141	0.211	0.246	0.193	0.053	0.193	0.088	0.07	0.105	0.158	0.211
0.187	0.158	0.023	0.158	0.193	0.123	0.299	0.316	0.193	0.281	0.141	0.281
0.094	0.141	0.164	0.316	0.176	0.035	0.211	0.123	0.053	0.088	0.053	0.211
0.066	0.141	0.117	0.239	0.159	0.035	0.211	0.123	0.141	0.171	0.193	0.281
AVG	AVG	AVG	AVG	AVG	AVG	AVG	AVG	AVG	AVG	AVG	AVG
0.1401	0.1584	0.2037	0.2083	0.1969	0.109	0.2197	0.1757	0.1705	0.1787	0.1599	0.2162
L,top	L,dw	L,top	L,dw	L,top	L,dw	L,top	L,dw	L,top	L,dw	L,top	L,dw
W,eff	0.148876	W,eff	0.205983	W,eff	0.14441	W,eff	0.196065	W,eff	0.174536	W,eff	0.18523

Figure A.25: CEMIII/B Control 70 days

PLA1-1		PLA1-2		PLA1-3		PLA1-4		PLA1-5		PLA1-6	
crack up	crack low										
0.43	0.861	0.545	1.528	0.746	0.732	0.488	0.538	0.631	0.538	0.366	0.667
0.387	0.517	0.517	1.141	0.804	0.778	0.287	0.56	1.004	0.474	0.344	0.581
0.56	0.581	0.459	0.474	0.861	0.56	0.344	0.538	0.43	0.495	0.495	0.495
0.667	0.5338	0.517	1.141	0.574	0.538	0.201	0.443	0.459	0.581	0.474	0.667
0.71	0.474	0.689	0.538	1.004	0.56	0.287	0.323	0.402	0.452	0.538	0.56
0.452	0.689	0.863	0.56	0.717	0.603	0.316	0.409	0.517	0.301	0.925	0.732
0.495	0.452	0.545	0.624	0.717	0.517	0.373	0.387	0.344	0.43	0.517	0.667
0.517	0.43	0.517	0.603	0.459	0.732	0.258	0.517	0.603	0.538	0.517	0.474
0.563	0.56	0.545	0.603	0.689	0.495	0.23	0.581	0.459	0.517	0.43	0.627
0.495	0.775	0.545	0.667	0.717	0.517	0.373	0.517	0.373	0.43	0.538	0.323
AVG	AVG										
0.5276	0.58728	0.5742	0.7879	0.7288	0.6032	0.3157	0.4813	0.5222	0.4756	0.5144	0.5793
L,top	L,dw										
W,eff	0.556375	W,eff	0.669828	W,eff	0.662046	W,eff	0.386946	W,eff	0.498174	W,eff	0.545566

Figure A.26: CEMIII/B PLA1 0 day

A

PLA1-1		PLA1-2		PLA1-3		PLA1-4		PLA1-5		PLA1-6	
crack up	crack low										
0.117	0.141	0.193	0.193	0.264	0.334	0.105	0.351	0.211	0.351	0.141	0.228
0.164	0.264	0.193	0.176	0.281	0.369	0.053	0.018	0.123	0.228	0.158	0.246
0.117	0.193	0.088	0.176	0.316	0.158	0.193	0.141	0.193	0.141	0.07	0.264
0.281	0.141	0.158	0.176	0.281	0.105	0.105	0.105	0.123	0.105	0.193	0.228
0.117	0.123	0.246	0.158	0.281	0.141	0.11	0.07	0.105	0.07	0.053	0.053
0.141	0.141	0.158	0.316	0.334	0.228	0.123	0.123	0.176	0.193	0.141	0.176
0.117	0.141	0.105	0.193	0.228	0.123	0.123	0.158	0.141	0.176	0.053	0.211
0.187	0.158	0.193	0.123	0.07	0.193	0.141	0.158	0.123	0.105	0.158	0.158
0.094	0.141	0.158	0.194	0.211	0.105	0.035	0.123	0.141	0.246	0.141	0.123
0.066	0.141	0.176	0.179	0.246	0.053	0.105	0.088	0.088	0.099	0.228	0.264
AVG	AVG										
0.1401	0.1584	0.1668	0.1884	0.2512	0.1809	0.1093	0.1089	0.1424	0.1714	0.1336	0.1951
L_{top}	L_{dw}										
W_{eff}	0.148876	W_{eff}	0.177162	W_{eff}	0.212221	W_{eff}	0.1091	W_{eff}	0.156005	W_{eff}	0.160492

Figure A.27: CEMIII/B PLA1 70 days

PLA2-1		PLA2-2		PLA2-3		PLA2-4		PLA2-5		PLA2-6	
crack up	crack low										
0.89	0.466	0.44	0.737	0.316	0.459	0.438	0.359	0.38	1.471	0.474	0.502
0.737	0.502	0.45	0.794	0.33	0.784	0.502	0.567	0.352	0.605	0.545	0.416
0.784	1.112	0.478	0.851	0.753	0.995	0.423	1.449	0.323	1.036	0.438	0.416
0.66	0.588	0.526	0.813	0.373	0.44	0.43	2.497	0.366	0.763	0.409	0.402
0.976	1.148	0.287	1.741	0.287	0.459	0.438	3.056	0.294	1.216	0.631	0.524
0.679	0.753	0.517	0.784	0.359	0.507	0.481	2.468	0.352	0.828	0.279	1.241
0.679	0.423	0.459	0.794	0.395	0.488	0.416	1.636	0.294	0.784	0.474	0.725
0.67	0.509	0.918	0.756	0.359	0.392	0.43	0.574	0.337	0.727	0.38	0.459
0.526	0.43	0.469	0.804	0.359	1.071	0.43	0.732	0.545	0.612	1.033	0.445
0.706	1.198	0.985	1.339	0.373	0.737	0.43	0.646	0.344	0.763	0.481	0.474
AVG	AVG										
0.7309	0.7129	0.5529	0.9413	0.3904	0.6313	0.4418	1.3984	0.3587	0.8805	0.5144	0.5604
L_{top}	L_{dw}										
W_{eff}	0.721825	W_{eff}	0.713056	W_{eff}	0.491737	W_{eff}	0.745807	W_{eff}	0.544006	W_{eff}	0.536744

Figure A.28: CEMIII/B PLA2 0 day

PLA2-1		PLA2-2		PLA2-3		PLA2-4		PLA2-5		PLA2-6	
crack up	crack low										
0.89	0.176	0.176	0.404	0.07	0.105	0.316	0.176	0.211	0.193	0.141	0.158
0.258	0.246	0.158	0.246	0.07	0.141	0.264	0.281	0.234	0.351	0.246	0.088
0.784	0.299	0.105	0.351	0.117	0.193	0.211	0.246	0.141	0.264	0.158	0.193
0.328	0.264	0.228	0.264	0.117	0.316	0.246	0.545	0.187	0.334	0.141	0.246
0.281	0.246	0.141	0.351	0.141	0.228	0.246	0.668	0.164	0.158	0.158	0.193
0.351	0.123	0.07	0.387	0.07	0.193	0.176	0.387	0.141	0.474	0.088	0.193
0.281	0.264	0.141	0.316	0.187	0.246	0.193	0.211	0.1176	0.351	0.193	0.246
0.234	0.193	0.07	0.474	0.047	0.228	0.228	0.07	0.047	0.281	0.387	0.211
0.187	0.141	0.07	0.316	0.211	0.141	0.193	0.123	0.234	0.088	0.053	0.299
0.211	0.151	0.123	0.158	0.141	0.404	0.264	0.387	0.023	0.334	0.105	0.211
AVG	AVG										
0.3805	0.2103	0.1282	0.3267	0.1171	0.2195	0.2337	0.3094	0.14996	0.2828	0.167	0.2038
L_{top}	L_{dw}										
W_{eff}	0.278821	W_{eff}	0.197574	W_{eff}	0.157749	W_{eff}	0.268021	W_{eff}	0.202565	W_{eff}	0.184181

Figure A.29: CEMIII/B PLA2 70 days



PHA1-1		PHA1-2		PHA1-3		PHA1-4		PHA1-5		PHA1-6	
crack up	crack low	crack up	crack low								
0.526	0.526	0.459	0.44	0.545	0.488	0.411	0.526	0.44	0.588	0.584	0.497
0.45	0.44	0.497	0.459	0.478	0.411	0.383	0.459	0.383	0.66	0.359	0.497
0.478	0.421	0.67	0.478	0.364	0.392	0.373	0.421	0.497	0.603	0.631	0.488
0.469	0.861	0.526	1.033	0.44	0.488	0.373	0.44	0.287	0.545	0.402	0.564
0.507	0.478	0.507	0.335	0.555	0.478	0.43	0.421	0.354	0.502	0.459	0.574
0.373	0.478	0.517	0.469	0.622	0.564	0.239	0.335	0.411	0.646	0.588	0.507
0.277	0.44	0.44	0.44	0.373	0.354	0.306	0.297	0.249	0.531	0.703	0.411
0.564	0.316	0.459	0.526	0.478	0.45	0.277	0.469	0.287	0.56	0.502	0.574
0.517	0.488	0.469	0.488	0.536	0.517	1.148	0.43	0.478	0.746	0.502	0.545
0.44	0.373	0.411	0.517	0.564	0.565	0.392	0.593	0.44	0.603	0.603	0.517
AVG	AVG	AVG	AVG								
0.4601	0.4821	0.4955	0.5185	0.4955	0.4707	0.4332	0.4391	0.3826	0.5984	0.5333	0.5174
L,top	L,dw	L,top	L,dw								
W,eff	0.470929	W,eff	0.506826	W,eff	0.482888	W,eff	0.436137	W,eff	0.474546	W,eff	0.52527

Figure A.30: CEMIII/B PHA1 0 day

PHA1-1		PHA1-2		PHA1-3		PHA1-4		PHA1-5		PHA1-6	
crack up	crack low										
0.228	0.299	0.281	0.176	0.141	0.264	0.229	0.176	0.228	0.328	0.281	0.141
0.158	0.141	0.176	0.088	0.281	0.158	0.176	0.193	0.158	0.281	0.264	0.211
0.176	0.141	0.176	0.141	0.228	0.264	0.246	0.123	0.228	0.117	0.334	0.141
0.211	0.176	0.158	0.228	0.176	0.228	0.211	0.228	0.176	0.164	0.088	0.211
0.158	0.105	0.299	0.193	0.176	0.299	0.228	0.158	0.299	0.234	0.141	0.193
0.193	0.141	0.176	0.053	0.141	0.211	0.211	0.228	0.211	0.258	0.281	0.141
0.123	0.141	0.281	0.141	0.105	0.176	0.07	0.158	0.193	0.117	0.176	0.193
0.105	0.158	0.176	0.193	0.088	0.176	0.07	0.141	0.123	0.234	0.193	0.176
0.141	0.176	0.193	0.176	0.105	0.246	0.299	0.193	0.105	0.211	0.07	0.158
0.316	0.141	0.158	0.141	0.564	0.176	0.105	0.167	0.053	0.164	0.211	0.176
AVG	AVG										
0.1809	0.1619	0.2074	0.153	0.2005	0.2198	0.1845	0.1765	0.1774	0.2108	0.2039	0.1741
L,top	L,dw										
W,eff	0.171049	W,eff	0.177452	W,eff	0.209854	W,eff	0.180441	W,eff	0.193141	W,eff	0.188216

Figure A.31: CEMIII/B PHA1 70 days

PHA2-1		PHA2-2		PHA2-3		PHA2-4		PHA2-5		PHA2-6	
crack up	crack low										
0.517	0.191	0.727	0.421	0.373	0.536	0.373	0.411	0.316	0.373	0.458	0.832
0.265	0.756	0.344	0.44	0.392	0.421	0.258	0.593	0.268	0.392	0.58	0.641
0.854	0.995	0.899	0.44	0.354	0.555	0.474	0.459	0.258	0.43	0.641	0.727
0.488	0.488	0.517	0.364	0.469	0.478	0.378	0.517	0.249	0.297	0.671	0.842
0.344	0.402	0.364	0.364	0.354	0.402	0.359	0.344	0.287	0.421	0.671	0.469
0.481	0.488	0.344	0.325	0.44	0.44	0.387	0.517	0.316	0.335	1.16	0.65
0.395	0.354	0.287	0.316	0.459	0.662	0.402	0.488	0.354	0.383	0.732	0.67
0.409	0.727	0.392	0.268	0.44	0.584	0.474	0.497	0.459	0.488	0.803	0.517
0.43	0.536	0.502	0.497	0.478	0.421	0.789	0.498	0.44	0.354	1.297	0.612
0.409	0.402	0.411	0.355	0.497	0.879	0.502	0.507	0.373	0.383	1.099	0.517
AVG	AVG										
0.4592	0.5339	0.4787	0.379	0.4256	0.5378	0.4396	0.4831	0.332	0.3856	0.8112	0.6477
L,top	L,dw										
W,eff	0.494675	W,eff	0.424978	W,eff	0.477334	W,eff	0.460666	W,eff	0.357464	W,eff	0.723329

Figure A.32: CEMIII/B PHA2 0 day

A

PHA2-1		PHA2-2		PHA2-3		PHA2-4		PHA2-5		PHA2-6	
crack up	crack low										
0.316	0.053	0.141	0.164	0.234	0.316	0.211	0.246	0.141	0.212	0.141	0.474
0.158	0.141	0.158	0.141	0.094	0.246	0.193	0.176	0.117	0.281	0.258	0.281
0.316	0.158	0.088	0.351	0.234	0.228	0.228	0.158	0.141	0.164	0.07	0.193
0.211	0.228	0.07	0.187	0.094	0.193	0.088	0.158	0.211	0.117	0.211	0.228
0.105	0.193	0.158	0.117	0.141	0.105	0.07	0.193	0.164	0.141	0.234	0.264
0.07	0.176	0.141	0.234	0.047	0.158	0.158	0.193	0.094	0.189	0.375	0.316
0.123	0.211	0.088	0.187	0.094	0.228	0.141	0.088	0.047	0.094	0.351	0.105
0.141	0.228	0.176	0.164	0.211	0.229	0.105	0.123	0.211	0.164	0.305	0.246
0.105	0.281	0.123	0.117	0.141	0.193	0.141	0.105	0.07	0.094	0.141	0.105
0.07	0.088	0.246	0.187	0.234	0.141	0.018	0.123	0.164	0.171	0.211	0.158
AVG	AVG										
0.1615	0.1757	0.1389	0.1849	0.1524	0.2037	0.1353	0.1563	0.136	0.1627	0.2297	0.237
L,top	L,dw										
W,eff	0.168401	W,eff	0.159714	W,eff	0.175578	W,eff	0.145295	W,eff	0.148553	W,eff	0.233312

Figure A.33: CEMIII/B PHA2 70 days

A.3. INFLUENCE ON DUAL DEGRADATION MECHANISMS CARBONATION

Figures A.34-A.37 present the tables pertaining to carbonation depths for CEMI specimen.

Control	Bottom	RS	LS	Top	Avg depth
0.742	0.357	0.204	0.178		0.36
0.089	0.191	1.084	0.23		
0.128	0.115	1.084	0.548		
0.268	0.217	0.74	0.332		
0.208	0.383	0.064	0.499		
0.319	0.134	0.68	0.485		
0.268	0.395	0.14	0.179		
0.226	0.274	0.60	0.34		

Figure A.34: CEMI Control

PHA	Bottom	RS	LS	Top	Avg depth
0.086	0.067	0.105	0.096		0.10
0.01	0.104	0.086	0.134		
0.057	0.067	0.124	0.077		
0.096	0.143	0.048	0.239		
0.057	0.163	0.143	0.096		
0.124	0.105	0.134	0.105		
0.067	0.067	0.134	0.124		
0.071	0.102286	0.1105714	0.124429		

Figure A.35: CEMI PHA

PLA1	Bottom	RS	LS	Top	Avg depth
0.269	1.315	0.102	0.842		0.46
0.434	0.957	0.702	0.497		
0.51	0.179	0.446	0.625		
0.421	0.102	0.548	0.166		
0.421	0.102	0.115	0.281		
0.599	0.14	0.867	0.077		
0.931	0.255	0.829	0.038		
0.512143	0.439714	0.5155714	0.360857		

Figure A.36: CEMI PLA1

PLA2	Bottom	RS	LS	Top	Avg depth
0.23	0.064	0.102	0.064		0.17
0.383	0.077	0.089	0.293		
0.268	0.102	0.153	0.077		
0.268	0.14	0.115	0.036		
0.344	0.170	0.101	0.242		
0.357	0.064	0.102	0.128		
0.268	0.051	0.153	0.14		
0.302571	0.096714	0.1292857	0.14		

Figure A.37: CEMI PLA2

Figures A.38-A.41 present the tables pertaining to carbonation depths for CEMIII/B specimen.

Control	Bottom	RS	LS	TOP	Average Depth	Bottom	RS	LS	TOP	Avg depth	Avg depth Control
0.268	0.459	0.753	0.395		0.428	0.383	0.526	0.395	0.051	0.399	0.414
0.319	0.746	0.319	0.191			0.563	0.293	0.497	0.472		
0.383	0.497	0.523	0.37			0.523	0.383	0.497	0.332		
0.434	0.485	0.51	0.268			0.497	0.501	0.191	0.23		
0.357	0.676	0.472	0.268			0.561	0.513	0.166	0.561		
0.651	0.599	0.242	0.281			0.434	0.548	0.23	0.357		
0.459	0.497	0.459	0.102			0.536	0.22	0.242	0.472		
0.410	0.5656	0.468	0.268			0.500	0.43	0.316857	0.353571		

Figure A.38: CEMIII/B Control



PHA	Bottom	RS	LS	Top	Avg depth	Bottom	RS	LS	Top	Avg depth	Avg depth PHA
	0.48	0.23	0.358	0.115	0.298	0.192	0.639	0.115	0.192	0.244	0.271
	0.496	0.179	0.371	0.128		0.384	0.55	0.077	0.179		
	0.457	0.345	0.281	0.09		0.32	0.269	0.026	0.179		
	0.512	0.396	0.064	0.077		0.205	0.281	0.128	0.294		
	0.467	0.307	0.243	0.243		0.435	0.358	0.102	0.153		
	0.492	0.243	0.179	0.115		0.269	0.192	0.09	0.205		
	0.556	0.486	0.32	0.102		0.345	0.294	0.102	0.243		
	0.494286	0.23	0.409	0.124286		0.537	0.294	0.153	0.102		
	0.294	0.23				0.335875	0.269	0.077	0.193375		
	0.3011	0.272778				0.349556	0.096667				

Figure A.39: CEMIII/B PHA

PLA1	Bottom	RS	LS	TOP	Average Depth	Bottom	RS	LS	TOP	Avg depth	Avg depth PLA1
	0.221	0.259	0.109	0.281	0.203	0.115	0.115	0.153	0.306	0.28	0.240
	0.16	0.4	0.141	0.198		0.064	0.37	0.153	0.459		
	0.189	0.243	0.15	0.08		0.14	0.191	0.115	0.497		
	0.249	0.23	0.128	0.099		0.423	0.332	0.255	0.191		
	0.221	0.211	0.198	0.128		0.179	0.408	0.23	0.23		
	0.179	0.179	0.24	0.198		0.332	0.281	0.268	0.459		
	0.281	0.329	0.09	0.291		0.383	0.319	0.485	0.319		
	0.21	0.2644	0.151	0.182		0.234	0.288	0.237	0.352		

Figure A.40: CEMIII/B PLA1

PLA2	Bottom	RS	LS	TOP	Average Depth	Bottom	RS	LS	TOP	Avg depth	Avg depth PLA2
	0.226	0.064	0.034	0.191	0.188	0.714	0.204	0.395	0.268	0.39	0.287
	0.14	0.051	0.013	0.14		0.472	0.344	0.319	0.408		
	0.102	0.064	0.089	0.446		0.293	0.395	0.306	0.332		
	0.153	0.038	0.077	0.064		0.485	0.23	0.497	0.383		
	0.14	0.153	0.153	0.421		0.344	0.242	0.217	0.421		
	0.128	0.448	0.281	0.23		0.574	0.191	0.268	0.714		
	0.226	0.077	0.536	0.574		0.332	0.485	0.523	0.459		
	0.159286	0.1279	0.169	0.295143		0.46	0.30	0.361	0.426429		

Figure A.41: CEMIII/B PLA2

Figures A.42-A.45 present the plots pertaining to TGA for CEMI specimen.

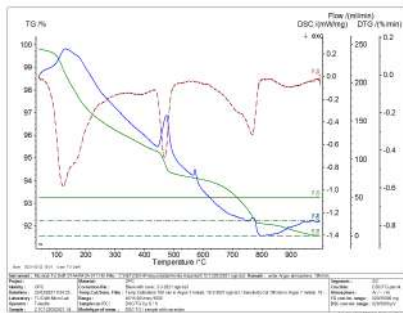


Figure A.42: CEMI Control

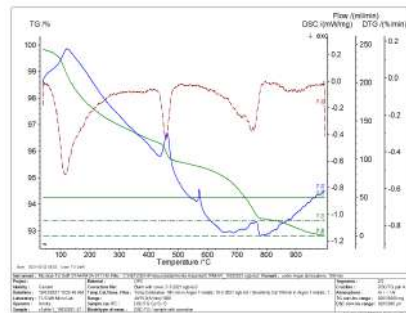


Figure A.43: CEMI PHA

A

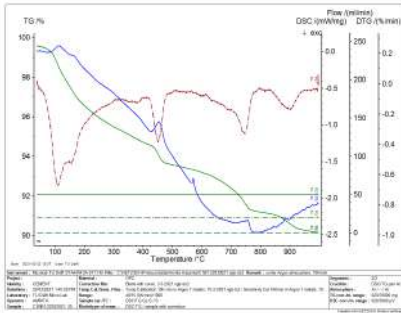


Figure A.44: CEMI PLA1

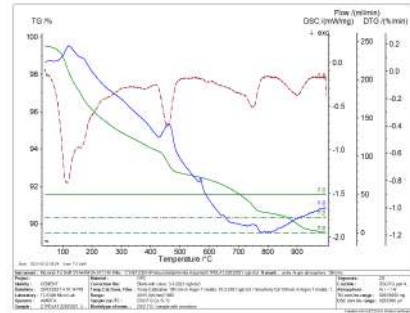


Figure A.45: CEMI PLA2

Figures A.46-A.49 present the plots pertaining to TGA for CEMIII/B specimen.

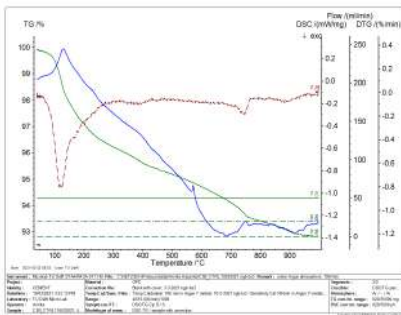


Figure A.46: CEMIII/B Control

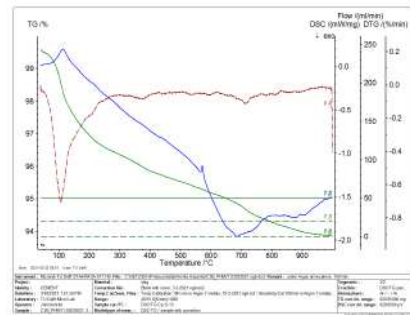


Figure A.47: CEMIII/B PHA

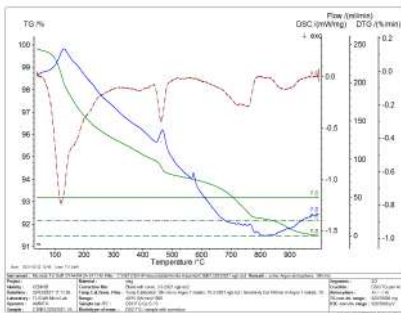


Figure A.48: CEMIII/B PLA1

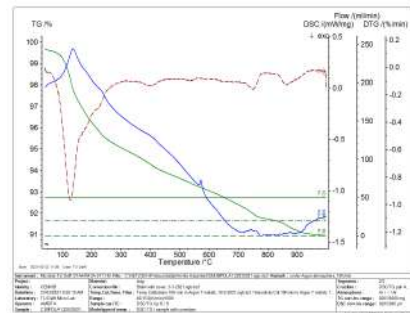


Figure A.49: CEMIII/B PLA2

SALT FROST ATTACK

Figures A.50-A.52 present the plots pertaining to frost attack mass loss for CEMI and CEMIII/B specimens.

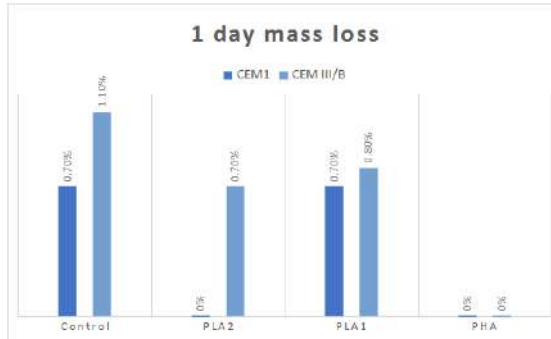


Figure A.50: Mass loss, day 1

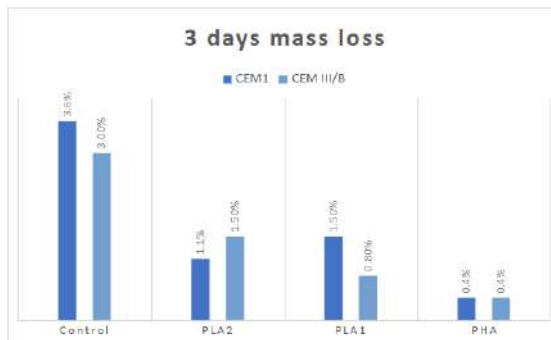


Figure A.51: Mass loss, day 3

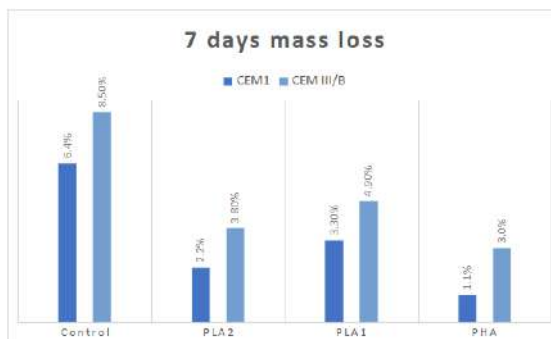


Figure A.52: Mass loss, day 7